BRNO UNIVERSITY OF TECHNOLOGY

VYSOKÉ UČENÍ TECHNICKÉ V BRNĚ

CENTRAL EUROPEAN INSTITUTE OF TECHNOLOGY BUT

STŘEDOEVROPSKÝ TECHNOLOGICKÝ INSTITUT VUT

ION-SELECTIVE MEMBRANE WITH ANTIMICROBIAL EFFECT

IONTOVĚ SELEKTIVNÍ MEMBRÁNA S ANTIMIKROBIÁLNÍM ÚČINKEM

DOCTORAL THESIS

DIZERTAČNÍ PRÁCE

AUTHOR

AUTOR PRÁCE

Ing. Evelína Gablech

SUPERVISOR

ŠKOLITEL

doc. Ing. Jana Drbohlavová, Ph.D.

CO-SUPERVISOR

ŠKOLITEL SPECIALISTA

Ing. Jan Křivčík

BRNO 2022

Abstract

This work deals with improvement of antimicrobial properties of commercial polymer membranes used in dairy industry for filtration of milk products such as whey. These membranes suffer from contamination caused by microorganisms present in milk during the filtration process. This biological contamination affects the life-time of the membrane and also filtration process itself. Thus, these membranes were modified with plasma treatment to incorporate amine functional groups for subsequent immobilization of silver and selenium nanoparticles to prevent the membranes from creation of biofilm of microorganisms. Antimicrobial activity of both types of nanoparticles and membranes with immobilized nanoparticles was determined against cell strains *Staphylococcus aureus* and *Escherichia coli*.

Abstrakt

Tato práce se zabývá zlepšením antimikrobiálních vlastností komerčních polymerních membrán používaných v mlékárenském průmyslu pro filtraci mléčných výrobků jako je syrovátka. Tyto membrány trpí kontaminací způsobenou mikroorganismy přítomnými v mléce během procesu filtrace. Toto biologické znečištění ovlivňuje životnost membrány i samotný filtrační proces. Pro ochranu membrány před vytvořením biofilmu z mikroorganismů byly tyto membrány modifikovány pomocí plazmových metod tak, aby došlo k funkcionalizaci aminovými skupinami pro následnou imobilizaci nanočástic stříbra a selenu. Antimikrobiální aktivita obou typů nanočástic a membrán s imobilizovanými nanočásticemi byla stanovena proti buněčným kmenům *Staphylococcus aureus* a *Escherichia coli*.

Keywords

Polymer membranes, silver nanoparticles, selenium nanoparticles, plasma treatment, functionalization, antimicrobial activity, cytotoxicity, immobilization of nanoparticles.

Klíčová slova

Polymerní membrány, stříbrné nanočástice, selenové nanočástice, plasmová modifikace, funkcionalizace, antimikrobiální aktivita, cytotoxicita, imobilizace nanočástic.

GABLECH, Evelína. *Iontově selektivní membrána s antimikrobiálním účinkem*. Brno, 2022. Dostupné také z: https://www.vutbr.cz/studenti/zav-prace/detail/143310. Dizertační práce. Vysoké učení technické v Brně, Středoevropský technologický institut VUT, Středoevropský technologický institut VUT. Vedoucí práce Jana Drbohlavová.

DECLARATION

I certify, that I performed dissertation work independently, under the supervision of doc. Ing. Jana Drbohlavová, Ph.D. All technical literature and other information sources presented in this work are properly cited in the text and listed in the reference list.

Brno: 28.2.2022

author´s signature

ACKNOWLEDGEMENT

I would like to thank to my supervisor doc. Ing. Jana Drbohlavová, Ph.D. and my supervisor specialist Ing. Jan Křivčík for their effective technical and pedagogical support and all their valuable advices during my studies a completation of this dissertation thesis.

Last, but not least, I would like to thank to my family for their patience and support during my studies. My thanks belong especially to my husband Imrich.

Brno: 28.2.2022

author´s signature

CONTENT

List of abbreviations

Anex	anion-exchange
Ag NPs	silver nanoparticles
ATP	adenosine triphosphate
AFM	atomic force microscopy
BrdU	bromodeoxyuridine
Catex	cation-exchange
CCM	Czech Collection of Microorganisms
CCP	capacitively coupled plasma
CFU	colony forming units
CPA	cyclopropylamine
DNA	deoxyribonucleic acid
DLS	dynamic light scattering
ED	electrodialysis
FBS	fetal bovine serum
FTIR	Fourier transform infrared spectroscopy
HR-TEM	high resolution transmission electron microscopy
IEM	ion-exchange membrane
Ionex	ion- exchange
IR	infra-red
LDH	lactate dehydrogenase
LDPE	low-density
MBC	minimum bactericidal concentration
MH Broth	Mueller-Hinton broth
MH Agar	Mueller-Hinton agar
MF	microfiltration
MIC	minimum inhibitory concentration
MPs	membrane processes
MTT	(3-(4,5-dimethylthiazol-2-yl) -2–5-diphenyltetrazolium bromide)
NF	nanofiltration
PEG	polyethylene glycol
PES	polystyrene
PVA	polyvinyl alcohol
PVP	polyvinylpyrrolidone

RF	radio frequency
RIE	reactive ion etching
RO	reverse osmosis
ROS	reactive oxygen species
SAXS	small angle X-ray scattering
USAXS	ultra-small angle X-ray scattering
Se NPs	selenium nanoparticles
SD	standard deviation
SDS	sodium dodecyl sulfate
SEM	scanning electron microscopy
SPR	surface plasmon resonance
TEM	transmission electron microscopy
UF	ultrafiltration
XRD	X-ray diffraction
XTT	(2,3-bis-(2-methoxy-4-nitro-5-sulfophenyl)-2H-tetrazolium-5-carboxanilide)

1 Introduction

The current issue in a dairy industry is how to keep a filtration process of milk products free from bacterial contamination. The most common treatments of milk products utilizes membrane processes (MPs) [1, 2]. Big advantage of MPs is a loss of very small amount of bioactive substances (such as microorganisms etc.) because the filtration is held under lower temperatures, chemical composition is preserved, energy consumption is low, as well as sensoric properties remain the same [3, 4]. MPs in dairy industry are exploited for removing of fat and microorganisms, decreasing of undesirable agents (lactose), enriching of milk with several components (whey proteins) or increasing the yield of milk products (desalination of whey) [1, 5]. One of the most important problem of the MPs is degradation of membrane during working conditions, namely congesting and biofouling caused by microorganisms creating biofilm on the surface of the membrane. This pollution very negatively affects an effectivity of filtration process and life time of the membrane [6, 7]. One of the frequent applications of these filtration membranes is desalination process of whey. The whey, contains very high amount of bioactive and organic components, which in combination with demands on membrane properties bring a lot of technological challenges [8, 9]. In practice, to avoid contamination of membranes, they are purified mechanically or with various aggressive chemicals such as oxidizing agents or acids, which can damage membrane as well. However, science brings new possibilities that can significantly prolong not only the life time of the membrane, but also can preserve the effectivity of MPs [7, 10].

Novel attitudes lately reported in few scientific papers how to prevent the membranes from biofouling include new design of membranes with various admixtures or adjusted polymers [4], photo/redox initiated surface grafting [11], engineered biofilms for targeted degradation of microorganisms [12], chemical reactions on membrane surface, physical coating and adsorption [13] and also surface modification with various types of nanoparticles [14].

Nowadays, nanochemistry frequently uses nanoparticles with unique properties compared to their macro-scaled counterparts coming from their high surface to volume ratio [15, 16]. In general, nanoparticles are clusters of atoms with size in the range of 1-100 nm [17-19]. Ideal nanoparticles evince small particle dimension, high surface area, quantum confinement or no agglomeration in colloidal state [16]. Nanoparticles have various physical, chemical and biological properties, which are very strongly driven by their shape, size and also size distribution that given by their synthesis approach [20]. In the last two decades, a lot of research has been dedicated to the synthesis and utilization of various nanoparticles [21]. The control of nanoparticles size or shape can be reached by various preparation techniques using reducing agents or stabilizers under different reaction conditions. Thus, it is a big advantage that nanoparticles can be prepared with desired properties for chosen applications [22, 23]. Specifically for antimicrobial application, it seems that silver nanoparticles (Ag NPs) and selenium nanoparticles (Se NPs) are the best candidates [24, 25].

Ag NPs can be utilized thanks to their remarkably distinct physical, biological and chemical properties in various areas of industry such as textile (nanosilver in clothes originally used in army [26] became commonly available in outdoor clothing, socks or underwear or even cleaning cloths), cosmetics [27], and they have very promising potential for various applications in pharmacy [28] or medicine [29]. According to the European Food Safety Authority (EFSA), they are also safe as biocidal additive in plastic food contact materials (FCMs) [30]. Apart from already mentioned antibacterial applications [17, 18, 31], Ag NPs have been also used in catalysis [32], sensing [33] and optics [34].

The antibacterial effect of Ag NPs is very closely interconnected with their size; general postulate is that the smaller is the silver nuclei, the higher is the antibacterial activity [35]. It is also well-known that silver-based materials are significantly toxic to microorganisms; such as *Staphylococcus aureus* or *Escherichia coli* [31, 36]. Silver is usually used in its nitrate form to originate the antimicrobial effect but in case of using Ag NPs, the available surface area to which microbes are being exposed increases very rapidly [37]. The newest research related to the safety of nanomaterials however shows that Ag NPs are being more and more questioned due to their significant environmental impact, especially to organisms living in the soil and aquatic ecosystems [38]. That is why the scientists are looking for an alternative candidate with less harmful impact to environment and human health.

Selenium (Se) is an essential micronutrient and in low concentrations very important and non-toxic to human body. Selenium can be present in the environment in following oxidation forms: elemental state (Se^0), in the form of selenates (Se^{6+}), selenites (Se^{4+}), and selenides (Se^{2-}) and can easily switch from one oxygen state to another [39]. Selenium exists in three allotropic forms: amorphous Se, which is red in color, crystalline trigonal, which is black in color, and crystalline monoclinic that are red in color [39, 40]. Se is a semimetal with very interesting photoelectrical and semiconductor properties [39, 41]. These remarkable photoconductivity and catalytic activity have been recently observed and intensively studied also for Se in the form of nanoparticles (Se NPs) [41, 42]. In addition, Se NPs evince also promising biological properties such as very strong antimicrobial effect. Thanks to them they are useful in a wide area of biomedical applications, namely for therapeutic or diagnostic purposes such as drug delivery, cancer prevention and therapy, biosensors, skin care products, point of care testing of SARS-CoV 2, and antimicrobial resistance [43]. Se NPs are able to defuse organisms such as *S. aureus* or *E. coli* [44, 45]. Like Ag NPs, Se NPs final properties are affected by their size and shape, thus, the smaller is the size of Se NPs, the higher antimicrobial effect is provided.

2 Aims of thesis

This thesis was realized in a cooperation with company MemBrain, ltd [46]. The company produces the commercial polymer ion-exchange membranes used in food industry for desalination of whey and for filtration of milk products. These membranes suffer during desalination process from the contamination with bacteria that create a biofilm, which damage and congest the membrane pores and subsequently debase not only membrane quality and life- time but also filtration process.

Milk products consist of a very high number of biological organisms, which can affect the MPs and also the condition of the membrane. Aim of this thesis is to modify the membrane to achieve antimicrobial properties. Thus, NPs were immobilized on the polymer membrane to prevent it from the contamination and eventually from degradation, as well.

Crucial part of this thesis was to find the proper antimicrobial agent. Ag NPs and Se NPs were chosen because of their very well-known antimicrobial properties.

To achieve the main goal, the thesis pursued the following specific objectives and activities:

1. The synthesis of Ag and Se NPs and their optimization to achieve the desired properties for subsequent utilization in membrane modification - most importantly the colloidal stability and suitable toxicological properties. The optimization process was based on tuning the physico-chemical properties of NPs via following synthesis parameters: concentration of reagents, utilization of different stabilizing substances, reaction conditions such as temperature or interaction with UV light. The prepared NPs were characterized by various methods determine their morphology: size and size distribution, shape as well as colloidal stability.
2. In the next step cytotoxicity of both types of Ag NPs and Se NPs were performed.
3. Subsequently, the antimicrobial tests were performed to prove the NPs antimicrobial effect.
4. The next part of this thesis was dedicated to the challenging immobilization of NPs onto polymer membrane. This stage included the plasma modification of surface of the polymer membranes to incorporate the desired functional groups for subsequent immobilization of NPs.
5. In the last part, polymer membranes with immobilized NPs were tested to determine the antimicrobial activity.

Company MemBrain ltd. provided two types of polymer membranes: anion-exchange (anex) and cation-exchange (catex). In this thesis only catex membrane were used due to better stability to various chemicals.

3 State of the art

3.1 Membrane processes

Membrane technologies are widely used in industries such as food, paper, and textile industry, pharmacy, biotechnology or chemical industry. In general, food industry employs membrane processes (MPs) because they are easy to process material but also thanks due to their ability to achieve highly selective separations. Dairy industry is one of the areas where MPs are used on the widest scale. They can be utilized in entire spectrum of workflow from primary production and treatment of milk to production of cheese or other milk products. Dairy industry usually uses MPs of first generation, namely based on pressure and usage of electromembrane [1, 2, 47]. A modern dairy industry utilizes MPs for separation of various individual components of filtered agent. These MPs are more economic and gentler to filtered substance in comparison to classic separation methods such as evaporation, distillation etc. MPs bring various advantages such as small loss of active substances, avoid changes in the state of matter or chemical changes, lower energy consumption, no waste products, no changes of sensory properties (low temperature of processes). Membranes are able to catch a huge part of microorganisms but also chemicals such as herbicides, pesticides, dyes, pharmaceuticals or sediments which could negatively affect the final product.

Individual MPs apply various mechanisms of separation and can be combined with each other, as well. The first attitude of physico-chemical principles divides MPs into three basic groups, see Table 1. MPs also consider dimensions of separated particles or molecules, affinity of filtered mixture to membrane material, properties of solvent and different diffusion rate [48].

Table 1: Mechanisms of membrane processes.

Stimulus	Type of separation method
Pressure	Microfiltration, ultrafiltration, nanofiltration, reverse osmosis
Electric	Electrodialysis, electrodeionization, electrofiltration, electrolysis, fuel cells
Temperature	Membrane distillation

Dairy industry utilizes for filtration of milk and whey mostly pressure MPs, namely microfiltration (MF), ultrafiltration (UF), nanofiltration (NF), reverse osmosis (RO) and from electric MP electrodialysis (ED).

MF is usually used for retention of fat, bacteria, spores and somatic cells from milk and whey. This process is also utilized for products, which require specific purposes such as whey protein concentrate or whey protein isolate. Microfiltration is also suitable for fractionation of milk proteins. UF is suitable for filtration of low molecular weight particles such as organic acids, peptides, minerals, water and lactose. UF is primarily used for milk to produce lactose free milk. Furthermore, UF is also used to concentrate whey proteins in milk. NF and RO are usually used for desalination and dewatering of whey [3, 5, 7].

Principle of pressure MPs lies in utilization of different pressure, properties of membrane and dominant transport mechanism. Figure 1 shows schematic illustration of separation process of pressure methods. Pressure difference, which is used as stimulus above and under membrane causes that low molecular substances get through the membrane and high molecular substances are caught on the membrane. Dimensions of separated particles and molecules decrease in sequence from MF, through UF and NF to RO, hence dimensions of membrane pores decreases

as well. It leads to higher pressure of MPs to overcome the membrane resistance against the transport, which keeps constant flow of separation process. Product of separation process is permeate with almost zero concentration of separated component and retentate, where separated components are concentrated. Even though there are significant differences between individual processes, in practice there is no exact boundary between them [48, 49].

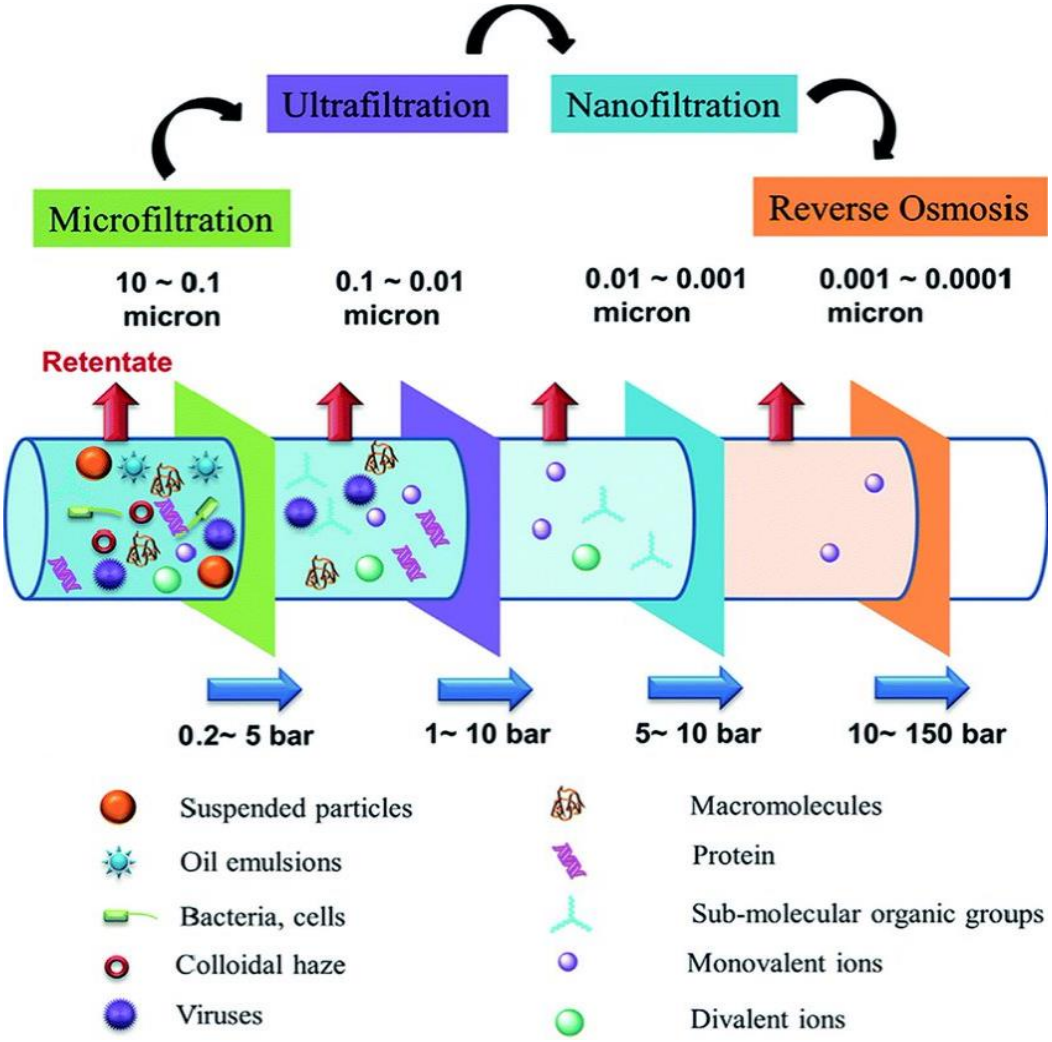

Figure 1: Schematic illustration of pressure membrane processes [48].

Electrodialysis depicted in Figure 2 is a separation process where direct current electric field affects dissociated substances in solvent. Such electrical potential between two electrodes causes movement of positively charged particles to negative electrode and simultaneously negatively charged particles move to positive electrode. Electrodialysis apparatus consist of a diluate chamber, which serves as a channel for depleted stream and concentrate chamber serves as a channel for enriched stream. A real device in working conditions can include a few hundreds of these chambers. Electrodialysis is in dairy industry usually used for processing of whey (for example desalination of whey). MPs can be used in many areas of dairy industry from basic treatment of milk, through thicken the milk or whey to separation of their individual substances (fat, proteins, lactose, mineral salts, etc.) and demineralization [49].

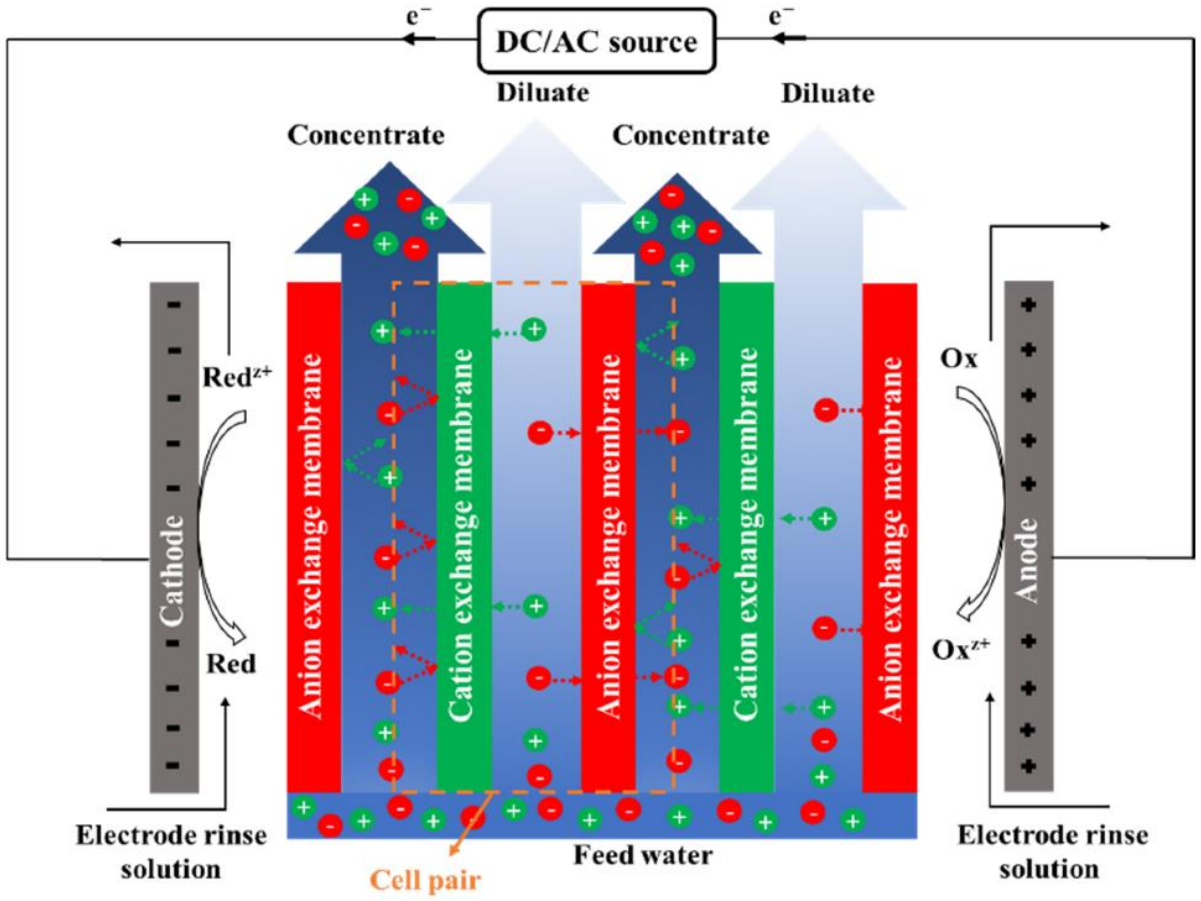

Figure 2: Schematic illustration of electrodialysis [49].

3.2 Membranes used in membrane processes

Membranes used in MPs can be biological or synthetic. Membranes can be divided into several groups based on their properties such as origin, physical state, material (fabrication), structure and morphology [50, 51].

Figure 3 shows the basic membrane types based categorized above-mentioned properties. Synthetic membranes are divided to inorganic and organic membranes. Inorganic membranes are usually made from silicon or metal materials. Organic membranes utilize polymers, which is most common material for membrane production and frequently used in dairy industry [51]. Dairy industry filtrates high amount of product, thus, membranes are usually set to big modules to make filtration process as effective and fast as possible. These modules can be planar, spiral or capillary [50, 51].

A special type of these membranes is ion exchange membranes (IEM). IEM are usually employed in ED processes. It is a type of membrane, which can transport ions with the same type of charge e.g. positive or negative (this membrane cannot transport neutral molecules or solvent itself) depending on ion-exchange material (ionex) that membrane contains. Charge of functional group in the membrane is compensated with equivalent quantity of opposite charged ions. Filtration of several compounds can be accompanied with penetration of so called counterions, which have the same charge as functional groups in membrane. In milk industry they are used mainly for desalination of whey [52].

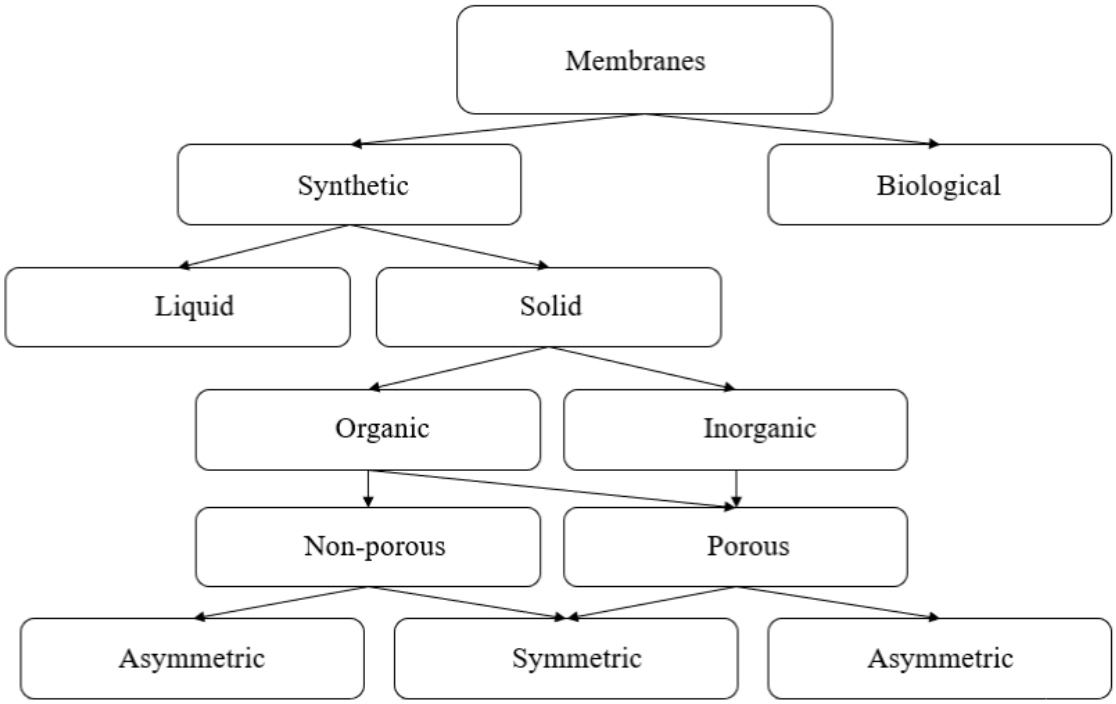

Figure 3: Basic distribution of membranes used in membrane processes.

IEM can be homogeneous or heterogeneous, and also composites, if there are additional compounds for desired properties. They are also divided into few groups according to type of ionex they contain [52]:

- **cation-exchange** membranes - allow penetration of only positively charged particles,
- **anion-exchange** membranes - allow penetration of only negatively charged particles,
- **bipolar membranes** - special type, which combines anex and catex layers.

Proper functionality of membrane is driven from its properties such as swelling capacity, thickness, ion exchange capacity, perm selectivity, transfer number, ion conductivity (electrical resistance of membrane), diffuse coefficient, hydraulic resistance, thermal stability, chemical stability and mechanical strength. These are the points that should be considered during development of membranes.

The most important properties are high perm selectivity, high permeability and long life-time. Selectivity is very important because it defines the effectivity of selection process and also purity of final product. Permeability defines speed of filtration process. Usually, in working conditions, poor permeability requires membrane with bigger area. Membrane should be resistant to mechanical, chemical and temperature factors and it usually depends on fabrication process and used materials.

Selection and suitable utilization of membrane is very related to exact filtration process and it is dependent on many factors. Generally, versatile membrane for all application does not exist, thus it is very important to consider following demands when it comes to final application:

- type of MPs,
- composition of filtered mixtures (dimensions of particles and molecules, properties of solvent),
- material and properties of membrane,
- membrane pollution and contamination (scaling, fouling, biofouling),

- sanitation of membrane,
- damage of membrane from inappropriate operating conditions,
- and storage of membrane.

A very common problem of IEM (and membranes used in food industry in general) is their contamination and congesting during filtration process, especially in dairy industry, where milk and milk products evince high biological activity. This fact makes the research and development of membranes for MPs challenging. Physical, chemical and biological factors affect contamination, congesting and life-time of the membrane. In general, three types of membrane contamination exist [52]:

- **scaling** - represents congestion of membrane as result of crystalized mineral substances on the surface of the membrane that obstruct penetration,
- **fouling** - represents congestion of membrane pores with particles (physical or chemical fouling),
- **biofouling** - microorganisms create a biofilm on the surface of the membrane.

Biofouling causes an extensive problem such as degradation of membranes and also affects the filtration process, which is described in details in the following chapters.

3.2.1 Biofouling of polymer membranes - creation of biofilm

As mentioned above, biofouling is a process when bacteria form a thin layer on the surface of polymer membranes (so-called biofilm). This biofilm then negatively impacts not only the properties of the membranes, but also the filtration process itself [53]. Biofilm formation is not yet fully described, especially with respect to the initial phase, but there are several theories how the biofilm from bacteria is formed. Biofilm formation consist of several stages [54-56]:

1. **Initial phase** - this stage can also be called as conditioning stage. At this phase, the bacteria reversibly interact with the polymer surface. When bacteria separate from the surface, there are remaining extracellular compounds on the surface of the membrane. These compound most likely play a significant role in a subsequent formation of biofilm.
2. Phase of irreversible attachment - also called as the phase of primary adhesion. In this phase bacteria irreversibly adhere to the surface of the membrane and the bonding is stable.
3. **Microcolonies formation** - also named as the maturing phase 1. In this phase, bacteria multiply and form colonies.
4. **Formation of biofilm** - can be also called as maturing phase 2. This is the phase when cells are completely adhered to the membrane surface and begin to form extracellular substances (mostly based on polysaccharides). When the entire surface is covered with this extracellular substance - a biofilm is formed. At this stage, the biofilm is stable and bacteria can multiply. In their scientific work published by Sedlařík et al. they stated that in order to deactivate the biofilm, it requires 100 times higher concentration of antibiotics in comparison to bacteria that are not part of the biofilm [55].
5. **Distribution phase** - the amount of multiplied bacteria rapidly increased, which cause the rupture of the biofilm. The bacteria are then released into the environment (in this case into milk or the filtered product, respectively)

Illustration of creation of biofilm is depicted in Figure 4.

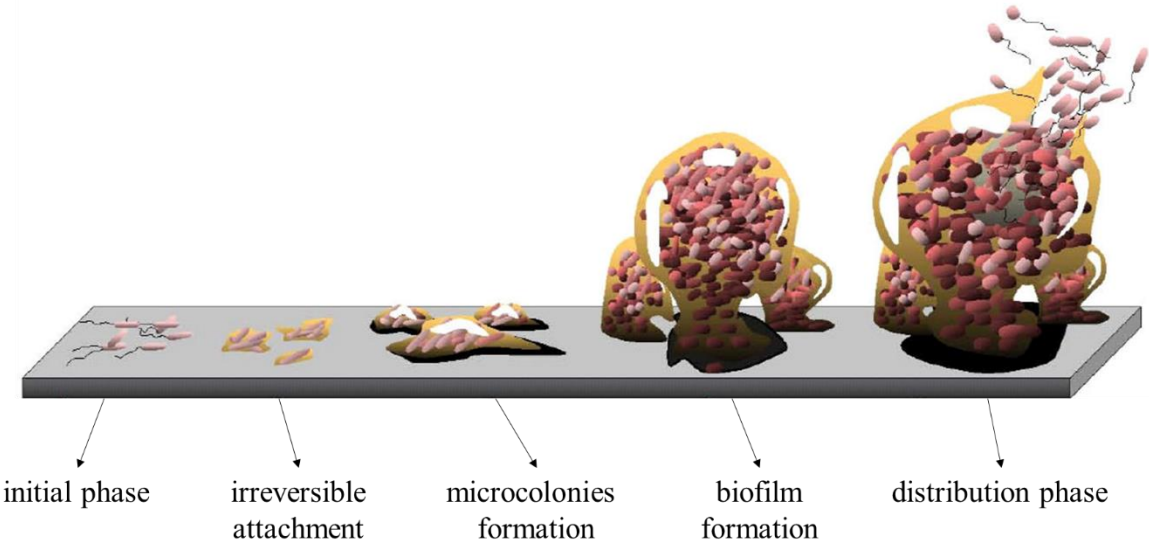

Figure 4: Biofouling process - formation of bacterial biofilm [55].

3.2.2 Filtration of milk products and biofouling of membranes

Original product entering the filtration process is always milk. Final milk products consist of high amount of bioactive and organic substances depending on species of cow and its surrounding environment. Milk products usually consist of water, lactose, fat, minerals, vitamins and salts, enzymes and of course variety of microorganisms [57]. Milk offers very favorable conditions for microbes to grow. Once the microorganism enters the milk, the number increases very rapidly. Contamination with microorganisms usually comes from outside: food, water, bedding, milker or milking apparatus, air, faeces, etc. [58]. There can be a big variety of microorganisms, some of them are pathogens, the others usually spoil the milk. The most common pathogens occurring in milk are family of *Enterobacteriaceae*, *S. aureus*, *Staphylococcus agalactiae*, *Brucella* and *Mycobacterium tuberculosis*. They usually cause diarrheal illnesses. Other types, which usually case spoiling, acid fermentation or acid production are bacteria from species of *Streptococcus* and *Lactobacillus* [4, 58].

These microorganisms present in milk cause problem named biofouling [57]. An example of biofouling on polymer membrane is depicted in Figure 5.

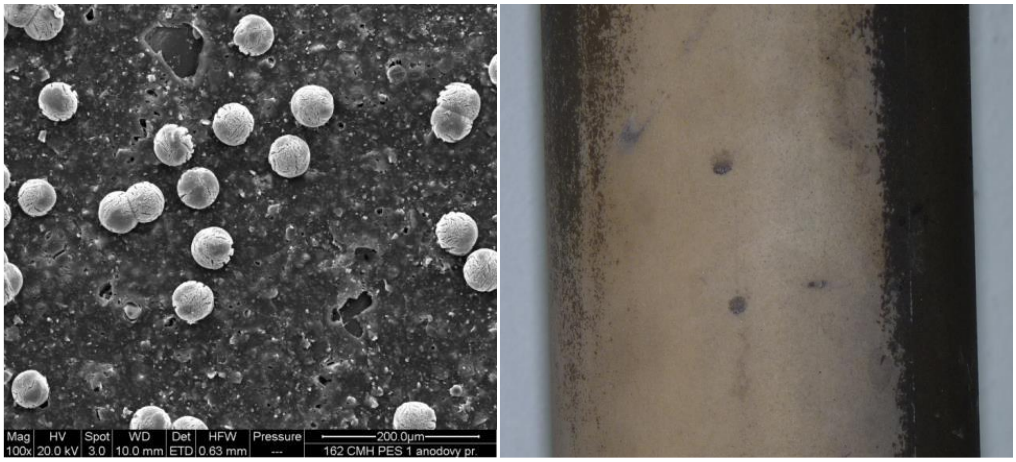

Figure 5: SEM image of polymer membrane with microbial contamination (left), photography of contaminated polymer membrane (right)[52].

Biofouling causes bigger damages unlike physical or chemical fouling. It is very difficult to clean membranes, which suffer from biofouling.They create a thin biofilm on the surface of membrane (or on every surface that milk comes to a contact) [8]. This causes a huge problem not only to membranes but also to products, which are filtrated. Very common problems are degradation and congesting of membrane, loss of filtration efficacy (usually membrane flux is reduced, which results in a higher operational costs), thus the final product suffers from poor quality [8, 59].

3.2.3 Cleaning of membranes and their prevention from contamination

Cleaning of membranes used for MPs should be periodical to preserve required quality of filtered product, to prolong the lifetime of the membrane and to prevent the membrane from congesting, especially in food industry. Membrane cleaning is provided usually when effectivity of filtration process is decreased (for example: increase of transmembrane pressure or decrease in permeate flux is observed). Unfortunately, biofouling increases the frequency of cleaning procedures [8, 59, 60].

Cleaning methods of membranes are divided into physical, chemical or mechanical [61]:

- **Mechanical cleaning** is one of the methods, where chemical compounds are not required. This is a big advantage because no chemicals are released into the permeate. This method employs various sponges or brushes to mechanically remove the dirt from the membrane. Unfortunately, sometimes this cleaning process can damage the membrane [61-64].
- **Physical cleaning** usually employs ultrasound. This cleaning process is held during operation conditions of membrane at certain frequency. This method is effective but very expensive and also pressure on membrane increases, which can cause erosion of the surface of the membrane. Thus, this method is not used very frequently in various industries [61, 63, 65].
- **Chemical cleaning** is utilized to remove compounds adsorbed on the surface of the membrane but also to clean an inner structure, where mechanical cleaning is not very effective. Chemical cleaning utilizes various cleaning mixtures and various conditions of surrounding environment (pH, duration of cleaning etc.), usually depends on laboratory. Effectivity of cleaning process is dependent on type of cleaning compounds and their concentration. In certain occasion, combination of different cleaning substances is used. If cleaning parameters are set incorrectly, properties of membrane can deteriorate or membrane can be even damaged [8, 64, 66]. Chemical cleaning can be enhanced with increased temperature. Unfortunately, there is also a study which refers to that, several microorganisms can survive the chemical cleaning, they develop a resistance against cleaning process [8, 10, 60]. Moderate conditions are usually selected for polymer membranes due to their lower chemical resistance and mechanical strength. Very important factor is also that if membrane is only dipped in the cleaning mixture or if the cleaning substance is filtrated through the membrane. Filtration through the membrane is, of course, more effective because it cleans the inner structure but it is also more expensive approach. Chemicals usually used for chemical treatment of membranes can be: alkaline (such as NaOH, KOH or NH_4OH), acidic (HCl, HNO_3, H_2SO_4), complex (ethylenediamine tetra acetic acid), oxidative (NaClO, H_2O_2, $KMnO_4$), enzymatic or surfactant. Above mentioned methods can be combined to achieve desired cleaning result (for example physical cleaning in combination with chemical cleaning) [67, 68].

Sometimes, to lower the number of cleanings, operating conditions of filtration process are adjusted (flow-rate). For example, during desalination process of whey, IEM membrane suffers from huge damage and pollution, which significantly affect not only its life time but also decreases the effectivity of MPs. Whey contains high amount of bioactive and organic compounds, which leads to often chemical and mechanical purification. Therefore, the electrical potential of MPs is often increased above limit values to achieve maximum salt transport. This approach is not very appropriate and cannot be repeated periodically because such adjustment can lead to membrane damage. In case of milk filtration, sometimes milk is treated with higher temperatures before filtration process but there are still a lot of microorganisms, which remain in the milk (sometimes multiple filtration techniques are used if required) [52].

However, new scientific researches try to avoid these invasive sanitation techniques and replace them with other non-invasive methods, which will not damage the membrane and prolong its life time and simultaneously will not change the MPs. This can be achieved by various approaches. One of them is the development a producing the membrane itself. Various admixtures and stabilizers are added to the polymer. The problem is that if the membrane should be protected properly, more stabilizers should be used at the same time. From chemical point of view, these compounds are only added to the polymers not chemically binded, thus they should have a very good compatibility with the polymer. If the compatibility of stabilizer with polymer is poor, stabilizer is released from the polymer during filtration process and contaminates the filtrate and also membrane becomes unprotected [69]. Other approach can be achieved by various modifications of membrane texture or surface, for example utilization of photocatalytic compounds [70], metal or semimetal nanoparticles with antimicrobial properties, which help to eliminate biofilm created from bacteria [53].

3.2.4 Polymer membranes for filtration of milk

The basic structure of membranes contains a binder - low density polyethylene (LDPE) and a filler - strong acidic or alkalic ionex based on styrene-divinylbenzene copolymer. The finely milled ionex provides ion conductivity of membrane. Another substance is reinforcing fabric from polystyrene (PES), which significantly affects operating limitations of membranes. The exact ratio and amount of substances of membranes is subject to corporate secret [52].

Membranes are fabricated by thermoplastic processing with maximum temperature of 160 °C and maximum pressure of 300–400 bar. Higher temperature than this maximum is not required due to limited temperature tolerance of ionex material [52].

Average working temperature for utilizing of polymer membranes is about 45 °C and pH 0–10 because of the reinforcing textile. Membranes can work only in swelled state (swelling is usually provided in deionized or in drinking water). In general, the higher is the operating temperature, the higher is the transport of salts, which is more advantageous in practical usage in most of application of membranes. For example, membranes can be used for electrodialysis process with high temperature when hot solution is processed, thus it is not necessary to cool it before procedure. Lifetime of membranes depends mostly on the type of application. The lowest lifetime of polymer membranes is usually at food industry and it is about 3 years but it can be 5–7 years for other applications. The most important parameter for any utilization is immunity to chemical cleaning in acids and alkalics. PES reinforcing fabric is sensitive to strong acids or alkalics, so the company tries to decrease concentration and usage of these materials, which is more ecologic, as well. Membranes are preferably used for water solutions without any content of solvents or organic compounds, which could decay membranes. It is recommended to store the membranes at temperature of 5–25 °C in dry, dark place [52].

Figure 6 shows swelled catex membrane. Surface of membrane is mostly smooth. Swelling causes changes in dimension of membranes and finely milled iones, thus surface becomes more structured. Swelling also causes partial crackles on the surface of the membrane, mostly in place of reinforcing textile [52].

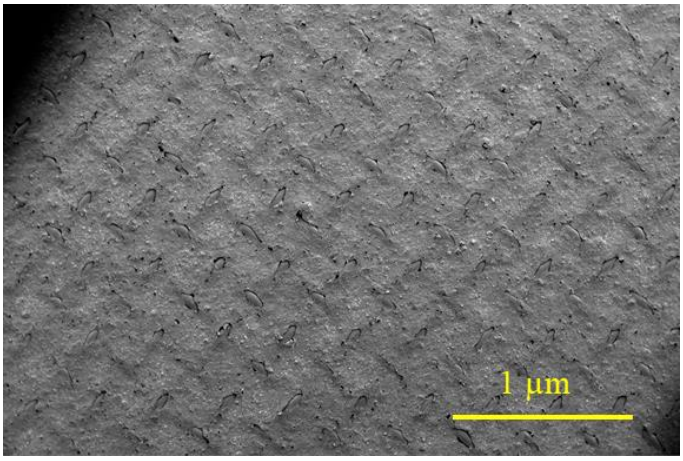

Figure 6: Catex polymer membrane in swelled state [52].

3.3 Nanoparticles as an antimicrobial agent

3.3.1 Silver nanoparticles as an antimicrobial agent

Silver was used already by ancient Greeks for treatment of ulcers, wound healing and as preservative agent for food and water. In fact, silver was very important antimicrobial material before the antibiotics were found and it is used in various areas till today [71].

Ag NPs have been widely studied during the last decade and they play an important role in nanotechnology. They evince very interesting and versatile chemical, biological and physical properties, which can be utilized in various areas of industry such as medicine, food, health care or in consumer products such as textiles. These include optical, thermal, electrical, high electrical conductivity and biological properties. One of the very interesting biological characteristics of silver and Ag NPs is its antibacterial activity. It is well known that silver is very effective against various types of bacteria and microorganisms such as *E. coli* or *S. aureus*, which can cause various diseases such as inflammatory diseases, diarrhea, etc. Thanks to these all-purpose properties they can be used in health-care related products (for example wound healing), medical device coatings, orthopedics, drug delivery, optical sensors, pharmaceutical industry, water treatment, imaging, diagnostics, anticancer drugs, clothing, cosmetics, biomedical devices or antimicrobial agents and much more [19, 72-74].

The biological activity of Ag NPs depends on their size, size distribution, shape, surface coatings, particle morphology, ion release or agglomeration. Al these factors determine their interactions and impact on final application because they significantly influence their antimicrobial activity and cytotoxicity [72]. Thus, optimization of Ag NPs synthesis is an important step to achieve desired properties such as good colloidal stability (at least 3 weeks due to experiments) and strong antimicrobial properties in order to protect polymer membrane from degradation caused by microorganisms present in milk products and whey. Size is very important because the smaller is the particle, the larger is the surface area to mass ratio, which provides greater interaction with cells or even allows the nanoparticle enter the cell [75]. Several studies revealed that shape of nanoparticles is important, as well. Asymmetric shapes show stronger antimicrobial activity probably due to the specific area that interacts with cell

[76]. The overview of various silver nanoparticles used as antimicrobial agent is summarized in the Table 2 below:

Table 2: Silver nanoparticles as antimicrobial agent (PEG - polyethylene glycol, SDS - sodium dodecyl sulphate, MIC - minimum inhibitory concentration, MBC - minimum bacterial concentration, NA - not available).

Ag NPs size and measuring method	**Ag NPs shape and measuring method**	**Chemicals for synthesis (P=precursor, R=reductant, S=stabilizer)**	**Synthesis conditions**	**Microorganisms and type of antimicrobial test**	**Ref.**
NA UV-VIS spectroscopy	NA	P: silver nitrate R: ascorbic acid S: chitosan (also reductant)	Heating in microwave oven (800 W, 4 min)	*B. subtilis*, *E. coli* MIC, MBC	[16]
NA UV-VIS spectroscopy	Spherical TEM	P: silver nitrate R: dextrose S: gelatin	Heating and stirring at 70 ºC for several h	*E. coli*, *P. aeruginosa* MIC, MBC	[20]
15 nm TEM	Spherical TEM	P: silver nitrate R: sodium borohydride	Vigorous stirring at room temperature	*E. coli* inhibition zones	[77]
5-40 nm TEM	Spherical TEM	Commercial Ag NPs	NA	*E. coli* concentration /contact testing	[78]
9-30 nm TEM	Spherical TEM	P: silver nitrate R: hydrazine hydrate S: sodium citrate or SDS or none	Stirring at room temperature	*S. aureus* MIC, inhibition zones	[35]
10-25 nm TEM	Spherical TEM	P: silver nitrate S and R: PEG	Stirring at room temperature	*S. aureus, S. typhimorium* inhibition zones	[24]
7-15 nm TEM	Spherical TEM	P: silver nitrate R: ethanol S: linoleic acid	Stirring at 70 ºC for 2 h	*S. basillus, S. aureus, P. aureginosa* inhibition zones	[79]

Zain et al. reported synthesis of Ag NPs using silver nitrate with concentration of 50 mM as a precursor of silver ions, ascorbic acid with concentration of 10 % (w/v) as a strong reducing agent and chitosan (1%, 2%, 3% w/v) as a weak reducing agent with stabilizing properties, as well. Size of Ag NPs was measured as a dependence to concentration of chitosan and was

measured by UV-VIS spectrometry. This analysis resulted in higher absorbance with increasing concentration of this agent. Antimicrobial activity of Ag NPs was proven by methods of minimum inhibitory concentration (MIC) and minimum bactericidal concentration (MBC) against *Bacillus subtilis* and *E. coli*. Antimicrobial activity of prepared Ag NPs was highly effective [16].

Mohan et al. prepared Ag NPs via green method using silver nitrate as a precursor reduced by dextrose and stabilized by gelatin. In this paper, size of Ag NPs was measured as a dependence of reaction time to absorbance measured by UV-VIS spectrometry. Aliquots were taken at different times and absorbance was measured (1 h, 5 h, 10 h, 24 h, 30 h, 40 h, 48 h). This measurement resulted as a blue-shift when reaction time increased. This indicates that with increasing reaction time, size of nanoparticles decreased. Shape of as prepared Ag NPs was confirmed as spherical by using TEM analysis. Antimicrobial study was held against Gram-negative bacteria *Pseudomonas aeruginosa* and *E. coli* using MIC and MBC methods. Efficacy of Ag NPs was compared with two controls, antibiotics ciproflaxin and imipenem. Ag NPs showed higher efficacy as these two drugs. They also reported that smaller sized nanoparticles evinced lower antimicrobial activity contrary to theory that the smaller is the silver nuclei, the higher is the antimicrobial activity. This anomaly was caused by passivation of Ag NPs by gelatin, which reduced its antimicrobial activity [20].

Yin et al. immobilized Ag NPs on thin film composite membranes to reduce biofouling. They prepared Ag NPs using silver nitrate as precursor and sodium borohydride as reducing agent. Ag NPs were immobilized via covalent bonding to thin polymer membrane (surface grafting). Ag NPs were employed to protect the membrane from bacteria *E. coli*. Membrane samples with applied Ag NPs showed inhibition zone of 5 mm whereas clear membrane without Ag NPs did not show any inhibition zone [77].

In another work, Haider et al. used commercial Ag NPs on polymer membranes for water treatment. Ag NPs were immobilized on membranes through amino groups. This study revealed that very effective antimicrobial inhibition towards bacteria *E. coli* was achieved even with low concentration of Ag NPs (6.6 % - percentage of released Ag ions). Ag ions release, which is supposed to be one of the key mechanism of Ag NPs antimicrobial activity (this will be discussed in details later in chapter 3.4.2), was effective 25 days [78].

Guzmán et al. tested antibacterial activity of Ag NPs against Gram-positive and Gram-negative bacteria of highly multiresistant strain as *S. aureus*. They prepared Ag NPs via several approaches, which resulted into Ag NPs with various sizes – silver nitrate was used as a precursor of silver ions reduced by hydrazine hydrate. Stabilization of Ag NPs was achieved by using sodium citrate or sodium dodecyl sulphate (SDS) or none of them. Antimicrobial activity was determined by MIC method and inhibition zones. Zones of inhibitions were measured after 24 h incubation at 35 °C. Presence of Ag NPs inhibited growth by 90 %. Decrease of particle´s size showed a lower susceptibility. They also determined MIC for each sample, which leads to inhibition of bacterial growth. Ag NPs were prepared via several approaches with or without stabilization (precursor silver nitrate, reductant hydrazine hydrate, stabilizer sodium citrate or without). This study also revealed that Ag NPs prepared using sodium citrate were more effective against Gram-positive and Gram-negative bacteria than NPs with no citrate stabilization layer [35].

Shameli et al. measured antibacterial activity of Ag NPs using disc diffusion method against *S. aureus* and *Salmonella typhimorium*. Polyethylene glycol (PEG) was used to stabilize Ag NPs with various stirring time during the synthesis. They found out that antibacterial activity decreased with increasing stirring time. They also tested antibacterial activity of Ag NPs and silver ions; Ag NPs were more effective in general [24].

Das et al. used Kirby-Bauer diffusion method to investigate the antibacterial activity of Ag NPs against *S. aureus*, *Staphylococcus basillus* and *Pseudimonas aureginosa*. The diameter of minimum inhibition zone was measured by ruler. Bacterial growth was inhibited more than by 97 % [79].

3.3.2 Selenium nanoparticles as an antimicrobial agent

Selenium is important semimetal trace element for antioxidation defense and reduces the redox state via specific metabolic pathways. Thus, in the last decades, Se NPs are deeply studied as promising agent for their biomedical potential. Se NPs exhibit low toxicity, degradability and high bioavailability. The major advance of Se NPs is strong ability as regulation of the reactive oxygen species which may trigger of the apoptosis and autophagy. Furthermore, the utilization of Se NPs for the anti-cancer treatment is remarkable. Due to their high stability, Se NPs can be used as nano-carriers for the anti-cancer, anti-inflammation or anti-infection treatments. As well, the Se NPs possess the benefits with therapy of arthritis, diabetes and nephropathy [80, 81].

Se NPs has also potential in suppressing the bacteria activity while directly killing them or blocking the evolution in a specific environment. This can be used for the treatment of bacteria with strong resistance to antibiotics, which is well-known issue of the last years and is predicted to be worse in the following years. Alongside the treatment of bacteria-based diseases, Se NPs can be used as a protection for liquids, which suffer from a high spread of bacteria, hence, the Se NPs are capable to stop or slow down these processes. For example, the milk-based liquids can contain *S. aureus* and *E. coli* that can proliferate at high speed, when these liquids are contaminated or improperly stored, which can be very harmful in case of ingestion. Se NPs are able to stop the biofouling process with high efficiency. Similarly to Ag NPs, the antimicrobial ability of Se NPs is influenced by many factors, such as the dimensions, shape and method of synthesis [82, 83]. Table 3 summarizes preparation procedures and utilization of Se NPs as antimicrobial agent. For instance, Guisbiers et al. published the antimicrobial effect of Se NPs prepared by pulsed laser ablation in deionized water using selenium pellets as a precursor. They employed Se NPs against *S. aureus* and *E. coli*, which are naturally present in health-care facilities, with interesting results. The ≈ 50 ppm concentrations inhibited ≈ 50 % of these pathogens within ≈ 24 h. Total inhibition was achieved in ≈ 110 h for *S. aureus* and ≈ 80 h for *E. coli*, respectively. These results underline the potential usage of Se NPs for one of the most drug-resistant pathogens [83].

Table 3: Selenium nanoparticles as antimicrobial agent (PVA - polyvinylacohol, BSA - bovine serum albumin, DLS - dynamic light scattering, NA - not available).

Se NPs size and measuring method	**Se NPs shape and measuring method**	**Chemicals for synthesis (P=precursor, R=reductant, S=stabilizer)**	**Synthesis conditions**	**Microorganisms and type of antimicrobial test**	**Ref.**
150 nm DLS	Spherical TEM	P: selenium pellets	Pulsed laser ablation	*S. aureus*, *E. coli* - inhibition of growth	[83]
50-80 nm TEM	Spherical TEM	P: sodium selenite	*In vitro* biological synthesis	*E. coli - relative mRNA expression*	[84]

NA	Rods TEM	P: sodium selenite R: ascorbic acid S: PVA	Stirring at 75 ºC for 15 min	*E. coli, S. aureus* - inhibition zones	[85]
10-50 nm TEM, DLS	Spherical TEM	P: selenium dioxide	In vitro biological synthesis	*B. cereus, E. faecalis, S. aureus, E. coli, S. typhimurium, and S. Enteritidis* - MIC	[86]
75-300 nm DLS	Spherical SEM	P: sodium selenite R: glucose, ascorbic acid S: chitosan, BSA	Stirring and heating	Gram- positive and Gram-negative bacteria strains - MIC	[87]
40-200 nm TEM	Spherical TEM	P: selenium dioxide R: sodium thiosulfate S: PVA	Stirring at room temperature	*S. aureus* - growth curves, MIC	[88]

Xu et al. found out that probiotic bacteria such as *Lactobacillus casei* can transform sodium selenite to Se NPs under driven conditions directly in organism intestine which have positive influence on digestion and other health benefits. One of the observed phenomena was the protection against *E. Coli* as a prevention from intestinal barrier function damage [84].

Other purpose of Se NPs is enhancement of wound dressing. Ahmed et al. published promising results of antimicrobial activity of Se NPs prepared by green method. Se NPs were prepared by using sodium selenite as a precursor reduced by ascorbic acid and stabilized with PVA. They demonstrated significant antimicrobial activity of wound dressing based on chitosan/polyvinyl alcohol film loaded with Se NPS against *S. aureus* and *E. coli*. These biopolymeric films are potentially promising for clinical applications such as faster wound healing in near future [85].

Ghada et al. prepared Se NPs by biosynthesis using *Bacillus licheniformis* and selenium dioxide as a precursor. Size of Se NPs was 10-50 nm and shape was spherical, both determined by TEM and DLS. They utilized as prepared Se NPs to inhibit the creation of biofilms against several foodborne pathogens such as *Bacillus cereus, Enterococcus faecalis, S. aureus, E. coli, Salmonella typhimurium,* and *Salmonella enteritidis.* Se NPs with concentration of 20 μg/ml were effective against growth of almost all strains except *B. cereus*, where higher concentration of Se NPs was required to stop the growth of the cell culture (75 μg/ml) [86].

Filipovic et al. examined antimicrobial activity of Se NPs with different coatings. They found that properties such as particle form, size and surface chemistry are crucial to determine the interaction with biological entities. They prepared three different samples, where sodium selenite was used as a precursor. First sample was stabilized with BSA, second sample was stabilized with chitosan, both reduced by ascorbic acid. Third sample was without stabilization compound, only reduced by glucose. They tested as prepared Se NPs against Gram-positive bacteria (*S. aureus, Enterococcus faecalis, Bacillus subtilis*, and *Kocuria rhizophila)* and also against Gram-negative bacteria (*E. coli, Salmonella abony, Klebsiella pneumoniae*, and *Pseudomonas aeruginosa*). Size of nanoparticles ranged from 70 nm to 300 nm determined by DLS. They provided results where efficacy of antimicrobial activity of Se NPs was higher against Gram-positive bacteria than against Gram-negative bacteria. They also found out that

positively charged Se NPs evince higher antimicrobial activity. The most sensitive to Se NPs was strain *Candida albicans* with MIC of 25 μg/mL [87].

Huang et. al. presented size control synthesis of Se NPs in their work. They prepared Se NPs via chemical reduction. Size of Se NPs varied from 40 nm to 200 nm. They reported that Se NPs with size of 80 nm have the strongest antimicrobial effect on *S. aureus* but they do not cause any damage to mammalian cells [88].

From the previous statements and examples, it is clear that the Se NPs are very competitive material to other inorganic materials such as Ag, Au, Zn, etc. in many fields of biomedicine. All things considered, the synthesis of Se NPs is also important parameter for the future utilization. It must be cheap, effective and well-controllable to keep the competitive, safe and sustainable by design character of Se NPs.

3.3.3 Synthesis of silver and selenium nanoparticles

In general, physical and chemical properties of nanoparticles NPs) are highly dependent on their shape, size and surface coatings [87]. A big potential lies in a possibility to prepare a nanoparticle with desired properties for exact application. These properties of nanoparticles can be tailored during their synthesis. NPs can be synthetized by both top-down and bottom-up methods.

- **The top-down** methods involve mechanical grinding of bulk metals followed by stabilization of resulted NPs.
- **The bottom-up** methods are the opposite; they include reduction of metals. There are two approaches how NPs can be prepared, either physical or chemical.

Physical route usually utilizes methods such as evaporation/condensation or laser ablation [89, 90]. Chemical routes are based on reduction of metal ions in solution to form small clusters. Chemical procedures can be also subdivided into several ways; classical, radiation chemical and biological or green approaches. The first one uses classic reducing agents, the second one uses a reduction process beginning from solvated electrons generated by the ionizing radiation [17, 19]. Biological methods utilize extracts of plants, fungus or microorganisms such as bacteria [19]. Green syntheses employ non-toxic substances. After the preparation of NPs, there are also some methods how to contribute to the better stability; usually via steric and electrostatic approaches. Steric stabilization is gained by the presence of bulk organic materials, for example polymers and large cations that impede the aggregation of particles. Electrostatic approach coordinates anionic species to metal particles. The result is the formation of electrical double layer (practically a diffuse electrical multilayer), which initiates electric repulsion among nanoparticles, thus impede merging of them [18, 19, 91].

In this thesis, wet chemical approach was selected for both cases of NPs (Ag and Se) because it is fast, easy and reproducible method and by setting appropriate conditions such as concentration of substances, temperature, radiation, etc. NPs with desired properties can be prepared.

3.3.4 Mechanism of antimicrobial effect of silver and selenium nanoparticles

Mechanism of Ag NPs and Se NPs antimicrobial activity is still not very well known and has not been completely explained yet. However, there are few theories and they all have in common few facts. It is believed that the mechanism of interaction with microbial cell is driven mostly from their design, i.e. size, shape, pH, ionic strength and capping medium. The first important fact is how the nanoparticle interacts with the cell and the second how it behaves

inside the cell. Scientific papers mostly mention the five following actions [92-94], which are illustrated in Figure 7:

- adhesion on the surface of the bacterial cell wall and membrane,
- penetration into the cell via several options such as phagocytosis, simple diffusion, facilitated diffusion, micropinocytosis, clathrin-mediated endocytosis and caveolae-mediated endocytosis,
- disruption of intracellular organelles and biomolecules,
- induction of oxidative stress,
- and modulation of signal transduction pathways.

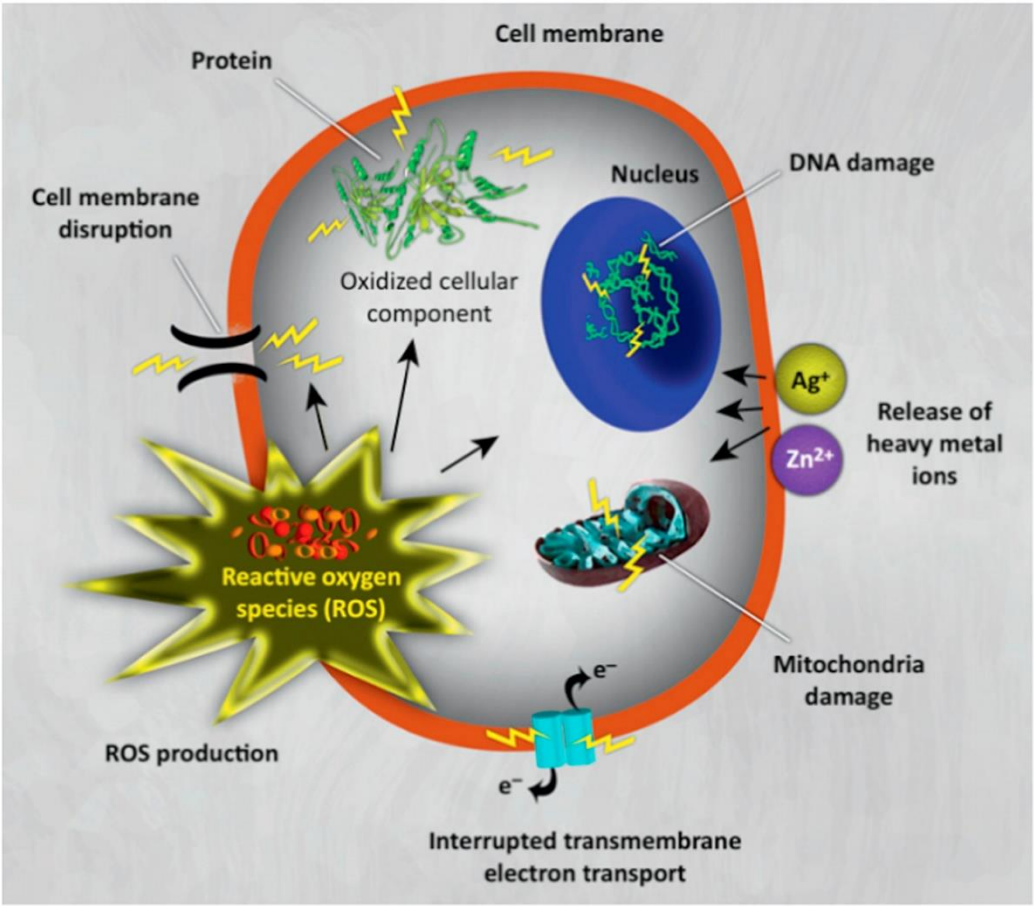

Figure 7: Mechanism of antimicrobial effect of metal nanoparticles [56].

Ag NPs and Se NPs interact with cells very similarly. The only difference is that Ag NPs release silver ions, thus, Ag NPs and also silver ions interact together with a cell. Ag ions interact mostly with nucleic acids and nucleosides.

Some researchers revealed that the Ag NPs and Se NPs can be attracted to cell via electrostatic forces. Due to electrostatic forces and their affinity to iron-sulfur proteins, Ag NPs and Ag ions, as well as the Se NPs can adhere to the cell wall or cytoplasm, which significantly changes the permeability of the cell wall. Consequently, they change the cell membrane arrangements, thus nanoparticles can penetrate through the cell wall or cause the disruption of cell wall. When the nanoparticles enter the inner space of the wall, it negatively affects the respiratory enzymes leading to creation of reactive oxygen species (ROS) and it also interrupts the release of adenosine triphosphate (ATP). ROS could be crucial to affect deoxyribonucleic acid (DNA). When nanoparticles interact with DNA via phosphorus and iron-sulfur, it can lead to changes such as DNA replication, propagation, and DNA damage. Additionally, these nanoparticles

probably impede also the synthesis of proteins. Ag NPs and Se NPs can cause a rupture of some organelles, subsequently followed by their lysis. These nanoparticles also interact with thiol groups with many vital enzymes and inactivate them. All these mentioned actions can cause the cell death [18, 75, 95-99].

3.3.5 Antimicrobial tests

In recent years, many new antimicrobial agents were developed to fight against antimicrobial resistance. Therefore, laboratories test the antimicrobial properties of these compounds to determine their effectivity against various types of microorganisms. There is a wide range of methods that can evaluate or screen the antimicrobial activity from dilution methods to rapid automated instrument methods. Manual methods provide high flexibility, they are fast and cheaper than fully automated testing. Some methods provide quantitative results but all of them can provide qualitative data such as susceptibility or resistance [100, 101]. The most known and basic methods are the disk-diffusion and broth or agar dilution methods, which are further described in the following subchapters. Growth curve test (sometimes called time-kill test or time-kill curve) is another strong tool for obtaining information about the dynamic interaction between the antimicrobial agent and the microbial strain and belongs among the most appropriate methods for determining the bactericidal or fungicidal effect [100, 102]. These methods usually utilize Mueller-Hinton agar (MH agar) or Mueller Hinton-Broth (MH broth) as a culture medium. Their composition is usually the same (beef extract, acid hydrolysate of casein, starch), the only difference is that MH agar containing solidifying agent, which causes the medium to solidify in room temperature. MH broth does not contain this substance and it remains in liquid form [103].

3.3.5.1 Diffusion methods

Diffusion methods are qualitative methods, where can be determined susceptibility of resistance of bacteria to active substance (in diagnosis it usually antibiotics, in this thesis the active substances are NPs). Principle of diffusion methods lies in diffusion of active substance into agar with previously inoculated culture. If the growth of culture is suppressed, so called inhibition zones occur. These zones are measured in mm and compared to reference values (in diagnostics usually guidelines, in scientific paper compared to most used antibiotics against chosen bacterial culture) [100, 104].

One of the most frequently used is agar disk-diffusion method. This method is also known as Kirby-Bauer test or sensitivity test. Usually, in diagnostics, it is used to determine the susceptibility of bacteria to antibiotics [105]. In scientific papers, this method can be used for determination of susceptibility for example to nanoparticles. Principle of this method is, that in the first step is prepared agar in Petri dish, after that agar is inoculated with culture (for example bacteria, yeast, etc.). It is important that agar medium should be appropriately enriched to support the culture growth. In the second step, filter paper disks containing the tested compound with desired concentration are placed on the agar surface (in diagnostics discs contain usually antibiotics, in scientific papers it can be colloidal solution of NPs) [24, 100, 106]. In the last step, as prepared Petri dish is incubated under suitable conditions to support the growth of the culture. [101]. This method is widely used because it is fast, cheap and reliable and it is possible to test a lot of samples at the same time [105]. Scheme of this method is depicted in Figure 8.

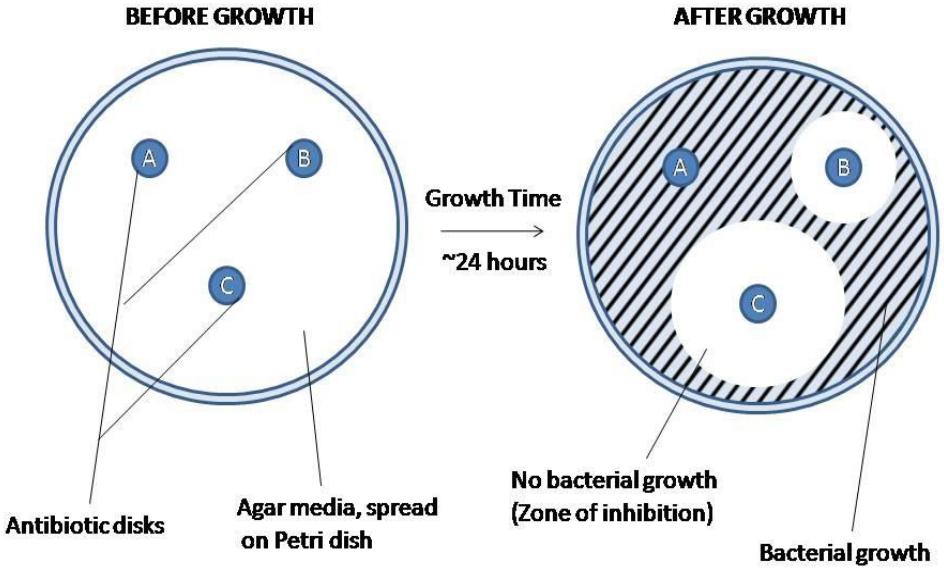

Figure 8: Schematic illustration of disk diffusion-method and inhibition zones [107].

Another diffusion method is agar-well diffusion method. Agar-well diffusion method is very similar to disk diffusion method but instead of paper disks with active antimicrobial substance, there are holes made in the agar [108]. At first, agar is inoculated with chosen bacterial suspension and put in the Petri dish. After that, holes are made in the agar (some suppliers can provide agar with already prepared holes). Subsequently active substance is pippeted into the holes. Then, the procedure is same as in the previous case. Petri dish with agar, culture and active substance are incubated at desired temperature to promote the growth of the culture. Active substance should be able to diffuse into the agar and stop the culture from growing, thus create inhibition zones, which are measured in mm. This method is depicted in Figure 9 [101, 109].

In this thesis, both methods were tested to determine the antimicrobial activity of Se NPs and Ag NPs.

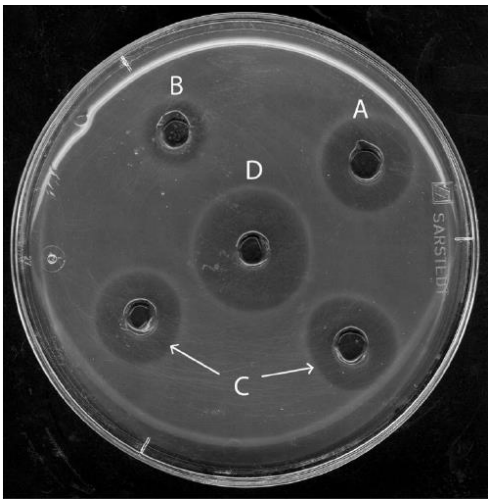

Figure 9: Agar-well diffusion method [110].

3.3.5.2 Dilution methods

Dilution methods are quantitative. They are used to determine the MIC or MBC. MIC is a minimal concentration of active substance (antibiotics or nanoparticles), which can stop the

growth of the culture. MBC is the minimum concentration of active substance, which suppress the growth of 99.9 % of the culture. Accuracy of dilution methods are higher than accuracy of diffusion methods. Principle of this method is that active substance is diluted to desired concentration (ideally in geometric order) and mixed with the fluid agar and with the culture. Following step is cultivation at desired temperature to support the growth of the culture. Growth of the culture is represented by turbidity of the mixture. If the growth of the culture was suppressed by the active substance, the mixture should remain clear. Final results can be read by spectroscopy measurement or cultivation of the aliquots on the agar plates subsequently followed by counting of the colonies, so called colony forming units (CFU) [100, 104, 109].

There are two types of dilution methods - micro and macro dilution methods. The only difference between them is the volume of the substances. As is obvious from the title micro dilution methods are provided in smaller volumes, usually on 96-well plates. Macro dilution methods are provided in test tubes. Usually, micro dilution method is used - because of less volume and it is also faster when it is made on 96-well plates but, of course, it depends on the incoming volume of the sample and on final application [100, 101]. An example of macro dilution method is shown in Figure 10.

In this thesis macro dilution method was used. Higher volume was needed because the sample of the polymer membrane with immobilized nanoparticles needed to be fully immersed in the medium.

Figure 10: Example of the macro dilution method - turbidity of the grown cultures are visible in first three vessels, fourth vessel is clear, thus without grown culture [111].

3.3.5.3 Growth curves

Another method that can help to determine the antimicrobial activity of NPs is measurement of growth curves or also call time-kill test [101]. Bacterial culture is diluted to desired concentration, as well as the active compound. Then active compound is added to the culture and incubated at appropriate conditions. In the end, results can be read by spectrometry.

In general, bacterial growth is described as a proliferation of bacterial cells starting as binary fission of one cell. Growth curve can provide several information. At first, it gives an information about the growth of population, when a given number of cells is placed into an appropriate environment and receive nutrients. Thus, the cells increase their mass and volume. Growth curve provides also information about multiplication of the culture. Growth of the

population is caused by multiple binary division of individual cells [112]. Growth curve depicted in Figure 11 has following phases [113]:

1. **Lag phase** - population is adapting to a new environment. In this phase, cells, which could not adapt to the new environment, die. Cells produce enzymes, proteins, and other substances, which are required for their further splitting. Thus, metabolic activity is increasing. In this phase, cells are maturing and usually do not multiply.
2. **Accelerated growth** - cells are fully adapted to the new environment. In the end of this phase, they metabolize very quickly and their division is in progress.
3. **Exponential phase** - cells multiply and grow very rapidly, in this phase. Population grows exponentially. This phase is limited by the amount of nutrients supporting the growth.
4. **Slow growth** - the speed of growth slows down. The amount of dying cells is increasing. Nutrients are nearly consumed.
5. **Stationary phase** - speed of multiplication of cells is decreased, state of equilibrium occurs, when the number of cells is not changing. Accumulation of metabolites start and nutrients are fully consumed.
6. **Death phase** - number of dead cells is higher than a number of new cells. The total number of cells may decrease.

Thus, to apply this procedure to determine the antimicrobial activity of NPs, there is a control of bacterial culture compared to the same bacterial culture with applied NPs with various concentrations, where individual growths are discussed.

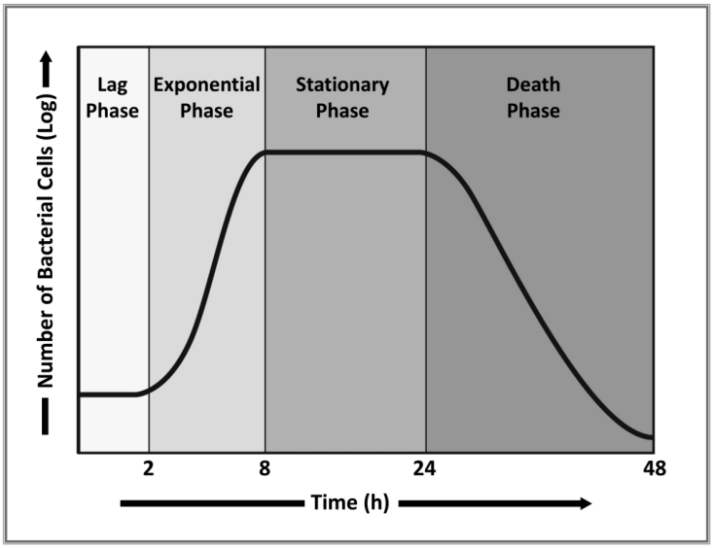

Figure 11: Growth curve phases [114].

3.3.6 Cytotoxicity assays

For every type of NPs being used in practice, it is extremely important to determine its safety. Although some types of NPs are widely used in various industries (such as Ag NPs in cosmetics, etc.), the Scientific Committee on Consumer Safety (SCCS) has identified certain aspects of nanomaterials that constitute a basis for concern over safety to consumers' health (when used in cosmetic products) [115]. These include:

- **Physicochemical aspects** - these are related to a very small dimensions of the components of particles, solubility and persistence, chemical structure and toxicity, physical and morphological properties, surface chemistry and surface functionalization,

- **Exposure aspects** - these are related to the frequency and the amount that is utilized, whether the amount of consumed product is high and if it can cause a potential accumulation in the body,
- **Other aspects** - these are related to new properties, activity and function and also specific concern arising from the type of application.

The evaluation of the final impact of nanoparticles on living organisms and environment is no less important and unfortunately still not very well known, since the nanoparticles are subject to chemical and physical transformation processes. The toxicity of nanoparticles presented in the environment is influenced by these "aging" transformations with relation to environmental conditions and nanoparticles properties. As mentioned above, Ag NPs are being already incorporated into commercial products as antimicrobial agents, which potentiate their emission to the environment. The toxicity of Ag NPs has been associated with the release of Ag ions (Ag^+), which are more toxic to aquatic organisms than Ag NP. In addition, some studies already showed that soil represents yet another important environmental compartment that can be regarded as a final sink for metal nanoparticles including Ag NPs [116-118].

Cytotoxicity describes how a specific compound is toxic to cells that are exposed to antimicrobial material. Cytotoxic effect can appear in different ways such as [119, 120]:

- change in cell morphology (damage or destruction of cell membrane),
- stopping the growth and dividing (decreased cell viability),
- suppression of the synthesis of proteins,
- or even cause cell death (necrosis, apoptosis, cell lysis).

Thus, cytotoxicity or viability assays are based on various cell functions. There are a lot of cytotoxicity and viability assays that can be provided. These assays are usually utilized to determine whether the tested compound have an impact on proliferation of cells or if their effect is directly cytotoxic.

Probably the most used assays are colorimetric assays. They are fast, cheap and reliable. Principle of these tests is to evaluate metabolic activity of cells. Compounds, which are utilized in these assays develop a color response and can be measured by spectroscopy [121-123].

An example of this test is MTT assay (3-(4,5-dimethylthiazol-2-yl)-2–5-diphenyltetrazolium bromide). Both, cytotoxicity or cell viability can be determined by this test. Principle lies in that NADH causes reduction of dye MTT to insoluble purple formazan. This final product is then measured by UV-VIS absorbance at a specific wavelength. At first, a detergent that dissolves formazan should be added to easily provide optical measurement. Thus, the cell viability is given by mitochondrial function of cells (activity of mitochondrial enzyme oxidoreductase) [121]. Another colorimetric test very similar to MTT assay is XTT assay (2,3-bis-(2-methoxy-4-nitro-5-sulfophenyl)-2H-tetrazolium-5-carboxanilide). XTT can be used for determination of cell viability of cytotoxicity, as well as MTT assay. However, XTT provides higher sensitivity and final product (orange-colored formazan) is soluble in water, thus, the step with dissolution of formazan is skipped. Another very popular colorimetric assay is BrdU cell proliferation assay (5-bromo-2-deoxyuridine). It detects changes in the number of cells in a division or changes in a cell population. Principle of this method lies in that BrdU is a thymidine analogue and it is incorporated to the cells of DNA synthetic phase. It is a label that can be tracked by antibodies. Results can be read by spectroscopy [121, 124].

All assays mentioned in this chapter were utilized to determine cytotoxicity of prepared Ag NPs and Se NPs. They are fast, cheap and reproducible and can provide solid information about toxicity of prepared NPs.

3.4 Immobilization of nanoparticles on polymers

As described above, one of the biggest problems of polymer membranes is biofouling. It is a process when several bacteria create a biofilm on a membrane and cause damages of the polymer material. Few approaches have been reported how to prevent the polymer from biofouling [125, 126]. In this thesis, NPs haven been chosen as auspicious antimicrobial agents. There are several ways how NPs can be immobilized on polymers to solve the biofouling problem [94].

One of the very promising option is plasma treatment of polymers and subsequent immobilization of NPs on the surface without using any aggressive chemical compounds [127, 128]. Various properties of polymers can be modified by utilization of plasma treatment, such as: wettability, surface energy, hydrophobicity or hydrophilicity, chemical inertness, surface morphology - increase or decrease surface crystallinity and roughness, surface electrical conductivity, surface lubricity and dyeability [127, 129].

Plasma modification usually possess low exposure time (from 5 s to 5 min.). Recently, this approach has been reported as a very successful way how to modify polymers [130, 131]. Plasma treatment is capable to alter the surface physical and chemical properties of polymer without changing the bulk properties. In general, plasma modification is utilized to change the surface chemistry of polymer in order to create new functional groups on the surface of the polymer [132]. Plasma treatment of polymer with various gas types (for example oxygen, nitrogen or ammonia plasma) change the surface energy of polymer and highly reactive species stable in vacuum are created. When these reactive species are exposed to various monomers, they create new surface functional groups such as amine, carboxyl or sulfonate [56, 127, 129]. Thus, by choosing a type of monomer, desired functionalities can be incorporated to the surface of the polymer [11].

Subsequently, various materials, such as NPs (or other compounds) can be immobilized via these functional groups [133-135]. Often an etch-step is performed prior to a deposition process, in order to remove weak boundary layers [136], and to produce radical sites on the surface, onto which the intended coating will be chemically bonded. Commonly used gases for polymers plasma treatment are argon, nitrogen, oxygen, ammonia, hydrogen, water, nitrogen dioxide, carbon dioxide and carbon monoxide [127].

There are few factors, which have impact on efficiency of the whole process: polymer type, plasma type (e.g. gas type), plasma energy, pressure, concentration of monomer, flow rate, and treatment time [132].

The biggest advantages of plasma treatment include following [127]:

1. Plasma treatment does not influence the bulk properties of the polymers.
2. By choosing a type of gas, it is possible to create desired type of chemical modification of polymer surface.
3. Plasma treatment does not require wet chemical techniques; thus, polymers are prevented from swelling and chemical solvents.
4. Plasma treatment provides uniform modification of polymer surface.

There are also some disadvantages that plasma treatment brings [127]:

1. Plasma treatment must be carried out in vacuum, which increases the cost of the whole process.
2. There is no uniform process of plasma treatment for all types of polymers. Parameters of experiment are usually developed for every sample and cannot be adopted for other sample.

3. It is very difficult to affect the amount of functional groups created on the polymer surface.

When plasma treatment of polymers is utilized, there are few ongoing surface reactions: reactions between surface species and reactions between gas molecules and surface species, cross-linking or degradation [129, 137].

These reactions can be used to achieve various purposes such as [11, 127]:

1. **Plasma polymerization** is driven by polymerization of an organic monomer in plasma (for example CH_4, C_3F) to prolong the main chain of the polymer.
2. **Cleaning and etching** are achieved usually by utilization of oxygen and fluorine containing plasmas resulting in removal of various materials from the surface of polymer forming volatile compounds. Oxygen containing plasma removes organic contamination. The difference between cleaning and etching by plasma treatment lies in the amount of materials that are removed from surface (etching usually provides reaction deeper in the polymer).
3. **Graft polymerization** is a process when various monomers are added and polymerized to create side polymer chains. Grafting density and length of grafted chains can be controlled by plasma parameters including power, pressure and sample disposition, and polymerization conditions such as monomer concentration and grafting time.

Many publications have been dedicated to plasma treatment of polymer with subsequent immobilization of various types of NPs to provide antimicrobial properties [53, 128].

Jiang et al. worked on immobilization of Ag NPs via aldehyde functionalized silicone rubber, stainless steel and paper surfaces. Formaldehyde groups were incorporated using radio frequency-plasma treatment on all types of substrates. Ag NPs were deposited after plasma treatment via Tollen´s method. They used SEM, atomic force microscopy (AFM) and XRD to investigate and confirm the presence of Ag NPs layer. Aldehyde functional groups were deposited via plasma treatment as follows: base pressure $\approx$ 6.7 Pa, formaldehyde pressure of $\approx$ 19.9 Pa, plasma $\approx$ 33.3 Pa, RF power of 50-150 W, reaction time from 5 s to 2 min, temperature of 170 ºC. Antimicrobial activity of as prepared samples was tested against *Listeria monocytogenes*. These surfaces were exhibited to microbial culture for 24 h. No viable bacteria were detected after 18 and 24 h [138].

Airoudj et al. demonstrated a method for Ag NPs immobilization on cotton fabrics. At first, cotton fabric was functionalized by with maleic anhydride plasma treatment at the pressure of 0.2 mbar and flow rate approximately 1.610^{-9} kg s^{-1}. The power of generator was 30 W. They investigated different deposition times to obtain a thickness of 30 nm. After that, Ag NPs were immobilized by wet chemical reaction. Samples of cotton fabrics were immersed in deionized water for hydrolysis to create carboxylic acid groups and subsequently silver nitrate with concentration of 50 ppm was added to attach the silver ions. Subsequently, Na BH_4 was added for reduction of silver ions to Ag NPs. Surface changes were analyzed by various methods such as SEM and XPS. Presence of Ag NPs was confirmed by UV-VIS spectroscopy and AFM analyses. Size of Ag NPs varied from 5 to 34 nm. Antimicrobial activity of these samples was tested against *E. coli* strain. Cotton samples with immobilized Ag NPs successfully inhibited the growth of bacteria [139].

Hosseini et al. reported on immobilization of Ag NPs on argon plasma treated styrene-butadiene-rubber cation exchange membrane. They investigated the duration of plasma treatment on distribution uniformity of Ag NPs. This experiment resulted in highly uniform distribution of Ag NPs on the membrane sample. They also found out that properties of membrane such as electrical conductivity, flux, current efficiency and ionic permeability were

enhanced with the increasing thickness of Ag NPs layer. Energy consumption of flow process decreased [140].

In this thesis, Ag NPs or Se NPs were immobilized on polymer membrane as a prevention from biofouling. Low-pressure plasma with polymerization of cyclopropylamine (CPA) and reactive ion etching (RIE) with ammonia plasma were used to incorporate amine functional groups on polymer membranes. These functional groups enabled further immobilization of both types of NPs (see Figure 12). Ag NPs prepared in this work were stabilized with sodium citrate. Sodium citrate has three carboxylic acid functional groups, which have solid reactivity with amine groups [141, 142]. Se NPs were stabilized with polyvinylpyrrolidone (PVP). This compound has an amide ring with carbonyl group, which has good reactivity with amine groups, as well [143].

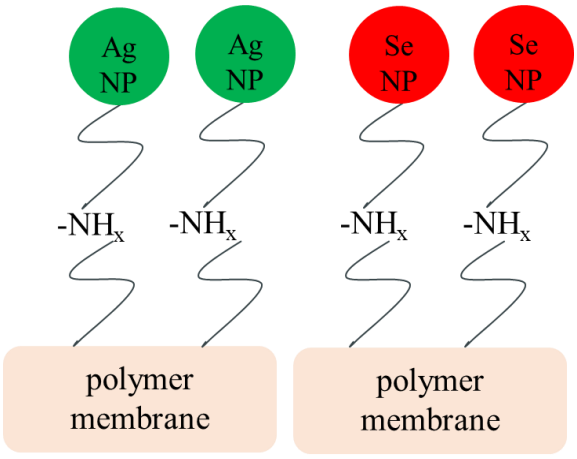

Figure 12: Polymer membrane with immobilized Ag NPs and Se NPs.

4 Experimental

4.1 Characterization methods

Various tests and methods were used to prepare the samples and determine their physical and biological properties of NPs (Ag and Se) and membranes with immobilized NPs. These methods are listed below in this chapter.

4.1.1 Morphology

Following methods were used to determine the morphology of prepared Ag NPs and Se NPs - mostly size (size distribution), shape and agglomeration.

Se NPs and Ag NPs were characterized by scanning electron microscopy (SEM) on Tescan FE MIRA II. In order to provide SEM analysis samples were drop-coated on a pieces of Si wafer covered with Ti thin film to avoid surface sample charging and dried at ambient temperature of 22 °C. Se NPs samples were also characterized by SEM in transmission electron microscopy (TEM)-mode (STEM) on high resolution scanning electron microscope FEI Verios 460L with an accelerating voltage of 30 kV. Sample were prepared as follows: 10 µl of Se NPs solution was drop-coated on carbon membrane for STEM/TEM analysis and dried at room temperature of 22 °C. TEM was provided on JEM 2100F (Schottky cathode, using a 200 kV electron beam).

One Se NPs sample was also additionally analyzed by Small angle X-ray scattering (SAXS) and ultra-small angle X-ray scattering (USAXS) methods to determine the average mean size of Se NPs. Experiment was performed on X-ray diffractometer (SmartLab, Rigaku) equipped with two bounce Ge (220) crystal monochromator and analyzer in high resolution setup (USAXS curves) and with pinhole collimation and 2D detector in low resolution high intensity setup (SAXS curves). This measurement was provided in cooperation with Mgr. Ondřej Caha, Ph.D.

4.1.2 Optical properties

UV-VIS spectroscopy (absorbance) was measured on Spectronic Helios Alfa spectrophotometer at Faculty of Chemistry, BUT. To purify Ag NPs centrifuge MiniSpin plus® was used. This measurement was also utilized the long-term colloidal stability of as prepared samples - samples, which formed agglomerates visibly seen at the bottom of the vessel were no longer used for this measurement.

4.1.3 Antimicrobial properties

Antimicrobial tests of NPs and polymer membranes with immobilized NPs were provided in cooperation with Mgr. Kristýna Šmerková, Ph.D. at the Mendel University. Several tests were performed, namely disk-diffusion method, MIC, measurement of growth curves, dilution method and macro dilution method. Cell cultures were incubated in Thermo-Shaker PST-60HL-4. Spectroscopy measurements were provided on Multiscan and TECAN Infinite.

4.1.4 Cytotoxicity assays

Cytotoxicity assays were provided in cooperation with Mgr. Zdenka Fohlerová, Ph.D. at BUT, Faculty of biomedical engineering. Qualitative MTT assay was provided to determine the cytotoxicity of Ag NPs. Qualitative XTT assay and quantitative BrdU proliferation assay were provided to determine the cytotoxicity of Se NPs. All these assays were provided in several repetitions for statistical analysis on 96-well plate. Final absorbance was measured on a microplate spectrophotometer Beckman Coulter Paradigm.

4.1.5 Plasma treatment of polymers

Part of the experiments was provided in cooperation with Mgr. Miroslav Michlíček, Ph.D. and Dr. Anton Manakhov from a team of doc. Mgr. Lenka Zajíčková, Ph.D. Deposition of amine groups was provided by low-pressure plasma treatment in a stainless-steel parallel plate reactor.

Second type of experiments were provided in CEITEC Nano Clean rooms (ISO 100) on instrument PlasmaPro 80 by Oxford.

4.2 Synthesis of silver nanoparticles

In this thesis, several approaches were employed to prepare Ag NPs. Ag NPs were synthetized via wet chemical reduction under different conditions such as temperature, duration of reaction, different stabilizers, concentration of reagents or irradiation of reaction mixture with UV light. All samples of Ag NPs were stored in the fridge at the temperature of 5 ºC in the dark vessel.

4.2.1 Chitosan-reduced silver nanoparticles

Chitosan is well known for its antimicrobial properties and is effective against Gram-positive and also Gram-negative bacteria (for example *S. aureus* or *E. coli*). Chitosan is also non-toxic to human body and can act not only as a reducing agent but also as a stabilizer. This synthesis was prepared according to article published by Tran et al. [144].

- *Materials:*

Silver nitrate (p.a., 99.5 %, PENTA), chitosan medium molecular weight (p.a., Sigma-Aldrich (p.a., deacetylation degree 75–85 %), acetic acid (p.a., 99.8 %. PENTA), deionized water (Millipore). All materials were used as purchased without further purification. All substances were diluted to aqueous solutions using deionized water (resistivity of 18.2 MΩ·cm, Milli-Q®). Final colloidal solutions were purified by centrifugation at 14 500 rpm 3x after synthesis (duration of each cleaning cycle was 30 min).

- *Method:*

Chitosan was dissolved in acetic acid aqueous solution (acetic acid was previously diluted with deionized water to concentration of 0.5 M) to obtain the concentration of 1 %. The dissolving process was kept at 65 °C for 12 h under moderate stirring on magnetic stirrer (200 rpm). The crucial step of the synthesis was to heat up 150 ml of 1 % chitosan solution to 95 °C and add dropwise 60 ml of solution of silver nitrate with concentration of 7 mM. The reaction was held under these conditions for 12 h. Color of the mixture changed into dark red in 5 min from adding the silver precursor into reducing agent, which pointed to the creation of Ag NPs. The sample prepared by this method is denoted as 1A**.** Value of pH of final colloidal solution was ≈ 6.18.

4.2.2 Glucose-reduced silver nanoparticles

Another green approach was tested. This synthesis was based on using of sugar as a reductant and PEG as stabilizing agent. The preparation method was modified according to work published by Shameli et al. [24]. PEG can act not only as a stabilizer but also as a reducing substance. PEG is non-toxic, evinces high biocompatibility with wide range of materials or organisms and proves excellent solubility in aqueous medium. Thus, PEG is frequently used in food industry. It is believed that the longer is the polymer chain, the higher is the reducing activity of PEG [145]. This synthesis was modified by adding the sodium citrate to the reaction mixture to enhance the reducing effect of sugar because no color change of the reaction mixture was observed, which usually points to creation of Ag NPs.

- *Materials:*

Silver nitrate (p.a., 99.5 %, PENTA), polyethylene glycol 4 000 (p.a., Sigma-Aldrich), glucose (D-(+)-Glucose monohydrate, p.a., MERCK), sodium citrate dihydrate (p.a., Sigma-Aldrich), deionized water (resistivity of 18.2 MΩ·cm, Milli-Q®). All materials were used as purchased without further purification. All substances were diluted to aqueous solutions using deionized water. Final solutions of colloidal nanoparticles were purified 3x after synthesis by centrifugation at 14 500 rpm (duration of each cleaning cycle was 30 min).

- *Method:*

Two samples were prepared via this method, namely 2A and 2B:

Synthesis of sample 2A: At first aqueous solution of all reagents were prepared as follows: 10 ml of silver nitrate with concentration of 1M, 20 ml of glucose with concentration of 1 M, 200 ml PEG with concentration of 0.1 % and 10 ml of sodium citrate with concentration of 1 M. At first silver nitrate was mixed with PEG solution. Subsequently, glucose solution was added into the mixture under vigorous stirring at 500 rpm for 5 min. Then, 60 ml of this mixture was transferred to a new beaker and heated at constant temperature of 60 °C in the dark for 3 h. Afterwards, the sample 2A was cooled naturally at room temperature for 1 h. The color of the sample 2A changed into dark green in 5 min from adding the solution of sodium citrate to the reaction mixture. Final pH of colloidal solution was ≈ 6.23.

Synthesis of sample 2B: In the first step, aqueous solutions of all reagents were prepared as follows: 10 ml of silver nitrate with concentration of 1M, 20 ml of glucose with concentration of 1 M, 200 ml PEG with concentration of 0.1 % and 10 ml of sodium citrate with concentration of 1 mM. PEG and silver nitrate were mixed together under vigorous stirring at 500 rpm for 5 min. Afterwards, 60 ml of this mixture was placed into a new beaker and heated at the temperature of 60 °C for 1 h. In the final step, sample 2B was naturally cooled at room temperature for another 1 h. Color of sample 2B changed in 20 min after the solution of sodium citrate was added to the reaction mixture to yellow. Final pH of colloidal solution was ≈ 6.25.

4.2.3 Hydrazine hydrate-reduced silver nanoparticles

Following type of Ag NPs was prepared according to article published by Guzmán et al. [35] . Few parameters of synthesis were modified such as: reagents concentrations, reaction conditions - temperature or employing UV-irradiation. They prepared various Ag NPs, where concentration of silver nitrate varied from 1 mM to 6 mM, concentration of hydrazine hydrate varied from 1 mM to 12 mM and concentration of sodium citrate varied from 1 mM to 6 mM. Various combinations of these concentrations were investigated. Silver nitrate was used as a precursor of silver ions and hydrazine hydrate as reducing agent. SDS and sodium citrate were used as stabilizers. Presence or absence in reaction mixture of these stabilizers was investigated, as well.

4.2.3.1 The effect of concentration

Six samples of Ag NPs denoted as 4A, 4B, 4C, 4A2, 4B2 and 4C2 were prepared using this method (4.2.3). Various concentrations of reagents were tested via this preparation process. Table 4 summarizes concentrations of individual substances for each sample and also color of final colloidal solution of Ag NPs:

Table 4: Synthesis of hydrazine hydrate-reduced Ag NPs (the effect of concentration) - composition of reaction mixtures and colors of final colloidal Ag NPs.

Sample name	Silver nitrate (mM)	Sodium citrate (mM)	Hydrazine hydrate (mM)	SDS (%)	Color of colloidal Ag NPs
4A	1	2	12	–	dark brown
4B	1	–	12	8	light green
4C	1	2	12	8	dark purple
4A2	6	2	2	–	dark brown
4B2	6	–	2	8	dark green
4C2	6	2	2	8	dark green

- *Materials:*

Silver nitrate (p.a., PENTA), hydrazine hydrate (p.a., Sigma-Aldrich), sodium citrate dihydrate (p.a., Sigma-Aldrich), SDS (p.a., MERCK), deionized water (resistivity of 18.2 MΩ·cm, Milli-Q®). All materials were used as purchased without further purification. All substances were diluted to aqueous solutions using deionized water. Final solutions of colloidal nanoparticles were purified 3x after synthesis by centrifugation at 14 500 rpm (duration of each cleaning cycle was 30 min).

- *Method:*

A beaker with the silver nitrate solution was placed on a magnetic stirrer at 500 rpm (vigorous stirring). After that, hydrazine hydrate solution was added as a reducing agent. In the final step was added the stabilizer, i.e., either sodium citrate or SDS or even both of them. The color of all samples changed immediately after adding the hydrazine hydrate into the reaction mixture. All samples have been stirred for 12 h at room temperature. Final pH of all samples was ≈ 6.18.

4.2.3.2 The effect of increased temperature

Another modification of hydrazine hydrate-reduced Ag NPs synthesis was employed, where an effect of increased temperature was investigated. Four samples were prepared at different temperatures, as it is summarized in the following Table 5:

Table 5: Synthesis of hydrazine hydrate-reduced Ag NPs (the effect of increased temperature) - concentrations of reagents and temperature.

Name of sample	Temperature (°C)	Silver nitrate (mM)	Sodium citrate (mM)	Hydrazine hydrate (mM)
4A1M	30	1	2	1
4A2M	40	1	2	1
4A3M	60	1	2	1

4A4M	80	1	2	1

- *Materials:*

Silver nitrate (p.a., PENTA), hydrazine hydrate (p.a., Sigma-Aldrich), sodium citrate dihydrate (p.a., Sigma-Aldrich), deionized water (resistivity of 18.2 MΩ·cm, Milli-Q®). All materials were used as purchased without further purification. All materials were used as purchased without further purification. All substances were diluted to aqueous solutions using deionized water. Final solutions of colloidal nanoparticles were purified 3x after synthesis by centrifugation at 14 500 rpm (duration of each cleaning cycle was 30 min.)

- *Method:*

Four samples were prepared via this synthesis at different temperatures: 30 °C, 40 °C, 60 °C, and 80 °C. The solution of silver nitrate was placed on a magnetic stirrer at 500 rpm and heated to desired temperature before the beginning of the reaction. Sodium citrate and hydrazine hydrate were pre-heated to desired temperature before the synthesis, as well. Afterwards, hydrazine hydrate solution and sodium citrate solution were added at the same time to the silver nitrate solution. The reaction was held at the dark place for 3 h with continuous heating at required temperature. The color of the reaction mixture changed immediately after adding the hydrazine hydrate and sodium citrate from light green to dark green for all samples. The value of pH of all prepared samples was about ≈ 6.24.

4.2.3.3 The effect of UV-irradiation

The preparation method was further modified by employing the UV-irradiation with different wavelengths. It is known that UV-irradiation can significantly affect the final properties of nanoparticles such shape or size [146]. Three different samples denoted as A, B and C were prepared by this synthesis. One additional sample denoted as X was prepared and it served as a control with no UV-irradiation applied. Table 6 shows the conditions of preparation procedure for each sample:

Table 6: Synthesis of hydrazine hydrate-reduced of Ag NPs (the effect of UV-irradiation) - concentration of reagents and wavelengths of UV light.

Name of sample	Wavelength (nm)	Silver nitrate (mM)	Sodium citrate (mM)	Hydrazine hydrate (mM)
X	dark	1	2	1
A	366	1	2	1
B	254	1	2	1
C	400	1	2	1

- *Materials:*

Silver nitrate (p.a., PENTA), hydrazine hydrate (p.a., Sigma-Aldrich), sodium citrate dihydrate (p.a., Sigma-Aldrich), deionized water (resistivity of 18.2 MΩ·cm, Milli-Q®). All materials were used as purchased without further purification. All substances were diluted to aqueous solutions using deionized water. Final solutions of colloidal nanoparticles were purified 3x after synthesis by centrifugation at 14 500 rpm (duration of each cleaning cycle was 30 min).

- *UV-source information:*

Three different wavelengths of UV light were used in this preparation procedure, namely, ≈ 254 nm, ≈ 366 nm. Surface power density of these two UV-sources was 5 mW/cm^2. The third irradiation UV- source had the wavelength of ≈ 400 nm. Surface power density of UV-source with wavelength of 400 nm was 6 mW/cm^2.

- *Method:*

Steps of this preparation procedure were identical as in the previous chapter 4.2.3.2 but individual samples were irradiated with UV lamp with various wavelengths. A beaker with the solution of silver nitrate was placed on magnetic stirrer at 500 rpm. UV source was placed 5 cm above the top of the beaker. Afterwards, hydrazine hydrate solution and sodium citrate solution were added at the same time to the beaker with solution of silver nitrate. The reaction was held for 20 min at the dark place - the UV-lamp was the only irradiation source and it was irradiating the reaction mixture during entire reaction process. The temperature of the surrounding environment was ≈ 22 °C. The color of reaction mixture changed continuously from the moment of adding the hydrazine hydrate and sodium citrate into the beaker from light green to dark green in about 1 min. The pH value of all final colloidal Ag NPs samples was ≈ 6.18.

4.2.3.4 The effect of UV-irradiation combined with decreased temperature

The UV-irradiation based synthesis was also modified in the combination with decreased temperature. Since the UV-irradiation caused heating of the reaction mixture, the cooling of the mixture during reaction was employed and investigated. Three different samples were prepared, AT, BT and CT. Detailed conditions of the preparation procedure are described in Table 7:

Table 7: Synthesis of hydrazine hydrate-reduced of Ag NPs – concentrations of reagents, wavelengths of UV lights and decreased temperature of reaction mixtures.

Name of sample	Wavelength (nm)	Silver nitrate (mM)	Sodium citrate (mM)	Hydrazine hydrate (mM)	Temperature (°C)
AT	366	1	2	1	15
BT	254	1	2	1	15
CT	400	1	2	1	15

- *Materials:*

Silver nitrate (p.a., PENTA), hydrazine hydrate (p.a., Sigma-Aldrich), sodium citrate dihydrate (p.a., Sigma-Aldrich), deionized water (resistivity of 18.2 MΩ·cm, Milli-Q®). All materials were used as purchased without further purification. All substances were diluted to aqueous solutions using deionized water. Final solutions of colloidal nanoparticles were purified 3× after synthesis by centrifugation at 14 500 rpm (duration of each cleaning cycle was 30 min).

- *Method:*

All steps of the preparation procedure were identical as in the previous chapter 4.2.3.3. However, a cooling system was employed to achieve the temperature of 15 °C during the entire reaction procedure. All substances were cooled down to this temperature before beginning of the synthesis. The reaction was held under these conditions for 1 h. The change of color of reaction mixture occurred in 15 min from the moment of adding hydrazine hydrate and sodium

citrate to the reaction mixture. Final color of all samples was dark green. Final pH of all samples was ≈ 6.19.

4.3 Cytotoxicity of silver nanoparticles

For determination of hydrazine hydrate-reduced Ag NPs cytotoxicity, colorimetric qualitative MTT assay was provided. Four samples of prepared Ag NPs were tested, namely X (dark), A (UV-254 nm), B (UV-366 nm) and C (UV-400 nm). Concentration of Ag NPs varied from 2.5 μg/ml to 220 μg/ml.

- *Materials:*

Ag NPs (prepared samples X, A, B, C - concentration varied from 2.5 μg/ml to 400 μg/ml), MTT dye (p.a., Sigma-Aldrich), medium Dulbecco´s Modified Essential Medium (DMEM) (p.a., Sigma Aldrich), DMEM medium was enriched by 10 % Fetal Bovine Serum (FBS) and 2 mM L-glutamin, penicilin (100 U/mL) a streptomycin (100 U/mL), solubilization solution (p.a., Sigma Aldrich), phosphate buffer saline (PBS) (p.a., Sigma Aldrich), mouse fibroblasts NIH-3T3 (ECACC, UK).

Ag NPs were dissolved in DMEM medium. All purchased materials were used as purchased without further purification.

- *Method:*

At first, cell culture was mixed with 100 μl of DMEM, placed in the 96-well and incubated for 24 h at 37 ºC in a humidified 5 % CO_2 incubator. Concentration of cell culture in each well was 1×10^4. After that, medium was removed and replaced by Ag NPs dissolved in medium with the volume of 50 μl. Subsequently, as prepared plate was incubated for 4 h and 6 h at the temperature of 37 ºC. After incubation, cells were washed 3x with pre-heated phosphate buffer saline (PBS) to 37 ºC. In the next step, MTT with the volume of 50 μl was added to each well, as well as 100 μl of medium and incubated for another 2 h in CO_2 incubator. In the final step was added 100 μl of solubilization solution to dissolve the formazan and let sit for 24 h. Results were read by measurement of absorbance at wavelength of 570 nm.

4.4 Antimicrobial activity of silver nanoparticles

Three different methods were used to determine the antimicrobial activity of Ag NPs, namely disk-diffusion method, measurement of growth curves and dilution method. Three samples of Ag NPs were tested: A (UV-254 nm), B (UV-366 nm) and C (UV-400 nm). Various concentrations of Ag NPs samples were tested against strains *E. coli* and *S. aureus*.

4.4.1 Disk-diffusion method

- *Materials:*

S. aureus (Czech Collection of Microorganisms - CCM), *E. coli* (CCM), prepared Ag NPs samples: A (UV-254 nm), B (UV- 366 nm), C (UV-400 nm): concentration of Ag NPs varied from 0.057 mg/ml to 5.207 mg/ml, antibiotics amoxicillin and penicillin were used as controls, MH broth (Oxoid, UK). All materials were used as purchased without further purification.

- Method:

MH agar was used as medium. At first agar was autoclaved at 50 ºC and placed to the Petri dish to cool down at a room temperature. Cell culture was cultivating for 24 h in MH broth at 37 ºC. Subsequently the culture was incubated for 2 h at 37 ºC. After that, 100 μl of cell culture was spreaded on the agar plate. In the next step, paper filter disks with desired concentration of Ag

NPs and controls were placed on the agar plate. In the last step as prepared Petri dishes were incubated for 24 h at 37 ºC. Inhibition zones around paper filter disks were measured in mm using micrometric ruler.

4.4.2 Growth curves

- *Materials:*

S. aureus (CCM), *E. coli* NCTC (CCM), prepared Ag NPs samples: A (UV-254 nm), B (UV-366 nm), C (UV-400 nm): concentration of Ag NPs varied from 0.31 mg/ml to 2 500 mg/ml, MH medium (Oxoid, UK), deionized water. All materials were used as purchased without further purification.

- *Method:*

This test was provided in 96- well plate. At first, bacterial culture was diluted with MH broth to 0.5 McF (McFarland standards), subsequently to 1:100. Ag NPs were diluted with deionized water to desired concentrations. In the next step, 100 µl of Ag NPs and 100 µl of diluted cell culture were pipetted to each well. As prepared plate was incubated at 37 ºC for 24 h. The absorbance was measured every 30 min.

4.4.3 Dilution method

- *Materials:*

S. aureus (CCM), *E. coli* (CCM), Ag NPs samples: A (UV-255 nm), B (UV-366 nm), C (UV-400 nm): concentration of Ag NPs was 7 mg/l, MH medium (broth and agar) (Oxoid, UK). All purchased materials were used as purchased without further purification.

- *Method:*

MH agar was used as medium. At first MH agar was autoclaved at 50 ºC. Ag NPs were added to fluid agar (final concentration of Ag NPs in agar was 7 mg/l). As prepared agar was transferred to Petri dish and cooled down at room temperature. Cell culture was grown in MH broth in 24 h and was diluted to concentration of $\approx 1.5\times10^3$ CFU/ml. Subsequently, grown culture was incubated at 37 ºC for 2 h. 100 µl of cell culture was pippeted on agar plates. In the final step, as prepared Petri dishes were incubated at 37 ºC for 24 h and grown colonies were counted as colony forming units (CFU). Control plates were prepared with the same procedure but without Ag NPs. Samples for testing against *S. aureus* were prepared fin 12 repetitions and samples for testing against *E. coli* were prepared in 11 repetitions for statistical analysis.

4.5 Synthesis of selenium nanoparticles

Se NPs were prepared via several methods. Wet chemical synthesis was employed and various reagents were used. Similarly, as for Ag NPs, final properties of Se NPs can be tailored during the synthesis process, as well. Final colloidal solution of Se NPs were stored in the fridge at the temperature of ≈ 5 ºC.

4.5.1 Ascorbic acid-reduced selenium nanoparticles

Se NPs stabilized with chitosan were prepared according to article published by Yu et al. [147]. One sample was prepared via this synthesis, denoted as Se NPs-chitosan. Selenous acid served as a precursor. Acetic acid played a role of reducing agent and chitosan was used for stabilization.

- *Materials:*

Selenous acid (p.a., Sigma-Aldrich), chitosan medium molecular weight (p.a., Sigma-Aldrich (p.a., deacetylation degree 75 % - 85 %), acetic acid (p.a., 99.8 %. PENTA), ascorbic acid (p.a., Sigma-Aldrich), deionized water (resistivity of 18.2 MΩ·cm, Milli-Q®). All materials were used as purchased without further purification. All substances were diluted to aqueous solutions using deionized water. Final solutions of colloidal Se NPs were purified 3× after synthesis by centrifugation at 10 000 rpm (duration of each cleaning cycle was 15 min).

- *Method:*

At first, acetic acid solution was prepared by dissolving of 1 g of acetic acid in 100 ml of deionized water. After that, 1 g of chitosan was added and dissolved - this mixture was placed on magnetic stirrer set to 200 rpm and moderate heating at the temperature of 30 ºC was employed. In the next step, 1 ml of selenous acid with concentration of 125 mM was prepared and it was placed on a magnetic stirrer (200 rpm). After that, 48 µl of chitosan solution was pippeted into selenous acid. In the last step, 5 ml of ascorbic acid with concentration of 100 mM was added to the mixture. In the end, the volume was topped up to 25 ml with deionized water. Reaction time was set to 15 min. Color of the final colloidal solution turned into ruby red in 3 min from adding the reduction compound to the mixture. Value of pH was ≈ 6.32.

4.5.2 Sodium hydroxide-reduced selenium nanoparticles

This method was modified according to Tran et al. [44]. Following reaction parameters were tested: the addition of sodium hydroxide, volume of reaction mixture and presence of absence of stirring the reaction mixture. Sodium selenite was used as a precursor, sodium hydroxide as a strong reducing agent and glutathione as a weak reducing agent and also as a stabilizer. Additionally, sodium hydroxide provides alkaline environment, which is sufficient for Se NPs creation [44]. In the environment with the pH lower than 6, it is not possible to achieve the reduction of sodium selenite because it oxidizes due to low pH. Therefore, the surface chemistry changes the interaction with other compounds used for the synthesis [44]. Table 8 shows the synthesis conditions of six samples of Se NPs denoted as A, B, C, D, E and F:

Table 8: Sodium hydroxide-reduced Se NPs - reactions conditions and concentration of reagents.

Name of sample	Sodium selenite (mM)	Glutathione (mM)	Sodium hydroxide (µl)	Stirring (rpm)	Demineralized water (ml)
A	25	100	-	-	-
B	25	100	150	-	9
C	25	100	-	-	9
D	25	100	150	220	9
E	25	100	-	220	-
F	25	100	-	220	9

- *Materials:*

Sodium selenite (p.a., Sigma Aldrich), L-glutathione reduced (p.a., Sigma Aldrich), sodium hydroxide (p.a., Sigma Aldrich), deionized water (resistivity of 18.2 MΩ·cm, Milli-Q®). All materials were used as purchased without further purification. All substances were diluted to aqueous solutions using deionized water. Final solutions of colloidal nanoparticles were purified 3× after synthesis by centrifugation at 10 000 rpm (duration of each cleaning cycle was 15 min).

- *Method:*

The synthesis of Se NPs was performed at laboratory temperature, which was 22 °C. In this preparation procedure, different concentrations of sodium selenite and glutathione (weak reducing agent and stabilization agent) were used. In several experiments the effect of addition of 1 M sodium hydroxide (strong reducing agent) or 9 ml of demineralized water were tested. When the sample was stirred, the stirring was set to 220 rpm during the reaction. The time of synthesis was set to 10 min. The pH of final colloidal solutions was ≈ 6.51.

4.5.3 L-cysteine-reduced selenium nanoparticles

Three different samples of Se NPs were prepared via this synthesis, namely A1, A2 and A3. Precursor and reducing agent were always the same for every sample, only the stabilizing agents were changed. Sodium selenite was used as a precursor and L-cysteine as reducing agent. The stabilizing agents were polyvinylpyrrolidone-29 (PVP-29), polyvinylpyrrolidone-40 (PVP-40) and bovine serum albumin (BSA). The following Table 9 shows the overview of chemical composition of prepared samples:

Table 9: Synthesis of L-cysteine-reduced Se NPs - composition of samples and concentration of reagents.

Name of sample	**Sodium selenite (mM)**	**L-cysteine (mM)**	**Stabilizing agent (mM)**
A1	25	25	PVP-29 (**0.1**)
A2	25	25	PVP-40 (**0.1**)
A3	25	25	BSA (**1**)

- *Materials:*

Sodium selenite (p.a., Sigma Aldrich), L-cysteine (p.a., Sigma Aldrich), polyvinylpyrrolidone with average molecular weight of ≈ 29 000 g/mol (p.a., Sigma Aldrich), polyvinylpyrrolidone with average molecular weight of ≈ 40 000 g/mol (p.a., Sigma Aldrich), BSA (p.a., Sigma Aldrich), deionized water (resistivity of 18.2 MΩ·cm, Milli-Q®). All materials were used as purchased without further purification. All substances were diluted to aqueous solutions using deionized water. Final solutions of colloidal nanoparticles were purified 3× after synthesis by centrifugation at 10 000 rpm (duration of each cleaning cycle was 20 min).

- *Method:*

A beaker with 25 ml of aqueous solution of precursor was placed on a magnetic stirrer with 200 rpm at constant ambient temperature of 22 °C. In the next step, the aqueous solutions of reducing agent and stabilizing agent, both 25 ml, were simultaneously added into the beaker.

Reaction time was 10 min. Ruby red color of the reaction mixture pointed to the formation of Se NPs. Value of pH of final colloidal solutions was about ≈ 6.23.

4.6 Cytotoxicity of selenium nanoparticles

Cytotoxicity of Se NPs was determined by methods XTT and DNA cell proliferation assay. Sample A1 (L-cysteine reduced and stabilized with PVP-29) was tested.

Three samples were tested:

- A1 in water (denoted as A1W)
- A1 in medium (denoted as A1M)
- A1 in medium – Se NPs without stabilization compound (denoted as A1-0M and used as control)

Se NPs samples were dissolved in medium or in deionized water. Sample without stabilization agent and sample dissolved in deionized water were used to observe if the stabilization compound or water can affect cytotoxicity of Se NPs.

Tests were performed on 96-well plate in triplets for statistical analysis. Seeding density of fibroblasts was 10^4 in each well. Cells were incubated with different concentrations of Se NPs for 24 h. Cells were harvested by trypsinization with 0.25 % trypsin-EDTA (trypsin-ethylenediaminetetraacetic acid). All tests were performed in duplicates for statistical analysis. Concentration of Se NPs varied from 0.005 mg/ml to 5 mg/ml.

4.6.1 XTT assay

- *Materials:*

NIH/3T3 fibroblasts (p.a., Sigma-Aldrich), medium DMEM enriched with 10 % FBS and 5 % penicillin/streptomycin (50 U/ml and 0.05mg/ml), dye XTT (p.a., Sigma-Aldrich), trypsin-EDTA, PBS (p.a., Sigma Aldrich). All materials were used as purchased without further purification.

- *Method:*

At first chosen density of cells was incubated with 100 µl of DMEM overnight. In the next step medium was replaced with Se NPs of various concentration mixed with 100 µl DMEM. After incubation of 24 h, this mixture was removed and fibroblasts were purified 3× using pre-heated PBS at 37 °C. Then 100 µl DMEM was mixed with 50 µl of XTT and added to each well to the cell culture. Subsequently as prepared 96-well plate was incubated for 2 h in a CO_2 incubator. In the last step, 100 µl of this solution was pipetted into a new 96- well plate to measure an absorbance at the wavelength of 570 nm.

4.6.2 BrdU proliferation assay

- *Materials:*

NIH/3T3 fibroblasts (p.a., Sigma-Aldrich), medium DMEM enriched with 10 % FBS and 5 % penicillin/streptomycin (50 U/ml and 50 µg/ml), BrdU (p.a., Sigma-Aldrich), trypsin-EDTA, PBS (p.a., Sigma Aldrich). All materials were used as purchased without further purification.

- *Method:*

At first chosen density of cells was incubated with 100 µl of DMEM overnight. Se NPs were dissolved in DMEM and 100 µl of this mixture was added to cell culture (again various concentrations). Fibroblasts were incubated with Se NPs for 24 h at humidified atmosphere at

37 °C. In the next step 10 µl of BrdU solution was added to each well followed by additional incubation for another 2 h. After that, labelling medium was removed and 200 µl of FixDenat solution was added to fix the cells for 30 min. Then, this fixing solution was removed and replaced by 100 µl of BrdU-peroxidase antibody solution and incubated at room temperature for 90 min. Then, the wells were rinsed using buffer solution. In the last step 100 µl of substrate solution was added for 20 min and subsequently was measured absorbance at the wavelength of 370 nm.

4.7 Antimicrobial activity of selenium nanoparticles

Antimicrobial activity of Se NPs was determined by two different methods: MIC and measurement of growth curves. Three samples of Se NPs were tested, namely L-cysteine-reduced Se NPs: A1 (stabilized with PVP-29), A2 (stabilized with PVP-40) and A3 (stabilized with BSA).

4.7.1 Minimum inhibitory concentration

- *Materials:*

S. aureus (CCM), *E. coli* (CCM), MH medium (Oxoid, UK), Se NPs samples A1, A2 and A3 (concentration varied from 0.191 mg/ml to 25.5 mg/ml). All materials were used as purchased without further purification.

- *Method:*

Bacterial cultures were diluted to 0.5 McF, subsequently 1:100 with MH medium. Se NPs were dissolved in MH medium to desired concentrations. Test was provided in 96-wll plate. 75 µl of Se NPs and 75 µl of bacterial culture were pippeted to each well and incubated in O/N atmosphere at 37 ºC for 24 h. In the final step, absorbance at the wavelength of 600 nm was measured.

4.7.2 Growth curves

- *Materials:*

S. aureus (CCM), *E. coli* (CCM), *MRSA* (CCM), MH medium (Oxoid, UK), Se NPs samples A1, A2 and A3 (concentration varied from 0.1 mg/ml to 12.25 mg/ml). All materials were used as purchased without further purification.

- *Method:*

This experiment was provided in 96-well plate. Bacterial cultures were diluted to 0.5 McF, subsequently 1:100 with MH medium. Se NPs were diluted with water to desired concentrations. Se NPs with the volume of 100 µl and bacterial culture with the volume of 100 µl were pipetted into each well. As prepared plate was incubated at 37 ºC for 18 h and absorbance was measured every 30 min.

4.8 Plasma treatment of polymer membranes and immobilization of antimicrobial nanoparticles

Polymer membranes were modified with plasma treatment to incorporate amine functional groups for subsequent immobilization of NPs. Two different methods were employed: low-pressure plasma treatment and reactive ion etching (RIE) with utilization of ammonia plasma. As mentioned earlier in this work, only catex membranes were used for all experiments due

better stability to various chemicals. Plasma modified membranes were stored in the freezer at the temperature of −15 ºC, in plastic bag containing silica gel to absorb the humidity.

4.8.1 Low-pressure plasma deposition of amine groups on polymer membrane

- *Materials:*

Cyclopropylamine (CPA) (purity 98 %, Sigma Aldrich), argon (purity of 99.998 %, Messer), glacial acetic acid (p.a., Penta), formic acid (p.a., Penta), polymer membrane (catex membrane, MemBrain ltd.). All materials were used as purchased without further purification.

- *Method:*

Polymer membranes were cut to ≈ (1×1) cm^2. At first, membranes were cleaned by pulsed Ar plasma for 10 min before the deposition process. Deposition of amine groups on membranes was done using capacitively coupled plasma (CCP) employing radio frequency (RF) generator with working frequency of 13.56 MHz. Plasma instrument with base pressure of ≈ 1×10^{-4} Pa was equipped with showerhead for uniform gas delivery. The deposition process with length of 1 h was realized via squared pulsed CPA/Ar plasma at pressure of ≈ 50 Pa with power of ≈ 100 W, while the duty cycle was 33 % at repetition frequency of ≈ 500 Hz. Flow rate of Ar and CPA was ≈ 28 cm^3/min and ≈ 2 cm^3/min, respectively.

4.8.2 Deposition of amine groups by reactive ion etching with ammonia plasma on polymer membranes

- Materials:

Argon (purity of 99.999 %, Linde), ammonia (purity of 99.7 %, SIAD), polymer membrane (catex membrane, MemBrain ltd.). All materials were used as purchased without further purification.

- Method:

Second approach of membrane functionalization was done using RIE instrument, which has similar configuration including CCP and RF generator working at the same frequency. Instrument base pressure was ≈ 5×10^{-5} Pa. Samples were precleaned using Ar plasma for 10 min. Then the deposition was done at pressure of 50 Pa with RF power of 50 W for 30 min. The used working gas was Ar with flow of 10 cm^3/min and NH_3 with flow of 40 cm^3/min. Higher RF power caused membrane damaging caused by plasma thermal exposure even if it was realized at higher working pressure.

4.8.3 Immobilization of nanoparticles on polymer membrane

Immobilization process of NPs was held as wet chemical reaction. Plasma treated membranes were immersed into the reaction mixtures of NPs. Membrane samples were immersed in reaction mixtures for 1 h. Subsequently dried for 24 h at the room temperature. As prepared membranes were stored in the dry box. These samples were stored in the dry box for 1 month to reduce the humidity to maximum because of subsequent optical measurements.

Table 10: Polymer membranes samples with immobilized NPs for macro dilution method.

Sample name	Plasma deposition type	Reaction mixture
M1	Low-pressure plasma	Silver nitrate
M2	Low-pressure plasma	Hydrazine hydrate-reduced Ag NPs

M3	Low-pressure plasma	Hydrazine hydrate-reduced Ag NPs stabilized with sodium citrate
M4	Low-pressure plasma	L-cysteine-reduced Se NPs stabilized with PVP-29
MA1	RIE	Silver nitrate
MA2	RIE	Hydrazine hydrate-reduced Ag NPs
MA3	RIE	Hydrazine hydrate-reduced Ag NPs stabilized with sodium citrate
MA4	RIE	L-cysteine-reduced Se NPs stabilized with PVP-29

4.9 Antimicrobial properties of polymer membranes with immobilized nanoparticles

Antimicrobial properties with immobilized NPs (Ag and Se) were tested against cell cultures *S. aureus* and *E. coli* using macro dilution method.

- *Materials:*

S. aureus (CCM), *E. coli* (CCM), MH broth (Oxoid, UK), catex polymer membranes with immobilized NPs. All materials were used as purchased without further purification.

- *Methods:*

Macro dilution method was used to determine the antimicrobial activity of polymer membranes with immobilized NPs. Bacterial cultures were diluted to concentration of 0.5 McF, subsequently to 1:100 with MH broth. Experiment was performed in test tubes and each tube contained with 1 ml of diluted culture. Polymer membrane with the dimensions of $\approx (0.5 \times 0.5)$ cm^2 were immersed in this solution. Samples were incubated for 24 h at the temperature of 37 ºC. Absorbance was measured at the beginning of the experiment (after immersing of polymer membrane with immobilized NPs in the medium), after 7 h and after 24 h.

5 Results and discussion

This chapter consists of discussion of achieved results. Sub chapters are in the same order as aim of thesis: synthesis of NPs, cytotoxicity assays, antimicrobial activity of NPs, plasma treatment of polymer membranes with immobilization of NPs and antimicrobial activity of polymer membranes with immobilized NPs.

5.1 Characterization of silver nanoparticles

5.1.1 Chitosan-reduced silver nanoparticles

SEM analysis of sample 1A depicted in Figure 13 shows prepared Ag NPs reduced by chitosan. SEM image outlines the inconsistent size of particles, which varies from 10 nm to 100 nm. It is visible that particles are aggregated (grown together) and form bigger cluster with size about 400 nm. Shape of Ag NPs seems to be mostly rounded. There is also a smooth coverage visible on the surface of the particles, which is probably created from chitosan for stabilization. However, big agglomerates created by smaller particles are very significant.

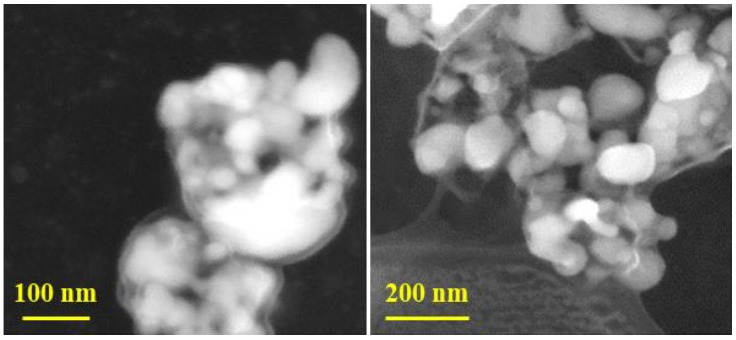

Figure 13: SEM image of chitosan-reduced Ag NPs, cluster (left), grown particles (right).

Typical absorption peak of Ag NPs is usually observable between 400 nm and 500 nm [148]. However, the absorption curve in Figure 14 does not show any relevant absorption peak of these Ag NPs in above mentioned region but there is observable broad peak visible from 600 nm, which indicates to agglomeration of Ag NPs as can be seen also in SEM image showed above. Tran et al. revealed that there must be found an appropriate ratio between silver nitrate and chitosan to achieve monodispersed colloidal solution of Ag NPs. With increasing ratio, the size of Ag NPs increased. They also found out that increasing temperature can support Ag NPs to result in colloidal solution with monodisperse size and shape distribution. They achieved monodispersed Ag NPs at the highest temperature of 100 °C and low ratio between silver nitrate and chitosan of [Ag+] = 13.33×10−3 mmol/l, and low concentration of chitosan 0.33 mg/ml [144]. The differences between syntheses could be caused by substances purchased from different companies (probably chitosan with medium molecular weight, which varies from 200 kDa to 400 kDa and also their deacetylation degree - depends on supplier) but also different reaction temperatures and concentrations of reaction substances.

However, stability of prepared Ag NPs was observable for 2 days after preparation. After this period agglomerates were seen at the bottom of the flask. In addition, characterization techniques revealed their aggregation from the very beginning. Thus, this sample was not sufficient for further usage because of very low colloidal stability

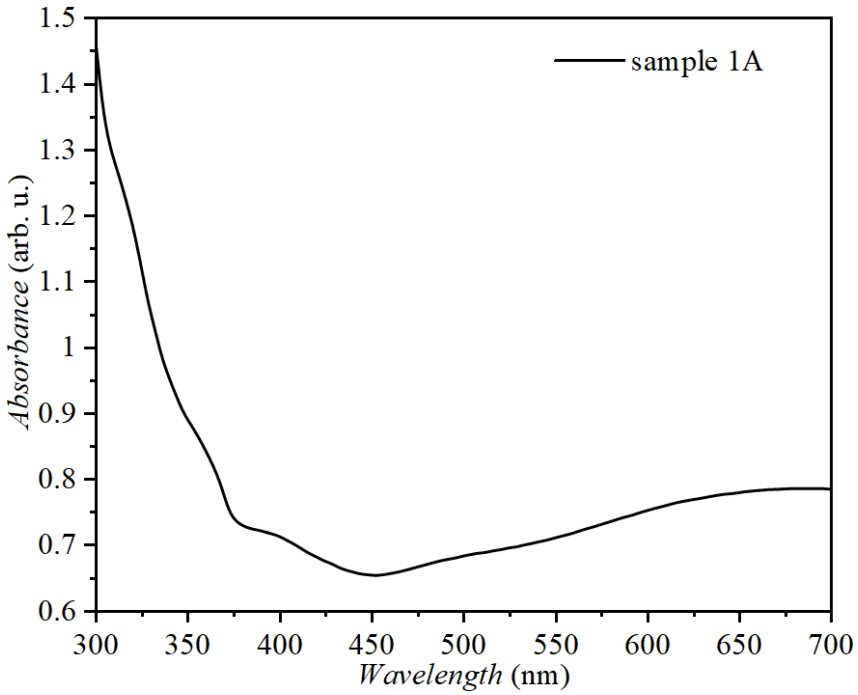

Figure 14: Absorption spectrum of chitosan-reduced Ag NPs.

5.1.2 Glucose-reduced silver nanoparticles

Glucose-reduced Ag NPs samples 2A and 2B were characterized using SEM and UV-VIS spectrometry. SEM images of both samples of Ag NPs are depicted in Figure 15; sample 2A (left) and sample 2B (right). View field of sample 2A was 1.089 μm and view field for sample 2B was 0.63 μm. Ag NPs of both samples have nearly spherical shape and very similar size and shape distribution. Size of Ag NPs is approximately of 100 nm and more. Both samples of Ag NPs are covered by stabilizing agent PEG as visible from SEM images. Both samples also evince agglomeration and some of particles are also probably grown together. Their colloidal stability lasted only for 2 days after preparation. After this period visible agglomerates were seen at the bottom of the flask.

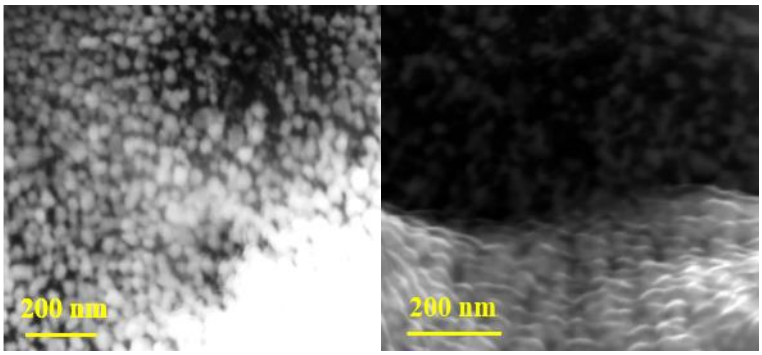

Figure 15: SEM images of glucose-reduced Ag NPs: sample 2A (left), sample 2 B (right).

Results from UV-VIS spectrometry of both samples can be seen in Figure 16. Absorption peak of sample 2A is visible very slightly at about 310 nm, which means that synthetized Ag NPs are probably very big sized or already aggregated. This fact was confirmed by SEM analysis, as well. Absorption peak of sample 2B is visible at 420 nm, which indicates that Ag NPs are really present in solution; absorption band at this wavelength is typical for Ag NPs [14].

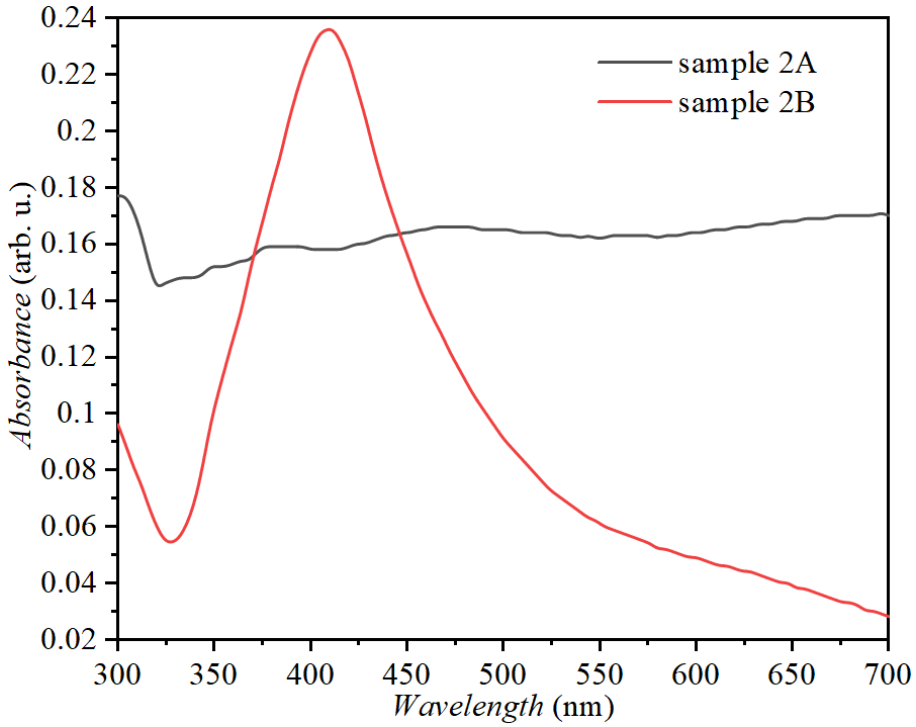

Figure 16: Absorption spectrum of glucose-reduced Ag NPs: samples 2A and 2B.

Results published by Shameli et al. were different. Their Ag NPs were spherical in shape without agglomeration and with size from 10 nm to 15 nm analyzed by TEM and size distribution function. They measured UV-VIS spectrometry for different duration of reactions (1 h, 3 h, 6 h, 24 h, 48 h). Typical absorption peak could be visible from 1 h of reaction and most significant was at 24 h of reaction time [24].

Results in this thesis are most probably different because of reducing agent - in the article was not specified the type of sugar. Synthesis presented in this work employed D-glucose as a reducing agent. The reaction after adding the glucose to silver nitrate solution for sample 2B was very weak because color of reaction mixture changed very slightly (very light orange color). Color of reaction mixture of sample 2A did not change at all after adding the reducing agent to silver nitrate. Thus, sodium citrate was added to enhance the reduction of silver ions.

However, colloidal stability of samples 2A and 2B was very low. It lasted only for 2 days, thus another set of experiments had to be provided to prepare Ag NPs with desired properties.

5.1.3 Hydrazine hydrate-reduced silver nanoparticles

Another method was used to prepare Ag NPs. This synthesis employed hydrazine hydrate as a reducing agent, silver nitrate as precursor and sodium citrate and SDS as stabilizers. This synthesis was optimized several times, where different factors were investigated, namely concentration of reagents, increased temperature of reaction mixture, utilization of UV-irradiation with different wavelengths and UV-irradiation combined with cooling of reaction mixture.

5.1.3.1 The effect of reagents´ concentration

Ag NPs samples prepared via this synthesis were analyzed by SEM and UV-VIS spectrometry. SEM analysis of samples 4A (left), 4B (middle) and 4C (right) is shown in Figure 17. View field of scanned samples was ≈ 2.55 μm.

Sample 4A: The color of colloidal solution of Ag NPs changed immediately into dark brown after adding hydrazine hydrate into the silver nitrate solution, which pointed to creation of nanoparticles. Figure 17 shows SEM image of this sample (left). In SEM image can be clearly seen that particles have spherical shape but size distribution is very wide. It varies in range from 20 nm up to 250 nm. A thin layer covering nanoparticles is observable, as well. This protection layer probably comes from sodium citrate, which was used as stabilizing agent for this sample.

Sample 4B: Change of color in this preparation procedure occurred right after adding hydrazine hydrate into the silver nitrate solution as in previous case. Color turned into green and after another 3 minutes into light green. Results of this synthesis are depicted in Figure 17 (center). These particles have spherical shape with size between 50 nm and 100 nm. Ag NPs are covered with thick layer created from SDS, which is used as the stabilizing agent for particles in colloidal solution [35].

Sample 4C: Ag NPs in this preparation process changed color immediately after adding the hydrazine hydrate to the silver nitrate solution into dark purple. These Ag NPs are shown in Figure 17 (right). Size distribution of Ag NPs is very broad. SEM analysis shows that Ag NPs have various size from 20 nm to 100 nm. Ag NPs are also covered with thick layer created from SDS and citrate, which were used as stabilizing agents. Shape of Ag NPs seems to be spherical.

It is obvious that protection layer that is created on each sample of Ag NPs is very different. Layer created from SDS is much thicker than layer created from sodium citrate. It is probably caused by their different chemical structure. Molecule of SDS is salt and organosulphate that consist of 12 carbon atoms with attached sulfate group. On the other side, sodium citrate is a salt of citric acid with only 6 carbon atoms and serves as an anticoagulant. Chemical structure makes SDS a strong detergent substance. Detergents with higher concentrations make the thick layer around the nanoparticles, thus the layer visible on Ag NPs is thicker than the layer from sodium citrate. All samples were stable for ≈ 1 week from synthesis, after this period, sediment could be observable at the bottom of the flask.

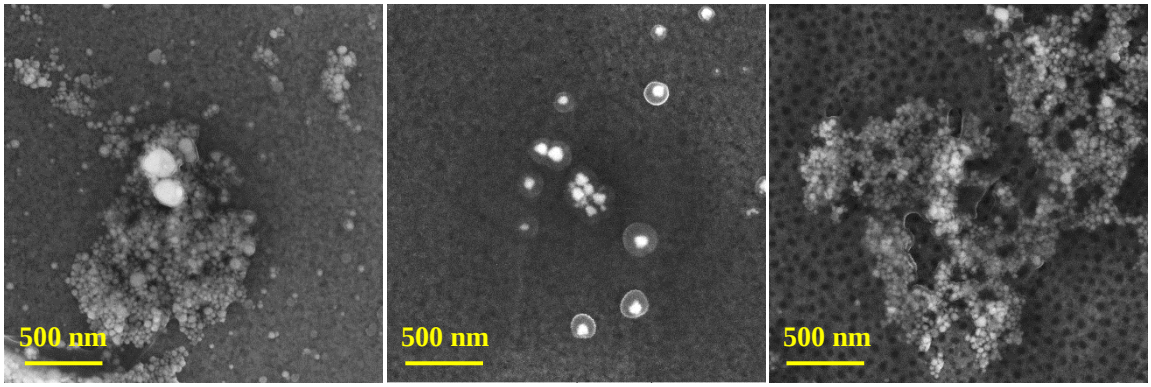

Figure 17: SEM image of hydrazine hydrate-reduced Ag NPs (the effect of concentration): 4A (left), 4B (center), 4C (right).

Furthermore, Figure 18 represents absorption spectroscopy of samples 4A, 4B and 4C.

Sample 4A: This absorption curve shows two peaks. Very distinct primary peak, which is visible at the wavelength of 440 nm and a secondary peak visible at the wavelength of 520 nm. In this case, secondary peak at the longer wavelengths can be induced by non-homogeneous size distribution of Ag NPs or their agglomeration. It is well known that bigger particles shows different SPR in comparison to smaller particles [148]. Agglomeration have impact on optical properties, as well. It can result in two or three peaks [149]. These Ag NPs evince very wide size distribution as confirmed by SEM analysis. Thus, double absorption peak could appear. In

this case, double absorption peak is most probably caused by size distribution of Ag NPs, as confirmed from SEM analysis, sample contains small particles but also big sized particles.

Sample 4B: Absorption peak of this sample is visible at the wavelength of 480 nm. Size of nanoparticles varies from 50 nm to 100 nm and they are not agglomerated. Thus, broader absorption peak of Ag NPs is be visible from UV-VIS absorption scan. The broadness of the peak can be also caused by a thick stabilization layer as SEM analysis confirmed [150].

Sample 4C: Absorption curve of sample 4C has got 2 absorption peaks, one at the wavelength of 440 nm and second at the wavelength of 520 nm. Double absorption peak of this sample is probably caused by very wide size distribution as well as by their agglomeration. As SEM analysis showed, size distribution of nanoparticles is highly heterogeneous, as well as their agglomeration is very significant. Spectral response of Ag NPs relates with the diameter of particles. Single particle shows different SPR than aggregated or agglomerated particles. Aggregated or agglomerated metal particles are electronically coupled so they have different electron oscillation pattern so they show different SPR from single nanoparticle [148].

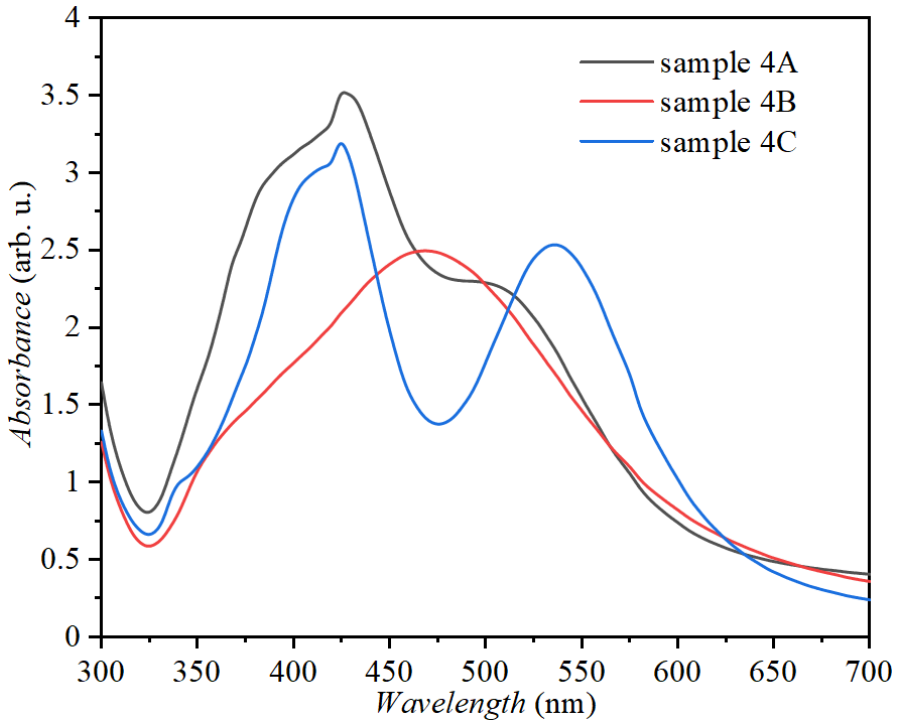

Figure 18: Absorption spectra of hydrazine hydrate-reduced Ag NPs (the effect of concentration): samples 4A, 4B and 4C.

Samples 4A2, 4B2 and 4C2 were also analyzed by SEM. View field of sample 4A2 was ≈ 2.52 μm and for the rest of the samples view field was ≈ 0.54 μm.

Sample 4A2: Change of color of the reaction mixture occurred immediately after adding the hydrazine hydrate to the silver nitrate solution into dark brown. Resulting Ag NPs prepared with above mentioned synthesis are depicted in Figure 19 (left). SEM image shows that Ag NPs evince anisotropic shape with very wide size distribution in range from 20 nm to 250 nm.

Sample 4B2: Ag NPs of sample 4B2 changed color immediately to dark green from adding hydrazine hydrate into reaction solution of silver nitrate. At first, mixture turned into purple and subsequently to dark green. Ag NPs from sample 4B2 are shown in Figure 19 (center). Ag NPs have nearly round shape and create bigger clusters, some of them are probably grown together. Layer covering surface is very significant and it is probably from SDS, which acts as a stabilizer

in this reaction. Size of particles seem to be up to 100 nm and the agglomerates have 500 nm and more.

Sample 4C2: Ag NPs of sample 4C2 changed color right after from adding hydrazine hydrate to silver nitrate solution into dark green. Ag NPs of sample 4C2 can be seen in Figure 19 (right). Ag NPs evince anisotropic shape, plate triangles with truncated tops but also spheres can be seen in SEM image. Particles are agglomerated and covered with thick layer, which is probably created from SDS and sodium citrate, which were used as stabilizing agents. Size of particles is up to 250 nm and size of clusters is up to 1 000 nm.

Colloidal stability of these samples was observed for 1 week from preparation procedure, after that sediment appeared at the bottom of the flasks.

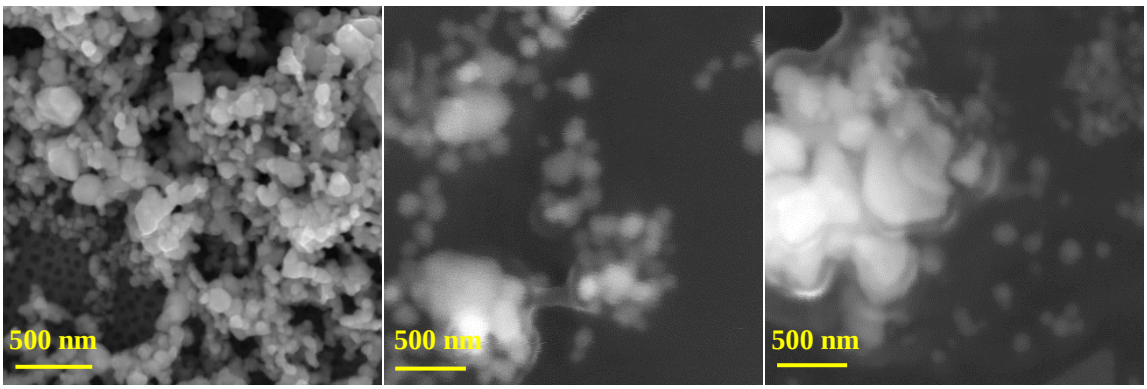

Figure 19: SEM image of hydrazine hydrate-reduced Ag NPs (the effect of concentration): sample 4A2 (left), 4B2 (center) and sample 4C2 (right).

UV-VIS spectroscopy analysis of samples 4A2, 4B2 and 4C2 is shown in Figure 20. Absorption curve of sample 4A2 does not show any relevant peak, it can be caused by low concentration of Ag NPs. Absorption peak of Ag NPs of sample 4B2 is very wide from 350 nm to 450 nm, which is probably caused by agglomerated nanoparticles confirmed also by SEM analysis. Absorption maximum of sample 4C2 is at 420 nm, which is typical for Ag NPs. There is also an indication of another peak at longer wavelengths between 600 nm and 700 nm, which can be caused by agglomerated Ag NPs, also confirmed by SEM analysis.

These experiments show that concentration of reagents and also different stabilizing agents such as SDS and sodium citrate can have significant impact on final colloidal solution, mostly on shape of Ag NPs. It was observed that if the concentration of silver nitrate was low (2 mM) and concentration of hydrazine hydrate high (12 mM), final Ag NPs evinced round shape. With increasing concentration of silver nitrate to 6 mM and decreasing concentration of hydrazine hydrate to 2 mM, anisotropic shape of Ag NPs prevailed. There is also difference between samples where sodium citrate was present or absent in reaction solution. The presence of sodium citrate supported the anisotropic shape of Ag NPs. Samples 4B and 4B2 did not include the sodium citrate and the final shape of Ag NPs was rounded as confirmed by SEM analysis. On the other side, in the rest of the samples (4A, 4C, 4A2 and 4C2), where sodium citrate was present, more anisotropic shape of Ag NPs was observed.

However, stability of all samples lasted only for ≈ 4 days after preparation procedure, thus these samples were not suitable for another experiments. This method was modified again, where a different factor was tested, namely, increased temperature, which is more described in the following chapter.

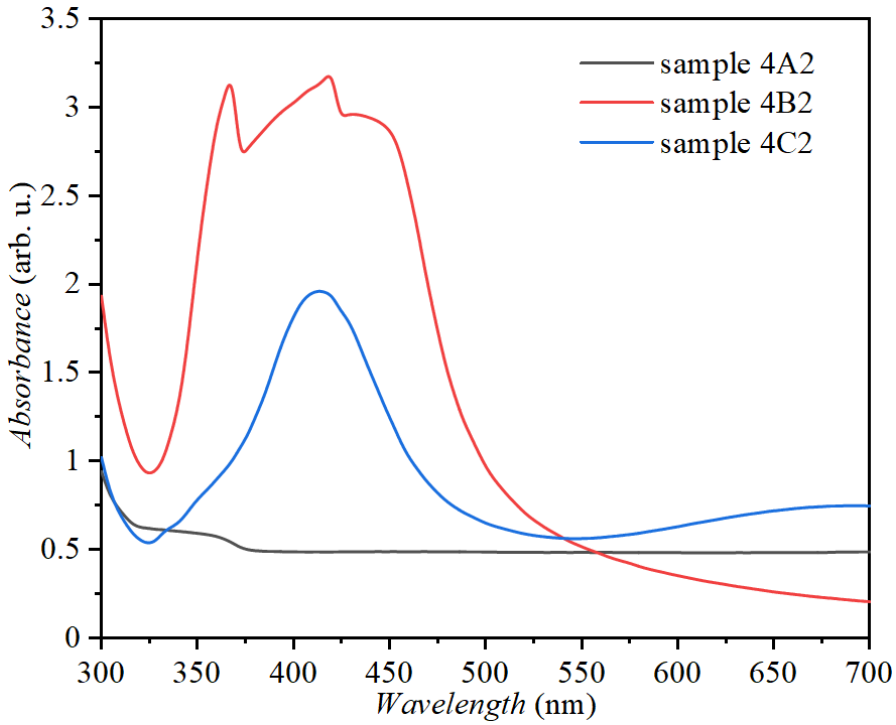

Figure 20: Absorption spectra of hydrazine hydrate-reduced Ag NPs (the effect of concentration): samples 4A2, 4B2, and 4C2.

5.1.3.2 The effect of increased temperature

Following samples were analyzed by SEM (view field for all samples was ≈ 0.54 μm) and also by UV-VIS absorption spectroscopy. SEM images of following samples are depicted in Figure 21. In this synthesis, the lowest concentration of reagents was used, 1 mM silver nitrate, 2 mM sodium citrate and 1 mM hydrazine hydrate because temperature was employed as another factor that can influence final properties of Ag NPs. In previous chapter was revealed that with increasing concentration of silver nitrate and presence of sodium citrate, anisotropic shape of Ag NPs is supported. In addition, SDS was not employed because of its very strong detergent properties. Samples containing SDS were very difficult to purify, which also caused difficulties with SEM analysis. SDS is the organosulfur and during SEM scanning samples were charged, thus the quality of the scanned image was poor. Therefore, samples had to be diluted multiple times.

Sample 4A1M - reaction temperature of 30 °C: Color of these Ag NPs changed immediately into dark green after adding reducing solutions to nitrate solution. Final Ag NPs can be seen in Figure 21 (left). Size and also shape distribution are very broad: there is no shape or population, which dominates. Thus, Ag NPs can be considered as anisotropic in shape with wide size distribution. Size of particles varies from 10 nm up to 100 nm. Ag NPs are agglomerated but not grown together.

Sample 4A2M - reaction temperature of 40 °C: Ag NPs of this sample started to form right after adding reducing agents into aqueous silver nitrate solution, which was observable as change of color of reaction solution into dark green. These Ag NPs are shown in Figure 21 (second from left). These Ag NPs have very similar size distribution in comparison to previous sample 4A1M. However, but Ag NPs from this sample seem to have more rounded edges. Size of Ag NPs varies from smaller particles with diameter of 10 nm to bigger particles with size about 80 nm. In comparison to previous sample 4A1M, size of Ag NPs decreased.

Sample 4A3M reaction temperature of 80 °C: This sample changed color into dark green right after adding reducing agents into solution of silver nitrate. Final Ag NPs are shown in Figure 21 (second from right). Size and shape of Ag NPs changed significantly. Particles evince spherical shape and their size decreased even more in comparison to previous two samples (4A1M and 4A2M). Size of Ag NPs varies from 10 nm to about 50 nm.

Sample 4A4M - reaction temperature of 60 °C: Color of this sample changed right after adding reducing solutions into silver nitrate solution into dark red, which pointed to creation of Ag NPs in reaction solution. Ag NPs of this sample are shown in Figure 21 (right). Shape of nanoparticles can be considered as spherical. Particles are not agglomerated and they are also covered with protection layer, probably created from sodium citrate to stabilize the colloidal solution. Size of Ag NPs is up to 50 nm.

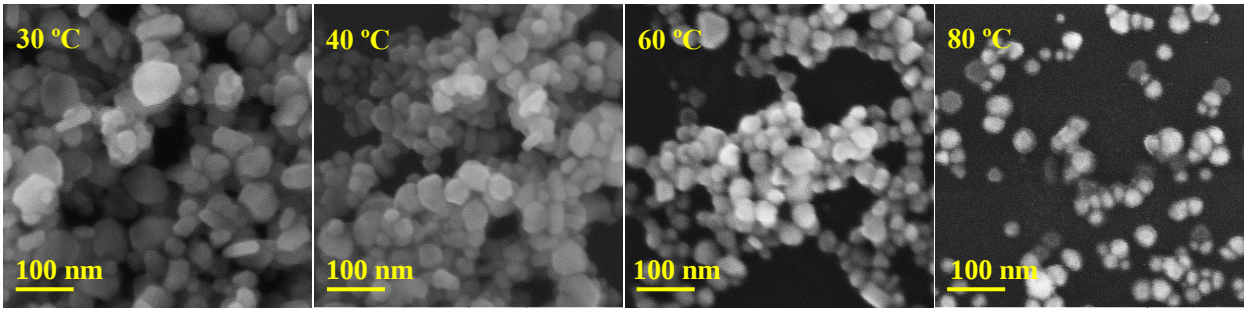

Figure 21: SEM images of hydrazine hydrate-reduced Ag NPs (the effect of increased temperature), from the left: 4A1M, 4A2M, 4A3M and 4A4M.

Figure 22 shows UV-VIS spectroscopy analysis of all samples mentioned in this chapter (4A1M, 4A2M, 4A3M and 4A4M).

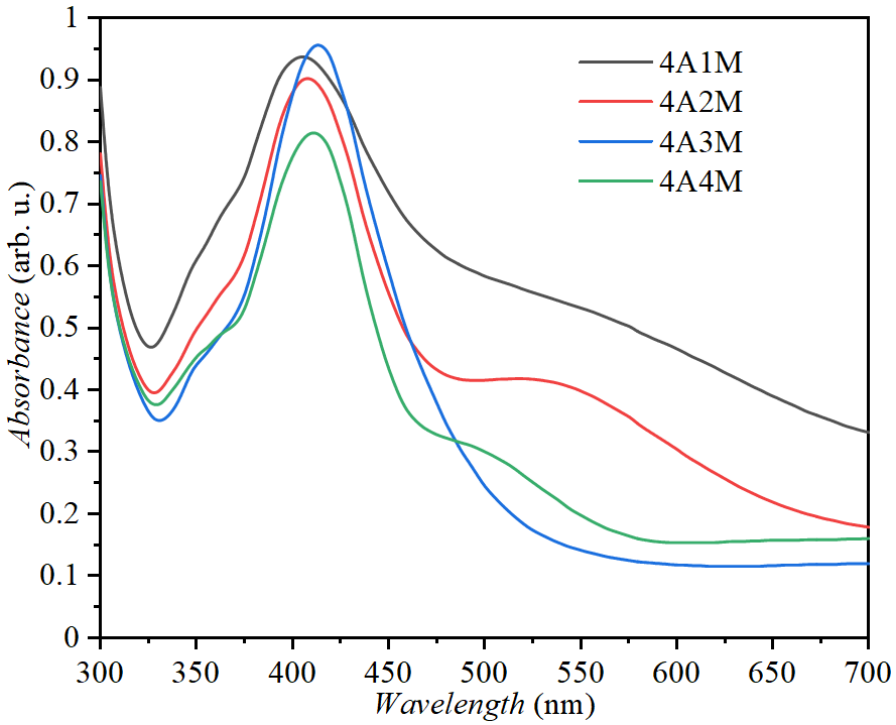

Figure 22:Absorption spectra of hydrazine hydrate-reduced Ag NPs (the effect of increased temperature):4A1M, 4A2M, 4A3M and 4A4M.

It is visible that broadness of absorption peak decreases with increasing temperature - as confirmed by SEM analysis, shape of particles became from anisotropic to isotropic. Size distribution should be mentioned as well - with increasing temperature, size and size distribution of Ag NPs decreased. The dependence between size and shape of nanoparticles and their optical properties is very clearly visible from this analysis. This set of experiments showed that temperature plays an important role that affects properties of final Ag NPs. The most significant properties that changed were shape and size of Ag NPs. With increasing temperature shape turned from anisotropic into spherical and size of nanoparticles decreased. This was confirmed by SEM analysis, where the change of shape and size of Ag NPs was clearly visible. UV-VIS spectrometry also revealed differences between samples. Samples with mostly anisotropic shape have different optical response from spherical nanoparticles. Particles with anisotropic shape can have specifics also in the infra-red (IR) region [151]. However, nanoparticles of all samples were stable only for ≈ 7 days, which is not sufficient for subsequent utilization. Thus, another modification of procedure was provided.

5.1.3.3 The effect of UV-irradiation

Figure 23 shows SEM analysis of samples X, A, B and C prepared via synthesis utilizing UV- irradiation with different wavelengths. Sample X was prepared in dark as a control.

Sample X - darkness: As can be seen on SEM image (Figure 23 - left), Ag NPs prepared in dark environment have spherical shape. Size distribution is very wide and ranges from 10 nm to 150 nm.

Sample A - wavelength of 254 nm: Ag NPs irradiated with the UV-source with wavelength of 254 nm are small, up to 50 nm (Figure 23 - second from the left). Agglomeration is also visible. In comparison to previous sample X, size of Ag NPs decreased. It is probably caused by the UV-irradiation, which gives additional energy to the reaction system.

Sample B - wavelength of 366 nm: These Ag NPs were irradiated with wavelength of 366 nm (Figure 23 – second from the right). Ag NPs. Morphology of these Ag NPs changed visibly. There is a mixture of smaller particles with spherical shape but also bigger particles with anisotropic shape are observable. Size distribution is wide and ranges from 10 nm to 50 nm.

Sample C - wavelength of 400 nm: Last sample of Ag NPs was irradiated with the UV- lamp with wavelength of 400 nm (Figure 23 - right). Ag NPs from this sample evince also anisotropic shape. According to the literature, with longer wavelengths the shape of Ag NPs can turn from spherical to anisotropic [152]. Number of particles with bigger size was increased in comparison to sample B. Size of Ag NPs vary from 10 nm to 50 nm. Agglomeration is visible.

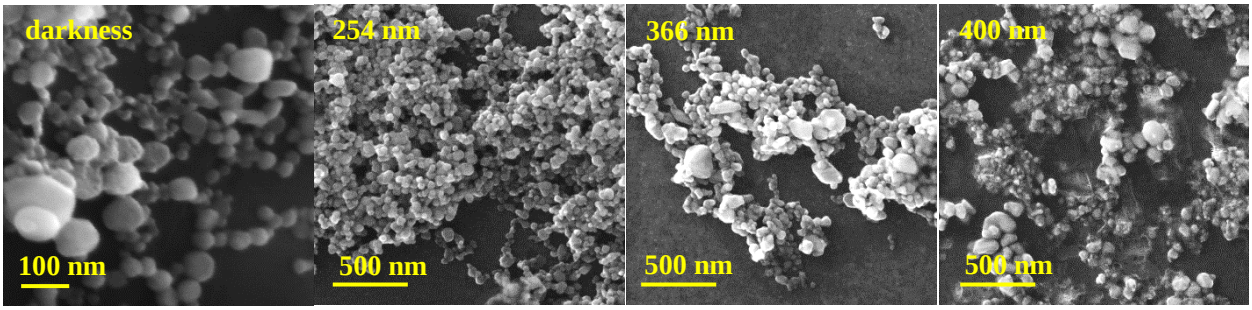

Figure 23: SEM images of hydrazine hydrate-reduced Ag NPs (the effect of UV- irradiation), from the left: samples X, A, B and C.

TEM analysis was provided only for three of these samples, namely A, B and C. TEM images can be seen in Figure 24 (sample A-left, sample B-center, sample C-right). This analysis confirmed that Ag NPs from sample A have spherical shape. Ag NPs from sample B can be

grown together, as visible from TEM image. Ag NPs from sample C are agglomerated with various shapes, this sample has the widest range of shape and size distribution of all prepared samples. Thus, with increasing wavelength of UV-irradiation shape of nanoparticles turned from spherical to anisotropic such as triangles with truncated tops, spheres and also rods. Number of Ag NPs with bigger size increased as well.

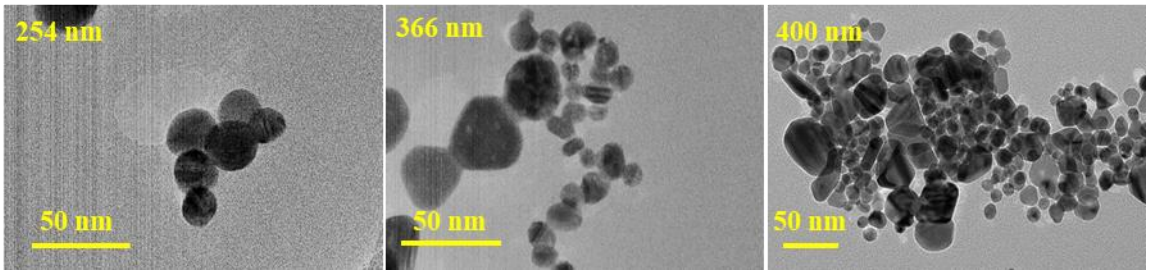

Figure 24: TEM images of hydrazine hydrate-reduced Ag NPs (the effect of UV-irradiation), from the left: samples A (left), B (center) and C (right).

Absorption spectra of samples X, A, B and C are shown in Figure 25. All samples have typical absorption maximum of SPR at the wavelength of 420 nm. Sample X evince the highest intensity of absorption peak of all samples, probably due to big particles. The absorption spectra of samples A and B are very similar with little difference that sample A shows higher intensity of SPR, which can be caused by smaller particles present in the solution as confirmed by SEM and TEM. Absorption spectrum of sample C is different, it has the highest intensity of UV-irradiated samples and exhibits also secondary absorption peak at higher wavelengths which is probably caused by bigger size of Ag NPs and also their anisotropic shape.

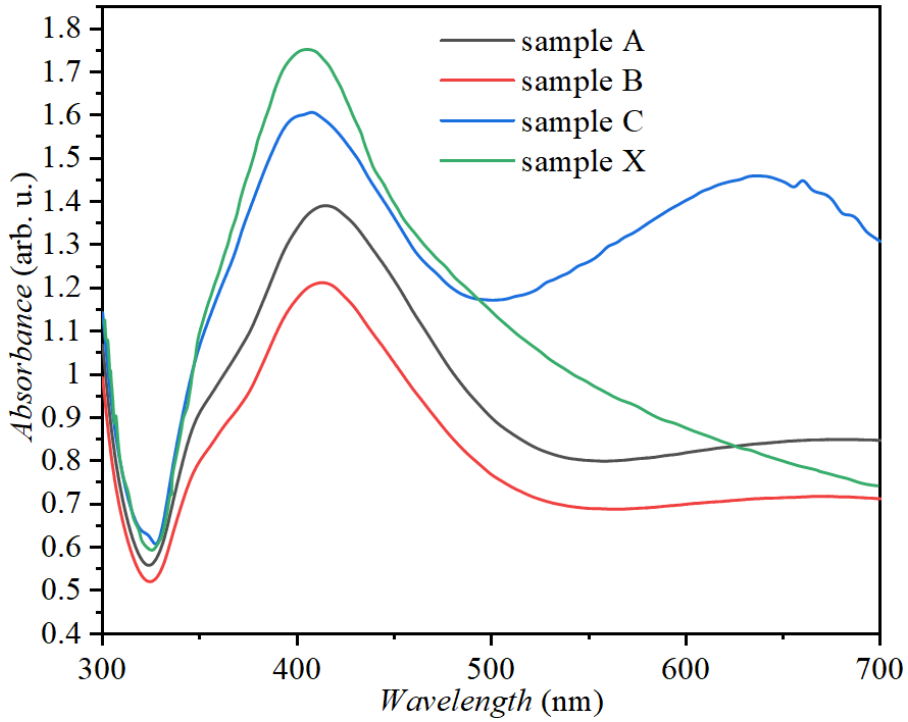

Figure 25: Absorption spectra of hydrazine hydrate-reduced Ag NPs (the effect of UV-irradiation): samples A (UV-254 nm), B (UV-366 nm), C (UV-400 nm) and X (darkness).

Stability of as prepared Ag NPs was measured within 3 weeks by UV-VIS absorption spectrometry (see Figure 26). Stability of samples A, B and C lasted for 3 weeks. Sample X

was stable for ≈ 7 days after preparation procedure. After this period, agglomerates could be seen at the bottom of the flask. Thus, long-term stability of this sample was not measured.

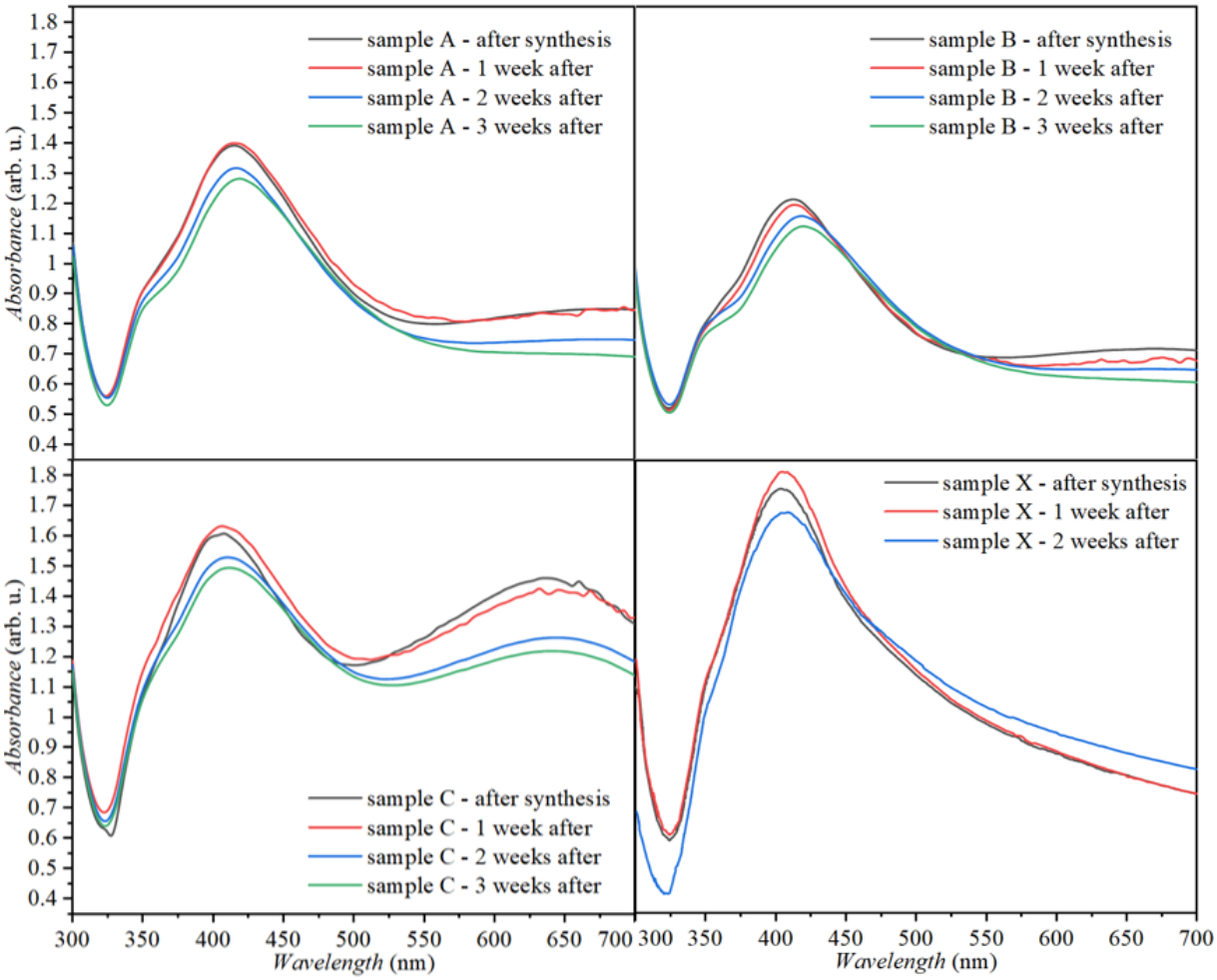

Figure 26: Stability of hydrazine hydrate-reduced Ag NPs (the effect of UV-irradiation): samples A (UV-254 nm), B (UV-366 nm), C (UV-400 nm) and X (darkness) measured by UV-VIS absorption spectrometry.

These experiments showed that UV-irradiation has significant effect on final properties of Ag NPs. Most significant changes appeared for shape and size of Ag NPs. With increasing wavelength of UV-irradiation, the shape of Ag NPs turned from spherical to anisotropic. UV-irradiation gives additional energy to the reaction mixture. The size of Ag NPs increased, as well. These particles were stable for 3 weeks as confirmed the UV-VIS spectrometry. After this period, sediments were seen at the bottom of the flask. Thanks to the stability of weeks, Ag NPs were sufficient for other experiments.

5.1.3.4 The effect of UV-irradiation combined with decreased temperature

One additional experiment was done. As we know from previous experiments, temperature influences the final properties of Ag NPs. When UV-irradiation was used, it is another energy that is given to the reaction system and it produces heat. Thus, UV-irradiation was combined with cooling of reaction mixture to temperature of 15 ºC.

Figure 27 shows SEM images of samples AT (UV-254 nm), BT (UV-366 nm) and CT (UV-400 nm). All samples of Ag NPs have anisotropic shape. Size and shape distribution are heterogeneous and very wide. Sample CT shows higher number of bigger plate particles.

Ag NPs in all samples are agglomerated and probably also grown together. Size of all samples varies from 20 nm to 100 nm.

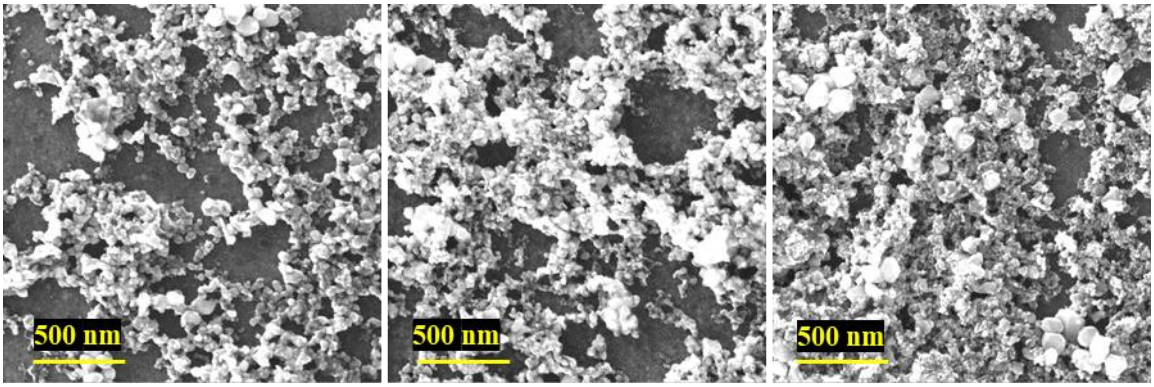

Figure 27: SEM images of samples hydrazine hydrate-reduced Ag NPs (the effect of UV-irradiation combined with decreased temperature), from the left: samples AT (UV-254 nm), BT (UV-366 nm) and CT (UV-400 nm).

UV-VIS spectrometry was provided as well. Figure 28 shows final absorption curves of all samples.

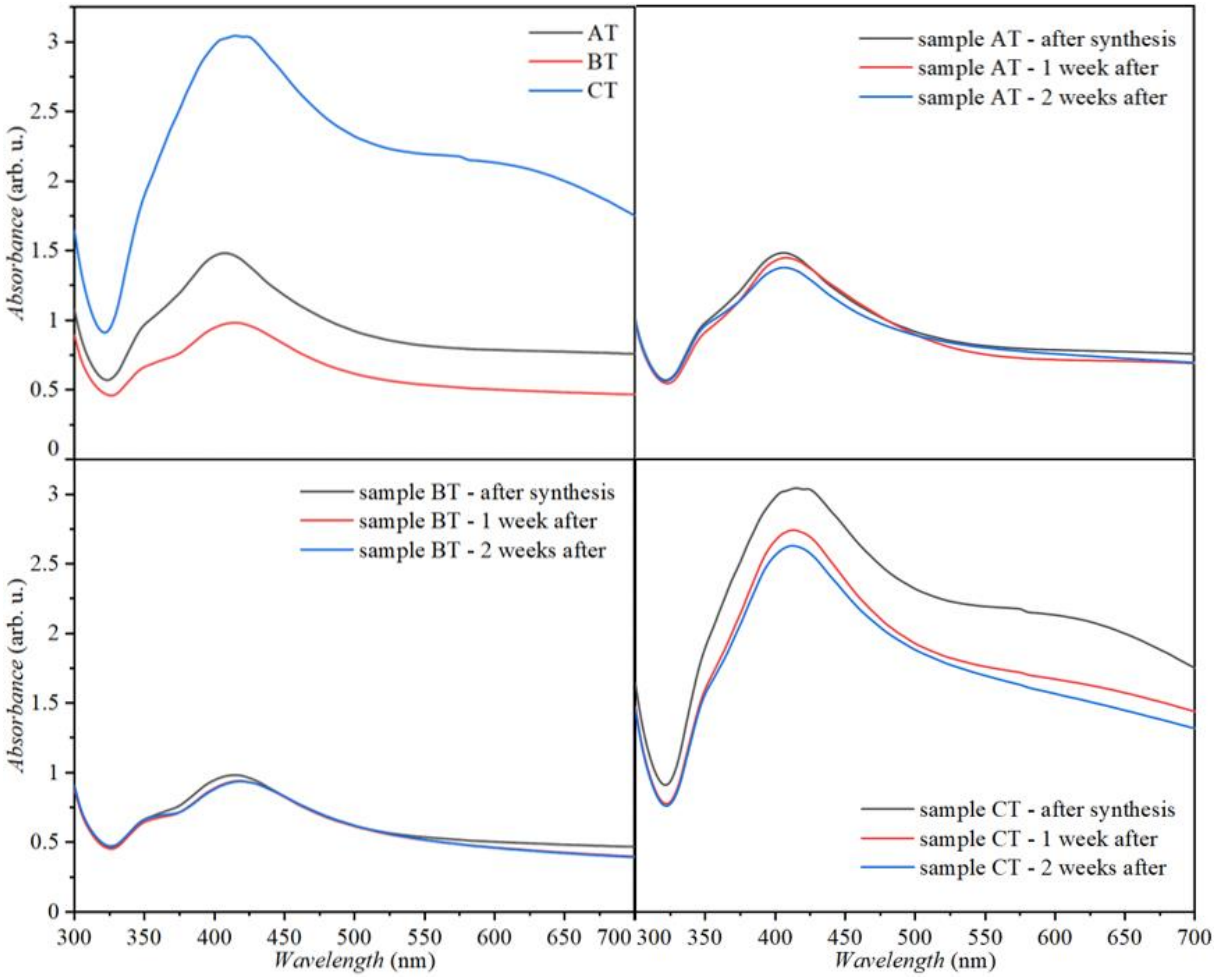

Figure 28: Absorption spectra of hydrazine hydrate-reduced Ag NPs. The effect of UV-irradiation combined with decreased temperature: samples AT (UV-254 nm), BT (UV-366 nm) and CT (UV-400 nm).

All samples have typical absorption maximum at the wavelength of 410 nm, which is typical for Ag NPs. Comparison of absorbance of all samples shows different intensity of the absorption peak, which can be cause by different sizes and shapes of Ag NPs. These absorption spectra are very similar to samples A, B and C from previous experiment, where only UV- irradiation was used for synthesis. Sample B has the lowest intensity and sample C has the highest intensity, which is most probably caused by anisotropic shape and by higher number of bigger particles.

Preparation procedure of these particles was demanding because of the cooling system. Stability lasted only for 2 weeks after synthesis. These Ag NPs were not further used for experiments because of very demanding preparation process utilizing the cooling system. These samples served mainly as a demonstration to a fact that not only increasing but also decreasing temperature can have significant impact on Ag NPs final properties.

5.1.4 Cytotoxicity of silver nanoparticles

Hydrazine hydrate-reduced Ag NPs samples prepared under UV-light: A (UV-254 nm), B (UV-366 nm), C (UV-400 nm) and X (darkness) were tested using MTT assay to determine their cytotoxicity. After the experiment, when Ag NPs were incubated with cell culture, viability of cells was calculated related to concentration of Ag NPs. Table 11 shows viability and standard deviation (SD) of cytotoxicity measurement of Ag NPs with different concentrations and also incubation time of individual samples that were tested:

Table 11: MTT cytotoxicity assay of hydrazine hydrate-reduced Ag NPs prepared with utilization of UV-irradiation - viability of cells after exposure to Ag NPs (NA - not available).

	4 h incubation		**6 h incubation**	
Ag NPs concentration (µg/ml)	A (viability % + SD)	B (viability % +SD)	C (viability % +SD)	X (viability % + SD)
220	95 ± 4	81 ± 6	NA	NA
200	NA	NA	70 ± 6	NA
110	96 ± 2	94 ± 4	NA	NA
100	NA	NA	74 ± 2	NA
55	96 ± 3	NA	NA	NA
50	NA	NA	86 ± 2	48 ± 6
30	98 ± 5	93 ± 2	NA	56 ± 7
25	NA	NA	90 ± 3	NA
20	96 ± 5	94 ± 2	NA	70 ± 4
10	97 ± 4	94 ± 1	93 ± 4	79 ± 1
5	NA	98 ± 3	93 ± 8	80 ± 4
2.5	NA	NA	NA	90 ± 6

Figure 29 shows graphical representation of the results of MTT assay tested on Ag NPs. However, during this assay, several difficulties occurred. All tested samples of Ag NPs possess high value of measurement error but most significantly sample B. These errors are attributed to very difficult preparation of Ag NPs for this test. MTT assay requires exact concentrations of Ag NPs to determine, which concentration causes cytotoxicity. Thus, Ag NPs were centrifugated at the speed of 14 500 rpm for 1 h and 30 min. After that, supernatant was removed and sediment with particles was placed to a small Petri dish. Subsequently Ag NPs were dried in the oven at 80 ºC for 1 h. The yield of Ag NPs was very small and it was very

difficult to scrub the dried Ag NPs from the Petri dish. Another point, which should be discussed is the drying temperature, which might change the properties of Ag NPs. Another obstacle was stability of Ag NPs. Ag NPs were originally dispersed in deionized water but water is not appropriate medium for cell culture used in this cytotoxicity assay (it can cause lysis or rupture of the cells), thus it could negatively affect not only the cell culture but also the results of the testing. Ag NPs had to be dissolved in DMEM medium but they agglomerated immediately - agglomerates could be seen by eye. Thus, vial with Ag NPs was placed to an ultrasound bath with for 10 min. This procedure helped to disperse the Ag NPs to colloidal solution but only for a limited period of ≈ 24 h. After this time, agglomerates of Ag NPs were visible at the bottom of the vial, again. Additionally, some resulting values of cell viability were excluded because of statistical reasons. Nevertheless, despite that there were issues with Ag NPs preparation and their colloidal stability. All of the samples evince a certain trend of cell mortality with increasing concentration. Graph also shows that viability of cell culture was only ≈ 90 % at the beginning of the test for sample X and for sample C. In this case it cannot be stated that decrease of cell viability is caused only by Ag NPs.

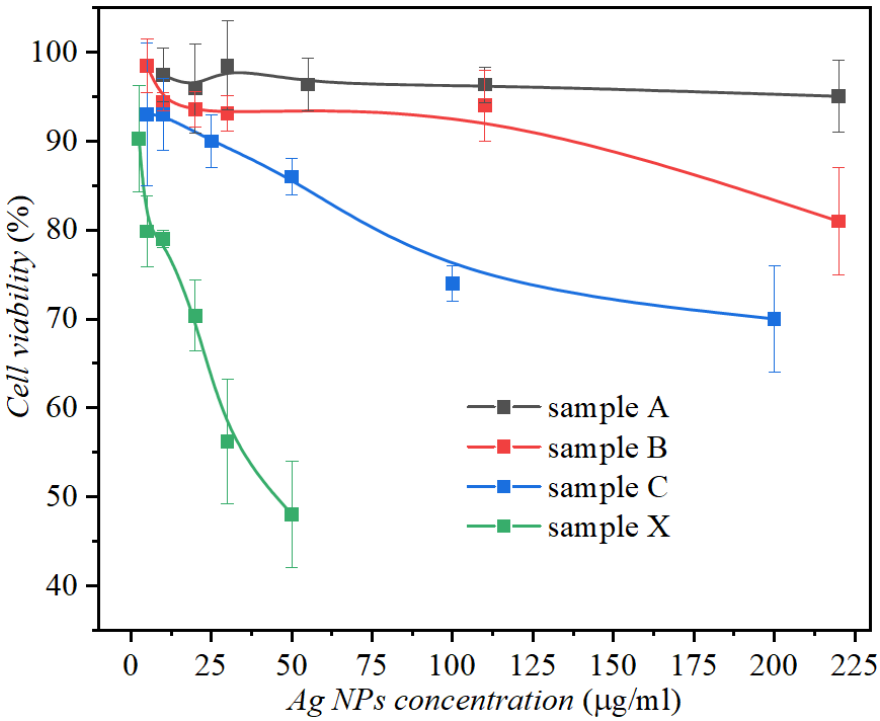

Figure 29: MTT cytotoxicity assay of hydrazine hydrate-reduced Ag NPs prepared under UV-irradiation - viability of cell culture related to concentration of Ag NPs samples A (UV-254 nm), B (UV-366 nm), C (UV-400 nm) and X (darkness).

Cell viability can be affected by many factors such as sterility of environment, incubation conditions, medium content etc. It points to that also a human factor needs to be considered when error measurement is provided.

5.1.5 Antimicrobial activity of silver nanoparticles

Three antimicrobial methods were employed to determine the antimicrobial properties of hydrazine hydrate-reduce Ag NPs: disk-diffusion method, measurement of growth curves and dilution method with subsequent counting of grown colonies. Three samples prepared under UV-irradiation were used, namely A (UV-254 nm), B (UV-366 nm) and C (UV-400 nm). Ag NPs were tested against strains *S. aureus* and *E. coli*.

5.1.5.1 Disk-diffusion method

Following Table 12 shows concentration of Ag NPs on individual paper filter disks dednoted from number 1 to number 6 for applied against *S. aureus* and *E. coli*:

Table 12: Disk diffusion method - tested concentration of hydrazine hydrate-reduced Ag NPs prepared with utilization of UV-irradiation (samples A, B and C).

Sample name	Filter disk number	Concentration
A	1	5.207 mg/ml
B	2	5.207 mg/ml
C	3	5.207 mg/ml
A	4	0.057 mg/ml
B	5	0.057 mg/ml
C	6	0.057 mg/ml

Figure 30 shows results from disk-diffusion method. Both controls, amoxicillin (conctrol for *E. coli*) and penicillin (control for *S. aureus*) inhibited the growth of bacterial cultures. Unfortunately, no inhibition zones were measured for Ag NPs used against strain *E. coli*. This can be caused by several factors: most probably because Ag NPs could not diffund into the agar from the paper filter disk. Another explanation could be that *E. coli* have a resistance against Ag NPs or that the concentration of Ag NPs is very low. Thus, these Ag NPs did not suprress the growth of the *E. coli* cell culture. However, inhibition zones for strain *S. aureus* were observed on all of the samples. Most significant inhibition zones show samples 3 and 4. Nevertheless, these inhibition zones are very small. Thus, it can not be stated that Ag NPs evince strong antimicrobial effect. This method did not show any relevant antimicrobial properties of Ag NPs. Thus, another method was utilized to determine whether the Ag NPs are or are not antimicrobial.

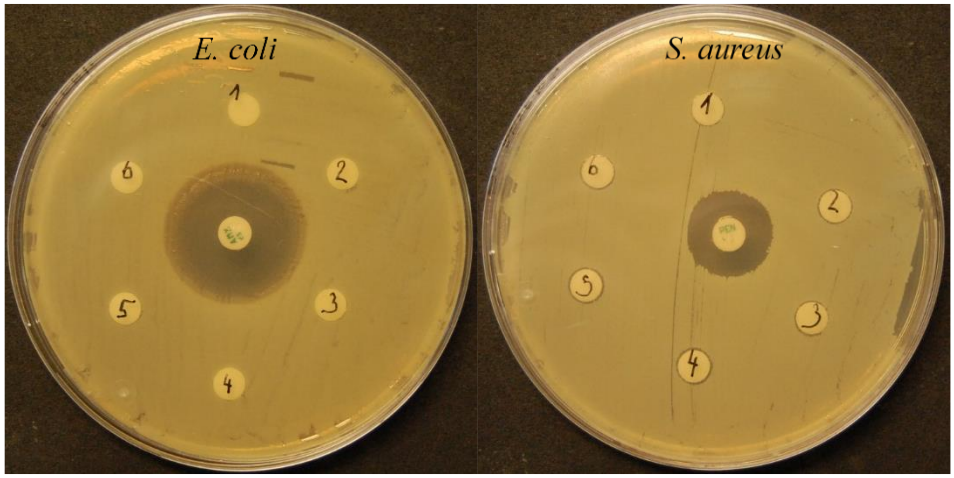

Figure 30: Disk diffusion method - hydrazine hydrate-reduced Ag NPs prepared under UV-irradiation applied against E. coli (left) and S. aureus (right).

5.1.5.2 Growth curves

Another method was employed to determine antimicrobial properties of Ag NPs, namely measurement of growth curves. Figure 31 show results from this experiment with applied samples prepared using UV-light, namely sample A (UV-254 nm), B (UV-366 nm) and C (UV-400 nm).

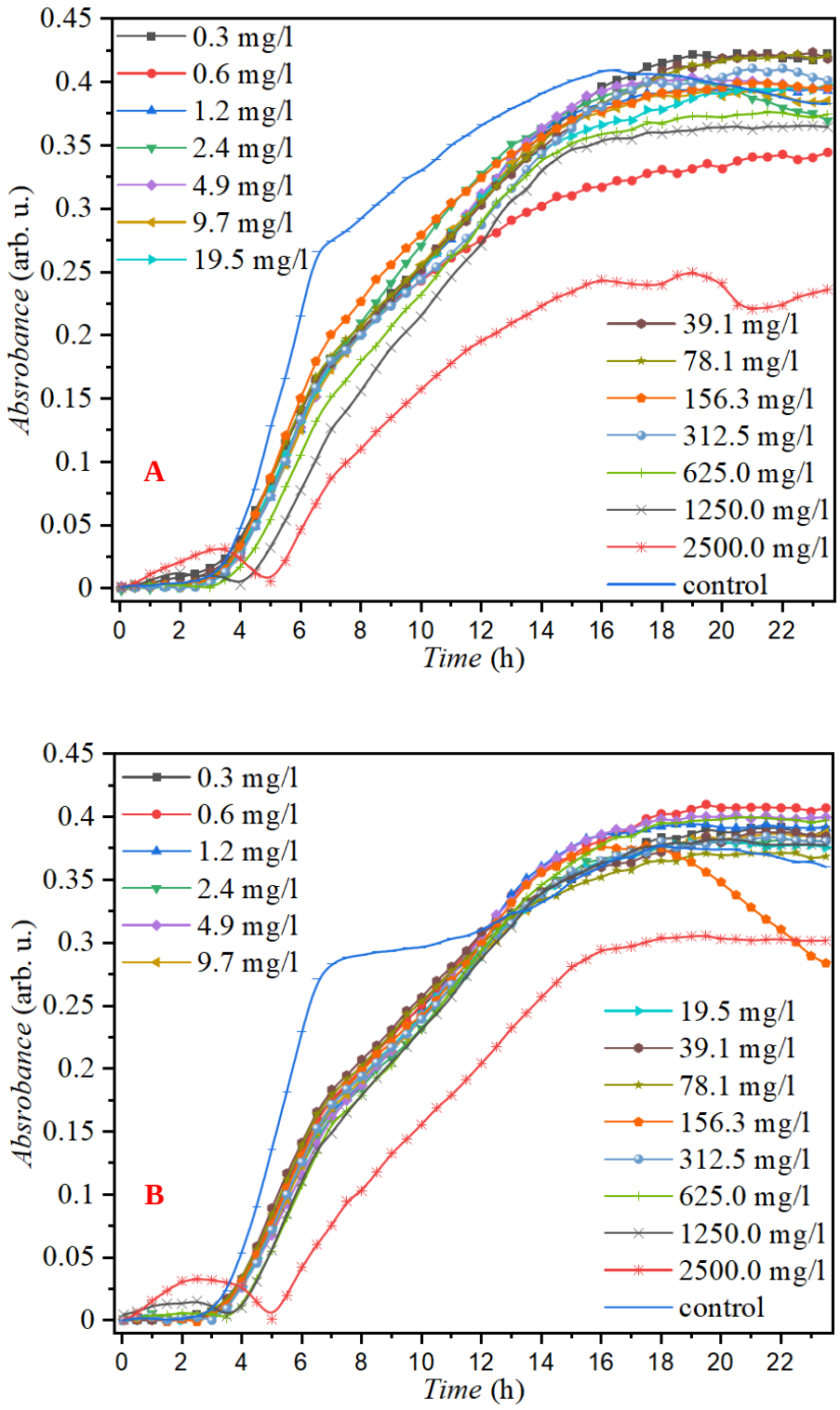

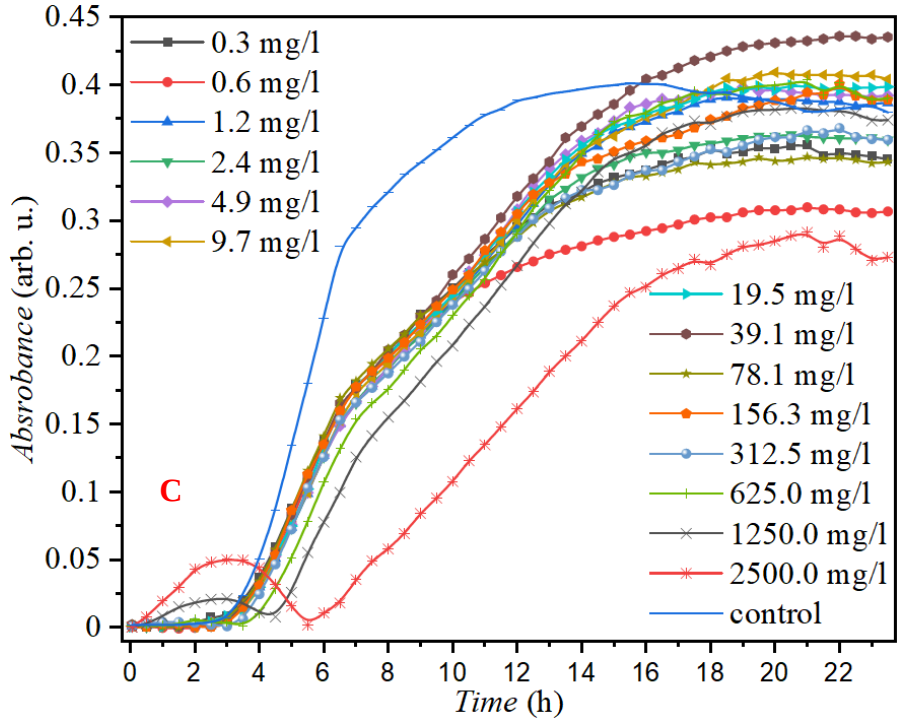

Figure 31: Growth curves of S. aureus with applied hydrazine hydrate-reduced Ag NPs prepared under UV-irradiation: A (UV-254 nm)-top, B (UV 366 nm) - middle, C (UV-400 nm) - bottom.

Ag NPs were applied with various concentrations to determine, which one of them can suppress or affect the growth of the cell cultures. Concentration of Ag NPs varied from 0.31 mg/ml to 2 500 mg/ml. The highest concentration of 2 500 mg/ml showed partial suppression of cell growth for all applied samples, where the cell culture did not grow to the maximum values as a control (control was only bacterial culture without Ag NPs). The most significant inhibition of growth is visible for sample A. Unfortunately, results are not significant and antimicrobial effect of Ag NPs could not be confirmed. This can by caused by fact, that the concentration of Ag NPs is too low or that Ag NPs are not effective against strain *S. aureus.* Dark color of colloidal solutions with higher concentrations could also decreases spectroscopy analysis accuracy.

The same experiment was provided for strain *E. coli.* Figure 32 shows results from measuring growth curves of *E. coli* with applied concentrations of Ag NPs. As in previous case, fourteen different concentrations of Ag NPs were applied (from 0.31 mg/ml to 2 500 mg/ml). The highest concentration of 2 500 mg/ml showed partial suppression of bacterial culture for all samples. The most significant result was observable for sample C, where the growth of cell culture was successfully stopped. However, this result could be affected by dark color of the colloidal solution and could cause issues during spectroscopy reading.

This method showed that several concentrations of Ag NPs can suppress the growth of bacterial cell culture or even stop the growth. However, results from testing Ag NPs against *S. aureus* were not significant and spectroscopy reading could be affected by dark color of the colloidal solutions of Ag NPs (especially at higher concentrations). Thus, another test was provided to confirm the antimicrobial properties of Ag NPs, where spectroscopy measurement is not necessary to determine the results.

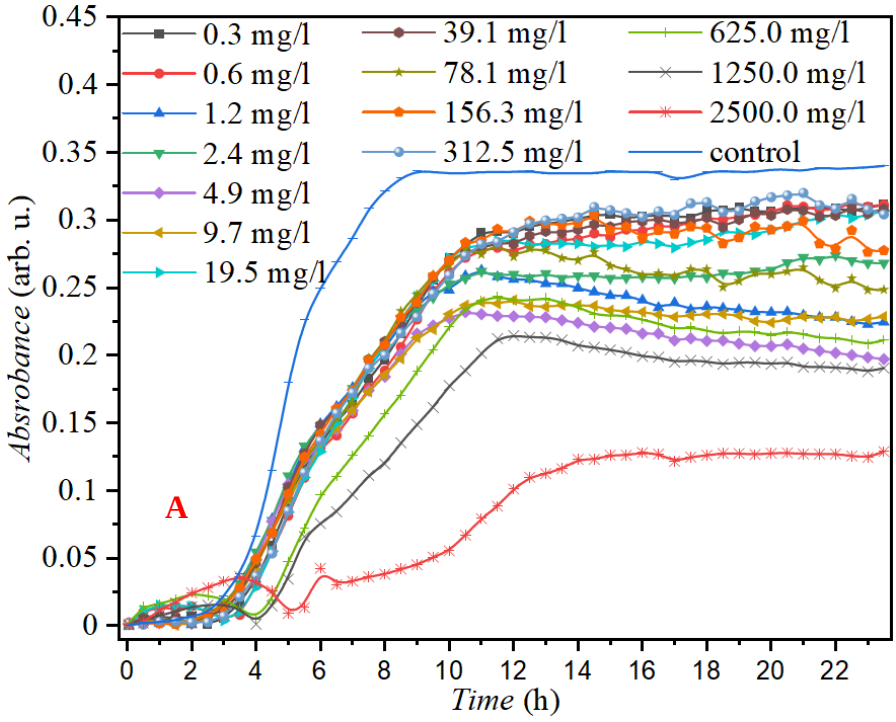
0.3 mg/l
0.6 mg/l
1.2 mg/l
2.4 mg/l
4.9 mg/l
9.7 mg/l
19.5 mg/l
39.1 mg/l
78.1 mg/l
156.3 mg/l
312.5 mg/l
625.0 mg/l
1250.0 mg/l
2500.0 mg/l
control
A
Absrobance (arb. u.)
Time (h)

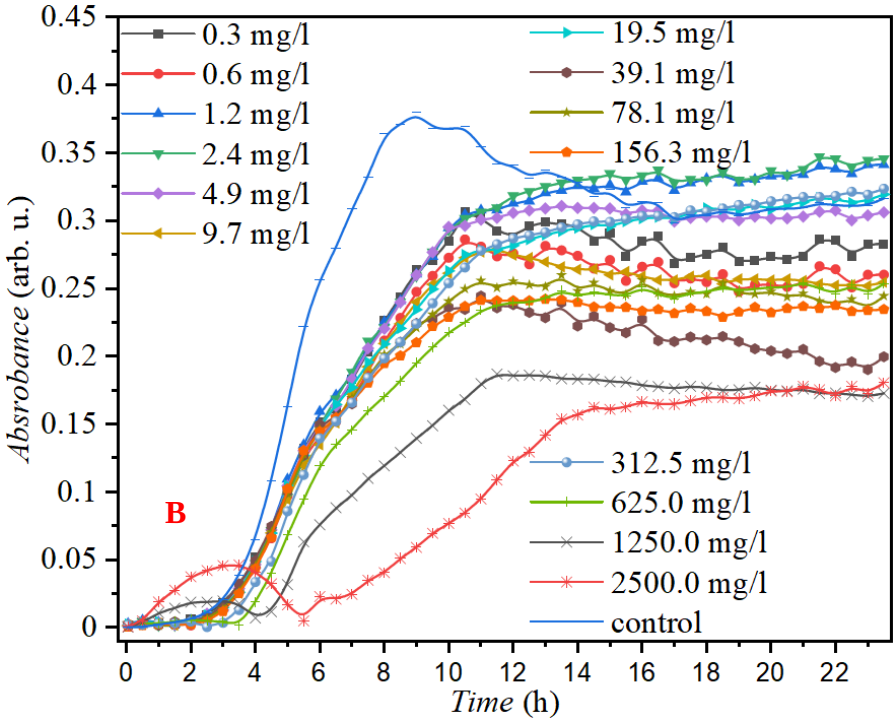
0.3 mg/l
0.6 mg/l
1.2 mg/l
2.4 mg/l
4.9 mg/l
9.7 mg/l
19.5 mg/l
39.1 mg/l
78.1 mg/l
156.3 mg/l
312.5 mg/l
625.0 mg/l
1250.0 mg/l
2500.0 mg/l
control
B
Absrobance (arb. u.)
Time (h)

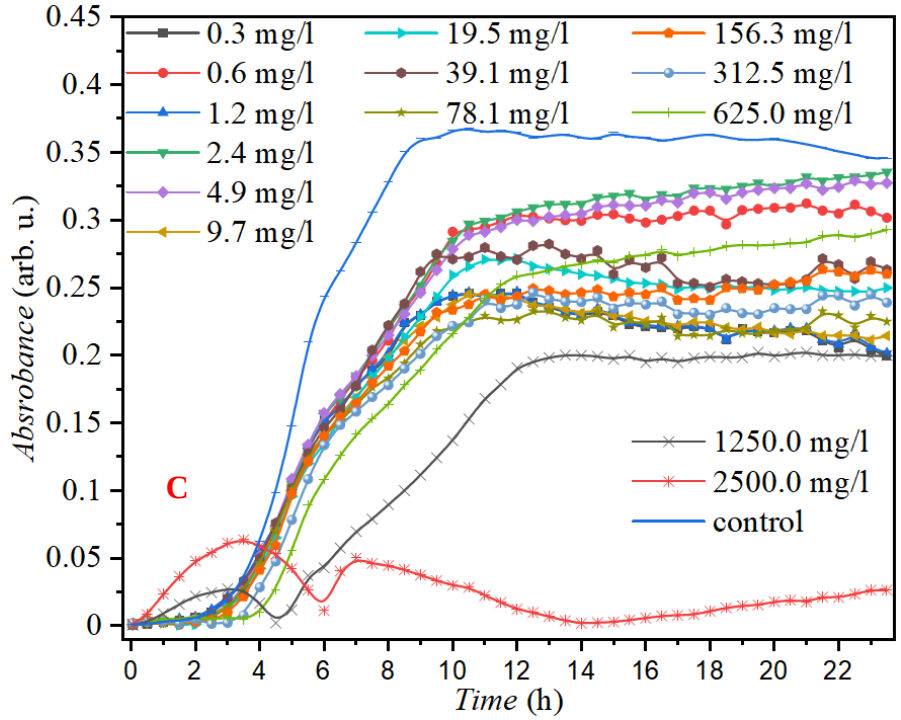

Figure 32: Growth curves of E. coli with applied hydrazine hydrate-reduced Ag NPs prepared under UV-irradiation: A (UV-254 nm) - top, B (UV-366 nm) - middle, C (UV-400 nm) - bottom.

5.1.5.3 Dilution method

Dilution method was employed to determine the antimicrobial properties of Ag NPs, where Ag NPs were added directly to the medium and cell culture was let to grow in such prepared medium. Grown colonies were manually counted in the final step. Figure 33 shows results from testing Ag NPs against *S. aureus*. This test determines how effectively Ag NPs can prevent cell culture from growing. As results showed, samples A and C seem to be the most effective. They were able to stop the growth of *S. aureus* almost of 50 %. Unfortunately, sample B did not prevent cell culture from growing (only very slightly).

Figure 34 shows results from testing Ag NPs against *E. coli* growth. Results are very similar to previous experiment, where Ag NPs were tested against *S. aureus* growth. Most effective were samples A and C. They stopped the growth of *E. coli* almost of 20 %. However, sample B supported the growth of this culture.

From the above-mentioned tests, it seems that Ag NPs possess a greater effect against *S. aureus* than *E. coli*. Reading the results of the growth curves by spectroscopy could be influenced by the dark color of colloidal samples (especially at higher concentrations). However, final tests using the dilution method, where spectroscopy was not required, showed that Ag NPs were more effective against bacterial culture *S. aureus*. In a respect to all these facts and also to the fact that also the disk-diffusion method showed at least partial antimicrobial activity, it can be concluded that Ag NPs evince partial antimicrobial effect against *S. aureus*. However, bacteriostatic rather than bactericidal effect should be considered because bacterial growth has not been completely stopped by any of the applied samples of Ag NPs with various concentrations.

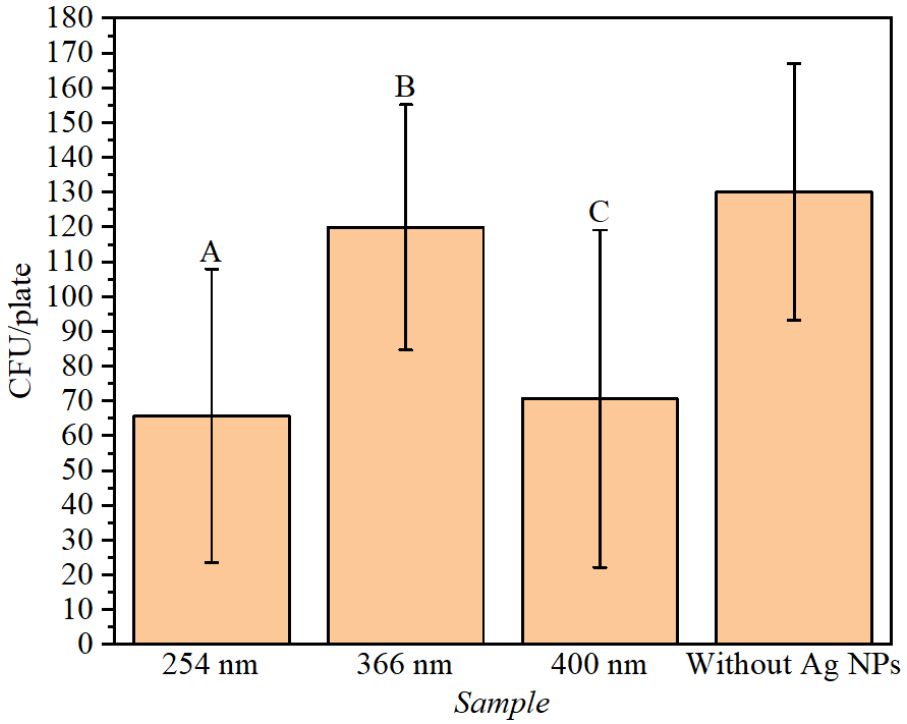

Figure 33: Colony forming units of S. aureus with applied hydrazine hydrate-reduced Ag NPs prepared under UV-irradiation: samples A, B and C.

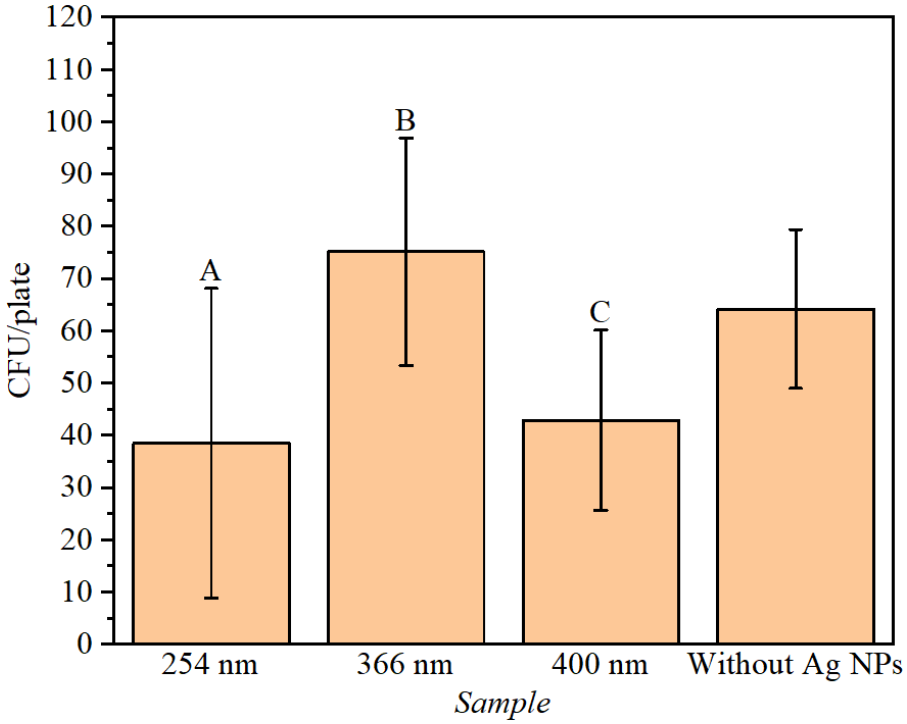

Figure 34: Colony forming units of E. coli with applied hydrazine hydrate-reduced Ag NPs prepared under UV-irradiation: samples A, B and C.

An interesting result was investigated for sample B, where the antimicrobial functionality occurred only minimally against *S. aureus* and for strain *E. coli* the growth of the bacterial culture even increased in comparison to the control. However, a correlation can be found

between antimicrobial action and the size and shape of Ag NPs. As mentioned several times in this work, particle size plays an important role. The smaller is the particle, the larger antimicrobial effect should occur. As we can see, samples A and C proved to be the most effective. We know from the characterization of these particles that sample A have small, mostly spherical particles with a size of about 50 nm and sample C is a mix of smaller particles (spherical) with larger particles (various shapes - spheres, rods, plate triangles with truncated tops). Therefore, the size and shape of Ag NPs also plays a role in this case. As for the culture of *E. coli*, Graves et al. published an article stating that *E. coli* is able to develop resistance against Ag NPs very quickly. This is due to the fact that the use of Ag NPs in the commercial sphere has rapidly increased in recent years (for example in cosmetics) [153].

5.2 Characterization of selenium nanoparticles

5.2.1 Ascorbic acid-reduced selenium nanoparticles

Se NPs reduced by ascorbic acid and stabilized with chitosan were analyzed by TEM and UV-VIS spectroscopy. TEM analysis is shown in Figure 35. Se NPs have spherical shape and size is about 100 nm. Se NPs are also covered by a layer, which is probably chitosan used for their stabilization. Some fragments are very significant, as well. It is probably chitosan, which did not completely dissolve in the acetic acid solution. Agglomerates were seen at the bottom of the flask right after the synthesis.

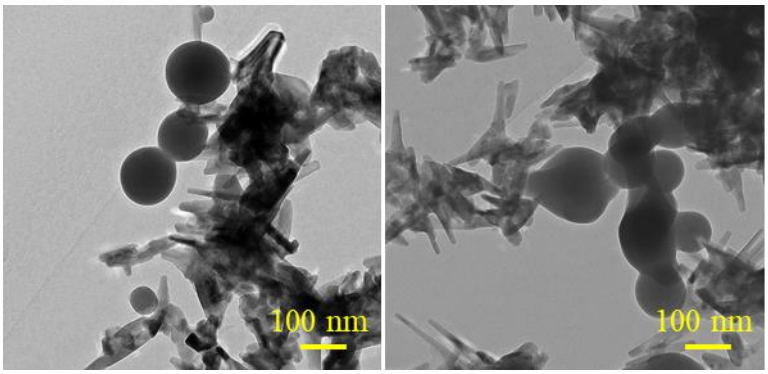

Figure 35: TEM image of ascorbic acid-reduced Se NPs, significant spherical shape (left), stabilization layer (right).

Figure 36 shows absorbance spectra of this sample determined using UV-VIS spectroscopy. The maximum of absorption peak is visible at the wavelength of 240 nm, which is typical for Se NPs. Se NPs prepared in this thesis were prepared according to published work from Yu et al. and results are similar. Se NPs in publication had spherical shape and also size about 120 nm. However, no fragments of chitosan were visible on TEM analysis they provided. The appearance of fragments of chitosan confirmed by SEM analysis are probably caused by that, the chitosan in this thesis was purchased from another supplier with different parameters such as deacetylation degree and purity. These Se NPs were not used because of the very low colloidal stability and fragments of chitosan present in the solution (stability lasted on for ≈ 1 day).

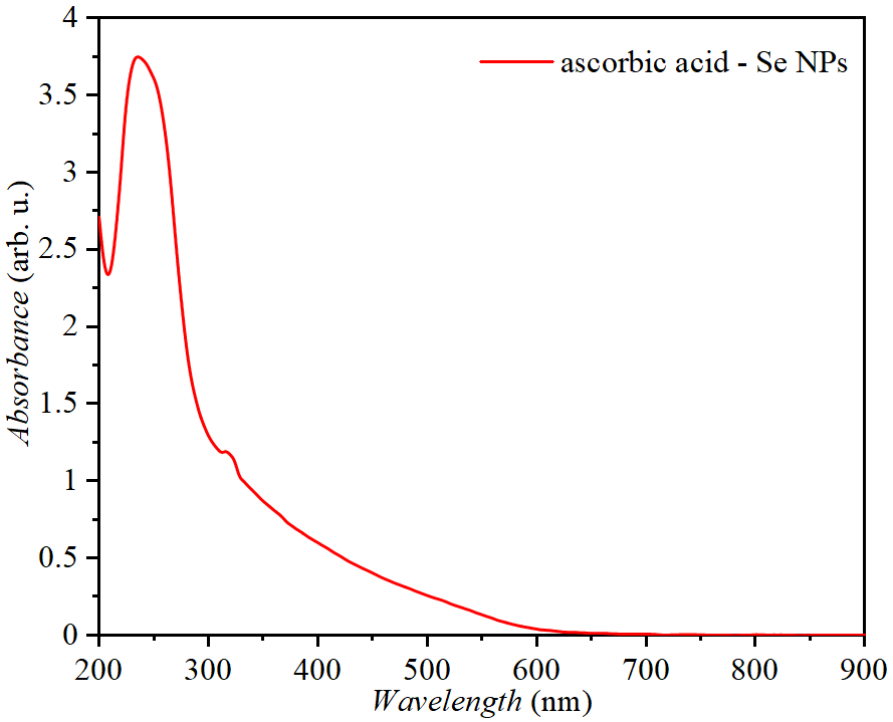

Figure 36: Absorption spectrum of ascorbic acid-reduced Se NPs.

5.2.2 Sodium hydroxide-reduced selenium nanoparticles

Sodium hydroxide-reduced Se NPs were analyzed by SEM to observe the morphology and size. shows SEM images of all prepared samples of Se NPs. As can be seen from these images, all samples of Se NPs have spherical shape. Size distribution is not narrow, most samples evince bimodal distribution. Size of Se NPs varies from 100 nm up to 200 nm.

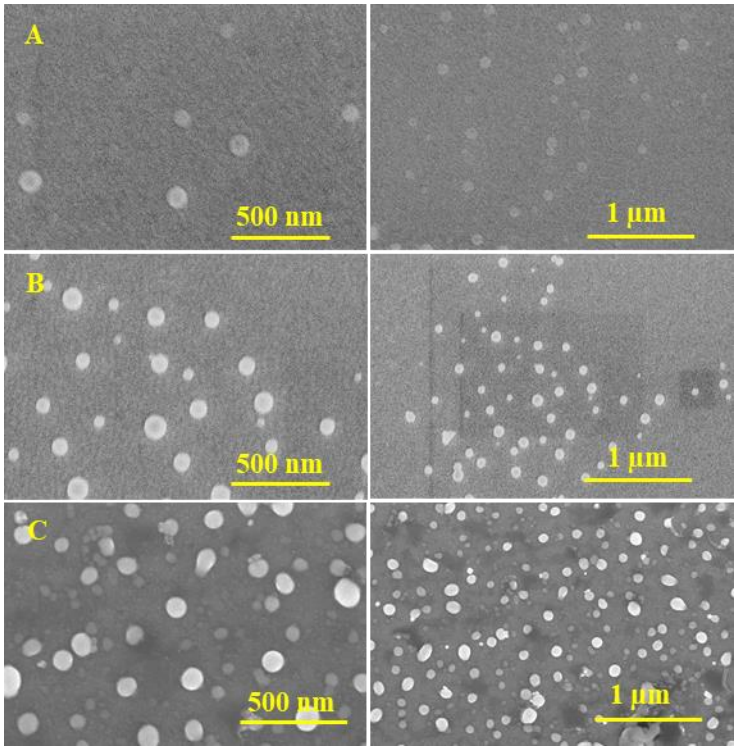

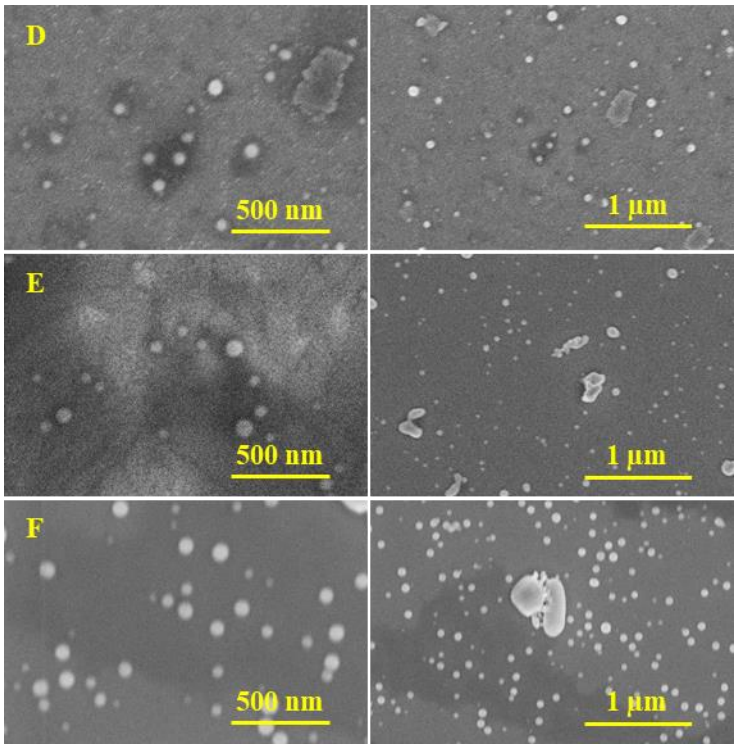

Figure 37: SEM images of sodium hydroxide-reduced Se NPs: samples A, B, C, D, E and F.

Spectrometry in UV-VIS region was performed to measure the absorbance of Se NPs samples. Figure 38 shows results of the measurement of all samples. The maximum of the absorption peak of all samples is between 320-350 nm. According to Lin et al. [154], Se NPs with size about 100 nm evince absorption maxima at the wavelength of about 350 nm. Absorption maximum is highly dependent on the size of Se NPs. The smaller is the size of Se NPs, absorption maximum appears at the lower wavelengths.

All samples are very similar to results published by Lin et. al. [154]. It seems that factors, which were investigated (presence or absence of sodium hydroxide, volume of reaction mixture and effect of stirring) did not have significant impact on final properties of Se NPs. The only property that was slightly changed is size of nanoparticles. As mentioned earlier, glutathione plays also role of reducing agent not only as a stabilizer (samples A, C, E and F). According to results, glutathione only, can effectively reduce sodium selenite to form Se NPs. Unfortunately, Se NPs prepared by this method were stable only for 3 days after preparation process, thus they were not suitable for further utilization.

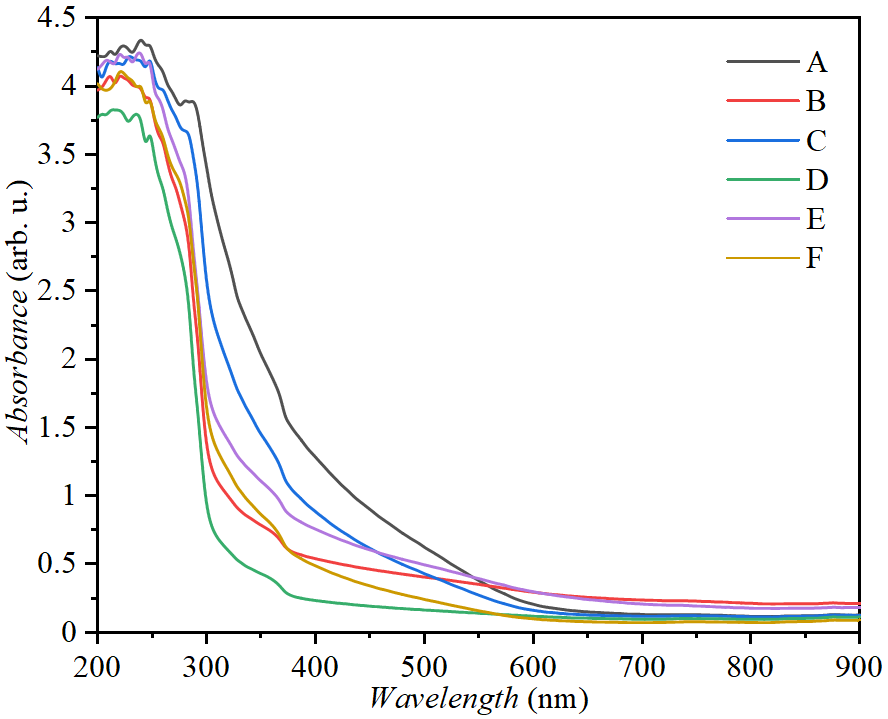

Figure 38: Absorption spectra of sodium hydroxide-reduced Se NPs: samples A, B, C, D, E and F.

5.2.3 L-cysteine-reduced selenium nanoparticles

In order to characterize the morphology and size of Se NPs, STEM analysis was performed. Figure 39 shows STEM images of sample A1 with two different magnifications with corresponding view fields of ≈ 3.45 μm (left) and ≈ 1.65 μm (right), respectively, where the PVP-29 was used as a stabilizing agent. The Se NPs do not tend to form agglomerates and they are well separated and spherically shaped. A dominant size of Se NPs is ≈ 40 nm, however the size distribution is not monodispersed.

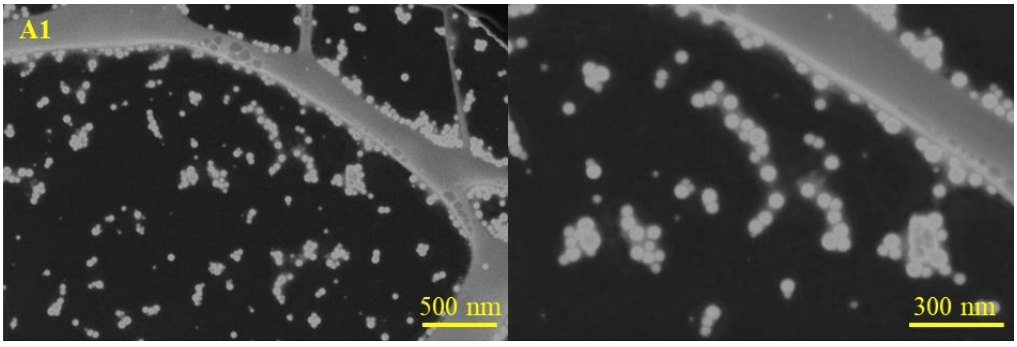

Figure 39: STEM image of L-cysteine-reduced Se NPs - sample A1 (stabilized with PVP-29).

Figure 40 shows STEM images of sample A2 with two different magnifications with corresponding view fields of 3.45 μm (left) and 1.65 μm (right), respectively, where the PVP-40 was used as a stabilizing agent. The shape of Se NPs is also spherical. A thin stabilizing layer of PVP-40 can be clearly seen on an individual particle as a white outer circle. A dominant size of Se NPs is the around ≈ 50 nm. It is obvious that size distribution of Se NPs is more monodisperse than in the sample A1.

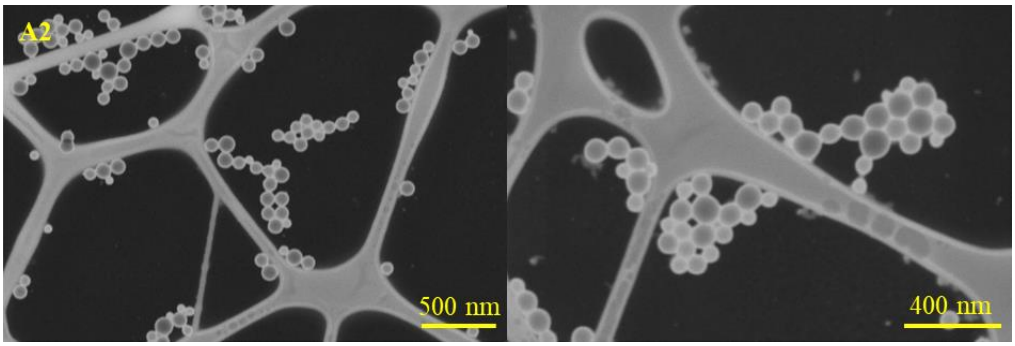

Figure 40: STEM image of L-cysteine-reduced Se NPs - sample A2 (stabilized with PVP-40).

Figure 41 shows STEM images of sample A3 with two different magnifications with corresponding view fields of 3.45 μm (left) and 1.65 μm (right), respectively, where the BSA was used as stabilizing agent. Formed Se NPs are separated and spherically shaped. Size distribution of Se NPs is highly polydispersed and size varies from 50 nm to 100 nm.

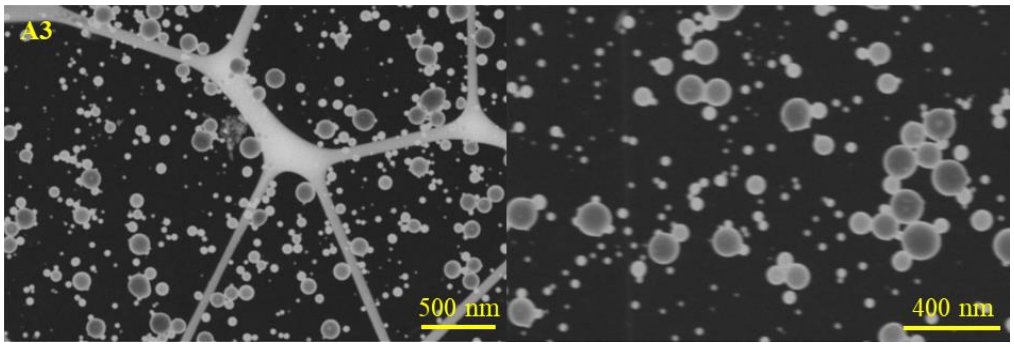

Figure 41: STEM image of L-cysteine-reduced Se NPs - sample A3 (stabilized with BSA).

Figure 42 shows UV-VIS spectroscopy of as prepared L-cysteine-reduced Se NPs. The color of all reaction mixtures changed into ruby red after ≈ 2 min. This change visually pointed to the formation of Se NPs. This analysis revealed that absorption maximum of Se NPs samples A1 and A2 is at the wavelength of 275 nm. Absorption maximum of Se NPs sample A3 is at 265 nm. As can be seen, sample A3 has a slightly shifted peak of absorption maxima, probably due to a different stabilizer in comparison to A1 (stabilized with PVP-29) and to sample A2 (stabilized with PVP-40).

The antimicrobial activity is very significantly affected by the size of particles, the smaller is the nanoparticle, the higher is the antimicrobial effect. Following this rule, sample A1 was found as a most suitable for immobilization on polymer membrane because of the smallest size among all prepared samples.

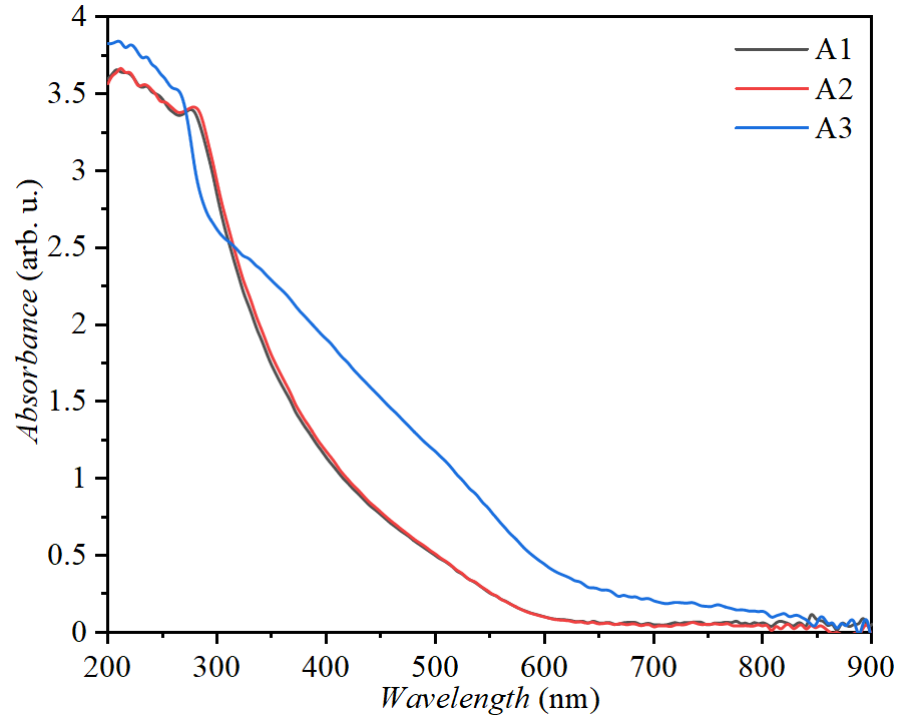

Figure 42: Absorption spectra of L-cysteine-reduced Se NPs - sample A1 (stabilized with PVP-29), A2 (stabilized with PVP-40) and A3 (stabilized with BSA).

SAXS and USAXS analyses to confirm the size of Se NPs were performed. Figure 43 shows experimental measurement of sample A1 where PVP-29 was used as the stabilizing agent.

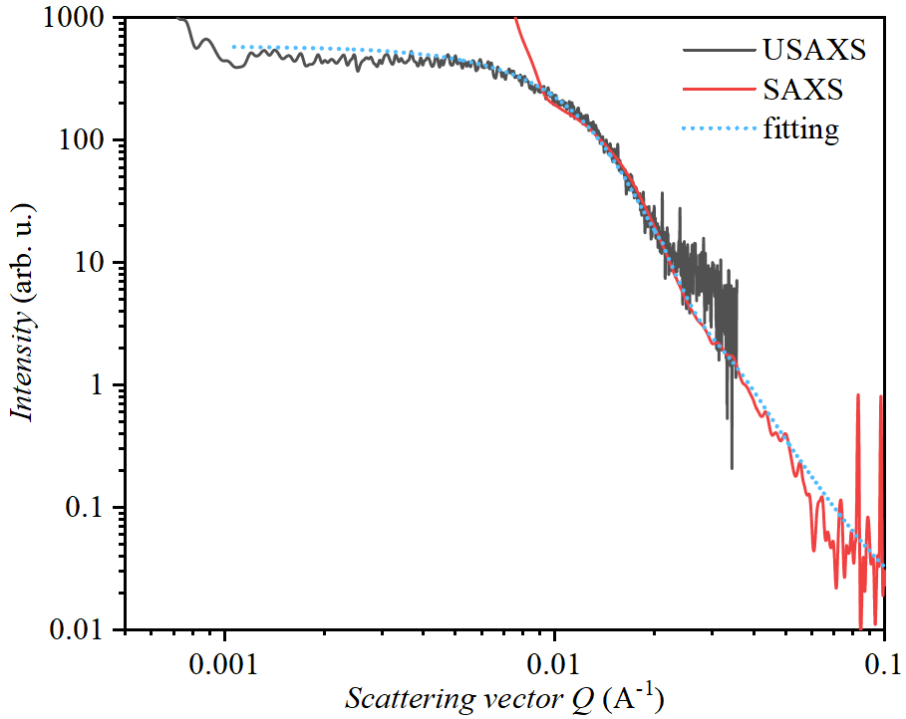

Figure 43: SAXS and USAXS measurement of L-cysteine-reduced Se NPs - sample A1 (stabilized with PVP-29).

The USAXS curve is multiplied by a factor of 25 to overlap with SAXS curve. The regions below 0.001\A-1 and 0.01\A^{-1} are affected by primary beam for USAXS and SAXS,

respectively. USAXS curve above $0.02\text{\AA}^{-1}$ is unreliable due to high background noise. Both curves were fitted with a model of spherical particles with mean diameter of (36 ± 2) nm and distribution width of (20 ± 2) %. This measurement is in correlation with STEM analysis, where dominant size of Ag NPs was determined around 40 nm. In conclusion, samples A1 and A2 are very similar. However, sample A2 evince higher size monodispersity and also slightly bigger size. Sample A1 was stabilized with PVP-29 and sample A2 was stabilized with PVP-40. Thus, it seems that the increasing length of polymer chains can potentially affect final size and size distribution. Sample A3, stabilized with BSA was completely different. Size distribution was highly polydispersed. Thus, it can be stated, that different stabilizers can have significant impact on final colloidal properties, mostly size and size distribution.

5.2.4 Cytotoxicity of selenium nanoparticles

XTT is qualitative assay and represents metabolic activity of the cell and can be related to viability of cells, under defined conditions. Metabolic activity of cells is given by mitochondrial activity, where cells produces NAD(P)H-dependent oxidoreductase enzymes, which can reduce the tetrazolium dye (XTT dye) to orange formazan [155]. In general, the darker is the resulting solution, the higher is the metabolic activity of the cell. Thus, the higher is the metabolic activity, the number of viable cells should be higher, as well. On the other hand, there is DNA cell proliferation assay, which is a quantitative analysis and reflects the proliferation of the cells. It should be noted that not all cells that are divided can survive, but still can contain BrdU. Additionally, metabolic activity is driven by several factors, not only from mitochondrial activity but also from cell proliferation rate, cell size, metabolic rate and cell survival. However, these two types of tests should not be compared because they represent different mechanisms in the cell [156]. L-cysteine-reduced Se NPs were tested (sample A1). This sample was stabilized with PVP-29 and few factors were investigated, namely Se NPs in water (sample A1W), Se NPs in medium (A1M) and Se NPs without stabilization layer dispersed in medium (A1-0M).

Thus, when cytotoxicity of various compounds is considered, in this case Se NPs, cytotoxicity can be caused by several factors, as well (metabolic activity, cell proliferation, mRNA yield, etc.). As can be seen from performed XTT assay (see Figure 44) and DNA cell proliferation assay (see Figure 45), Se NPs might be causing cytotoxic effect at higher concentrations (2 mg/l and 5 mg/l). To be more detailed, XTT test showed that Se NPs at lower concentrations can increase the metabolic activity. Se is a micronutrient and at very low concentrations, it can enhance several cell mechanisms such as metabolic activity. On the other hand, high concentration of Se NPs might have an impact on cell mechanisms such as decrease of metabolic activity or even cause cytotoxicity (cell death). This corresponds to well-known hormetic effect of Se, i.e. positive influence at adequate dose and negative at high dose [157]. As the XTT graph shows, metabolic activity decreased very significantly with increasing concentration of Se NPs (2 mg/l and 5 mg/l). DNA proliferation assay showed similar information about the concentration of Se NPs, even if it represents different mechanisms in cell. With lower concentrations, the proliferation of cells increased, but with increasing concentration of Se NPs, cell proliferation rapidly decreased. Thus, both of these tests showed that with very low concentration of Se NPs some of the mechanisms of cells can be supported even enhanced but with high concentrations of Se NPs, these mechanisms can decrease very rapidly.

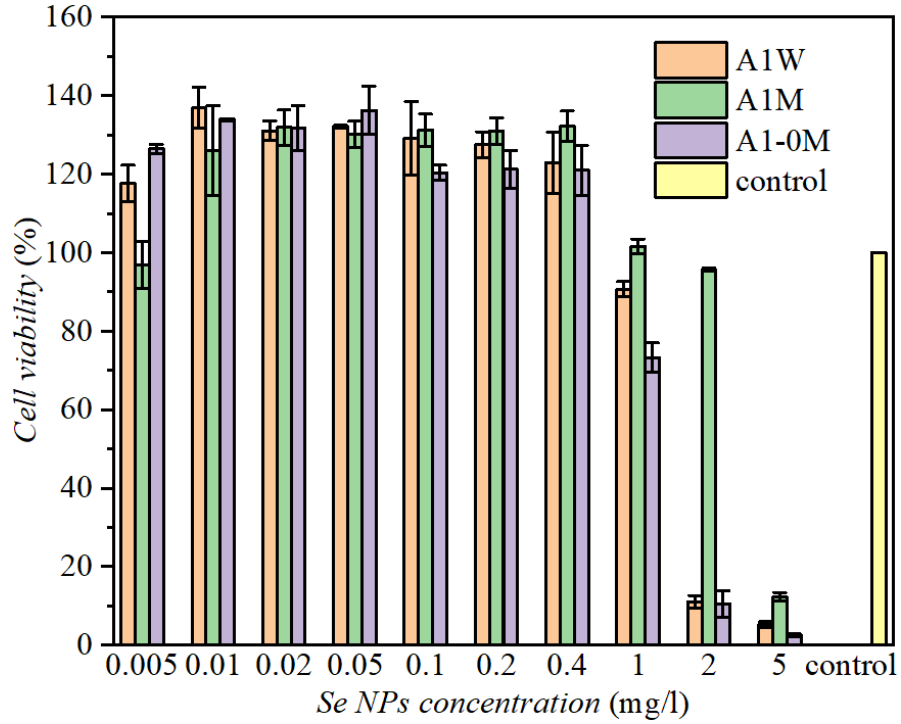

Figure 44: Results of XTT assay with applied concentrations of L-cysteine-reduced Se NPs.

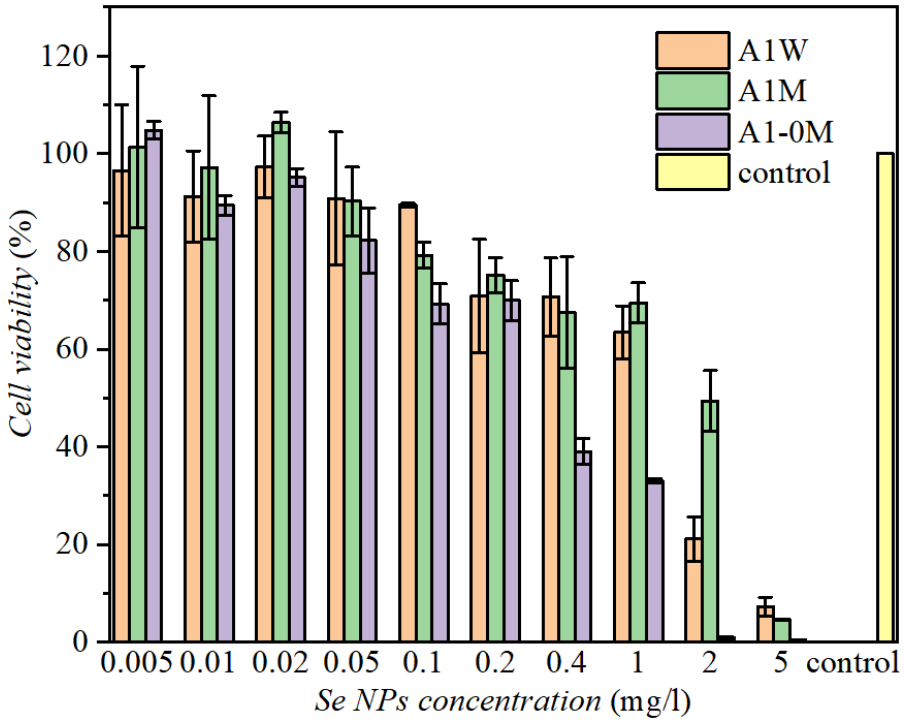

Figure 45:Results of BrdU cell proliferation assay with applied concentrations of L-cysteine-reduced Se NPs.

It can be seen that L-cysteine-reduced Se NPs have a certain cytotoxic effect at highest concentrations. On the other hand, with very small concentration of Ag NPs, metabolic activity of cells increased, probably due to fact, that Se is also a micronutrient. It is also obvious, that investigated factors such as dispersion in water or medium and absence of stabilizing compound can have impact on final cytotoxic effect of Se NPs. It is obvious that Se NPs without stabilizer

(sample A1-0M) evince the most significant cytotoxicity at highest concentrations. In this case, there was not present a stabilizing layer, thus, cell culture was exposed directly to Ag NPs surface and Ag ions. The lowest cytotoxic effect was observed for Se NPs sample dispersed in medium (sample A1M).

5.2.5 Antimicrobial activity of selenium nanoparticles

Antimicrobial activity of L-cysteine-reduced Se NPs was tested with two methods: MIC and measurement of growth curves. Three samples were tested, sample A1 (stabilized with PVP-29), A2 (stabilized with PVP-40) and A3 (stabilized with BSA). Influence of few factors were investigated: size and size distribution and also different stabilizing agents. Concentration of Se NPs varied from 0.096 mg/ml to 12.25 mg/ml.

5.2.5.1 Minimum inhibitory concentration

Figure 46 shows results from testing Se NPs against strain *E. coli*. It is obvious that all three samples of Se NPs (A1, A2 and A3) show very similar effect on this bacterial culture. In this case, it also appears that increasing or decreasing concentrations of Se NPs did not have any significant effect on the growth of the bacterial culture. *E. coli* growth was suppressed only partially. Se NPs suppressed the growth of bacterial culture by approximately of 20-30 %. As no MIC has been determined, this indicates, that these Se NPs evince bacteriostatic rather than bactericidal properties. There is also a possibility that the Se NPs concentration was too low to stop the growth of the bacterial culture. It can be also assumed that as in the above-mentioned tests of Ag NPs, it can be assumed that *E. coli* is able to develop antimicrobial resistance very quickly. Therefore, it was not possible to unambiguously determine the antimicrobial properties of nanoparticles with this test. Thus, another method was used to gain more information about Se NPs antimicrobial properties.

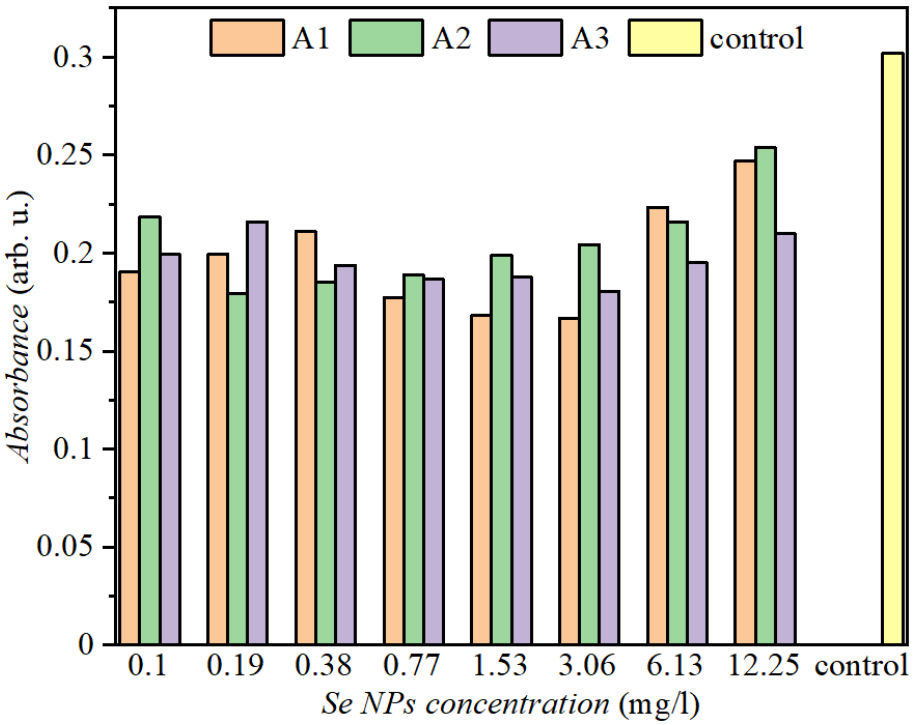

Figure 46: MIC results of L-cysteine-reduced Se NPs applied against E. coli: sample A1 (stabilized with PVP-29), sample A2 (stabilized with PVP-40) and sample A3 (stabilized with BSA).

The MIC test of all three Se NPs samples was also performed for *S. aureus* bacterial culture shown in Figure 47. For sample A1, the concentration of 0.096 mg/ml appeared to be the most

effective, however, the growth of bacteria was not stopped completely. Sample A2 slowed the growth of the bacteria very slightly. Sample A3 stopped the growth of *S. aureus* by approximately 50 % with the concentration of 0.191 mg/ml. However, an interesting phenomenon was observed - with increasing concentration of Se NPs, bacterial growth increased rather than decreased.

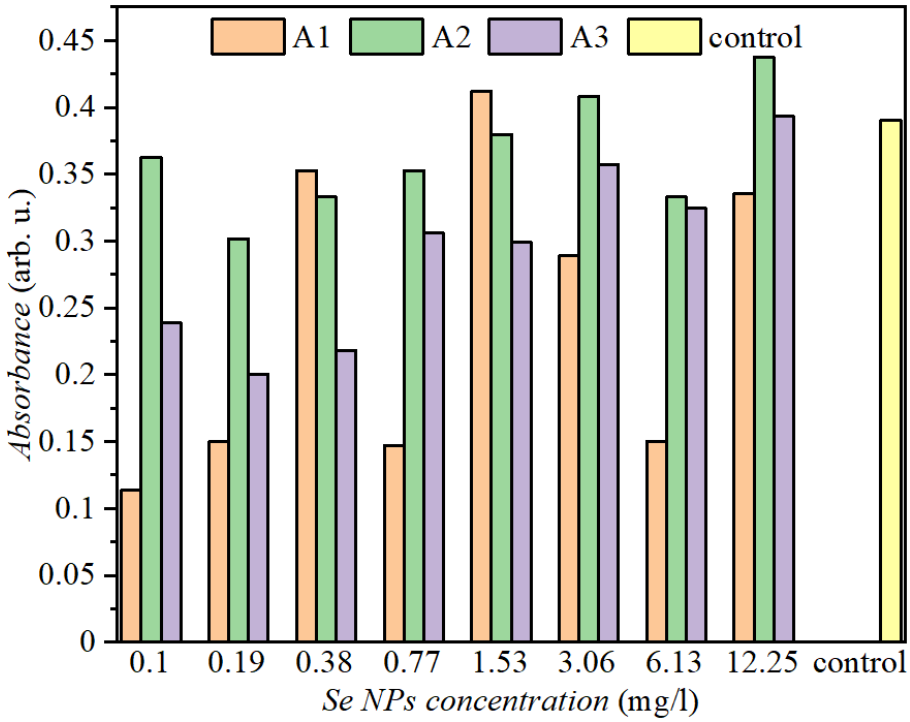

Figure 47: MIC results of L-cysteine-reduced Se NPs applied against S. aureus: sample A1 (stabilized with PVP-29), sample A2 (stabilized with PVP-40) and sample A3 (stabilized with BSA)

These set of experiments have shown that L-cysteine-reduced Se NPs samples evinced only partial antimicrobial activity against both of the cell cultures. Unfortunately, it was not possible to determine a MIC in the tests applied for *E. coli* and *S. aureus*, as none of the chosen concentrations stopped the growth of the bacteria. However, at higher concentrations the growth of bacteria stopped only partially or not at all. This fact is interesting because scientific publications mostly state that the antimicrobial effect of Se NPs increases with increasing concentration. As can be seen, there are also differences between samples. It seems that, in case of testing Se NPs against *E. coli*, the size distribution or stabilizer does not have any significant effect on final antimicrobial properties. However, in case of testing Se NPs against *S. aureus*, there are several differences between samples. It seems that sample A1 (stabilized with PVP-29) evinced the strongest antimicrobial effect at most of the chosen concentrations (except of the 0.38 mg/l, 1.53 mg/l and 12.25 mg/ml). Sample A2 (stabilized with PVP-40) seems to evince the lowest efficacy of antimicrobial properties. Sample A3 (stabilized with BSA) was most effective at the lowest concentrations. It seems that size of Se NPs and also their stabilization layer, can have potential influence on the final antimicrobial properties of Se NPs and it also shows different reactivity to Gram-positive or Gram-negative bacteria. However, another type of antimicrobial testing was performed for comparison, especially to examine above mentioned phenomenon (see following chapter).

5.2.5.2 Growth curves

Measurement of growth curves was also provided on bacterial strain *S. aureus*. Figure 48 (sample A1 stabilized with PVP-29, sample A2 stabilized with PVP-40, sample A3 stabilized with BSA) shows results of measurement with applied samples of L-cysteine-reduced Se NPs.

Figure 48 (A – top) shows that sample A1 effectively suppressed the growth of bacterial culture at the lowest concentrations (from 0.096 mg/ml to 0.766 mg/ml). With increasing concentration of Se NPs, the lag phase of the growth curve was significantly prolonged. This effect was also observed for the remaining two samples A2 and A3. The prolonged lag phase could indicate a bacteriostatic effect of Se NPs.

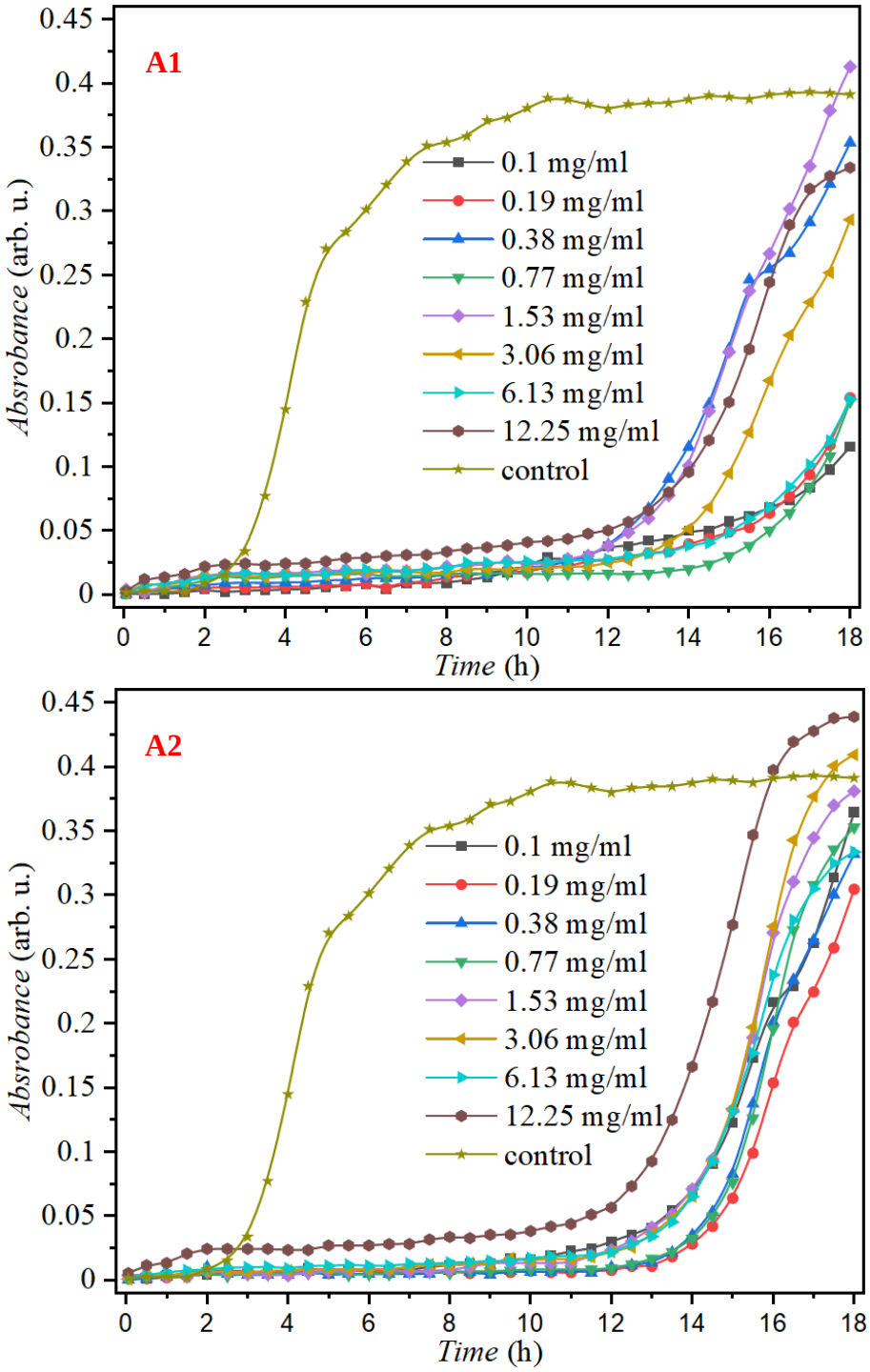

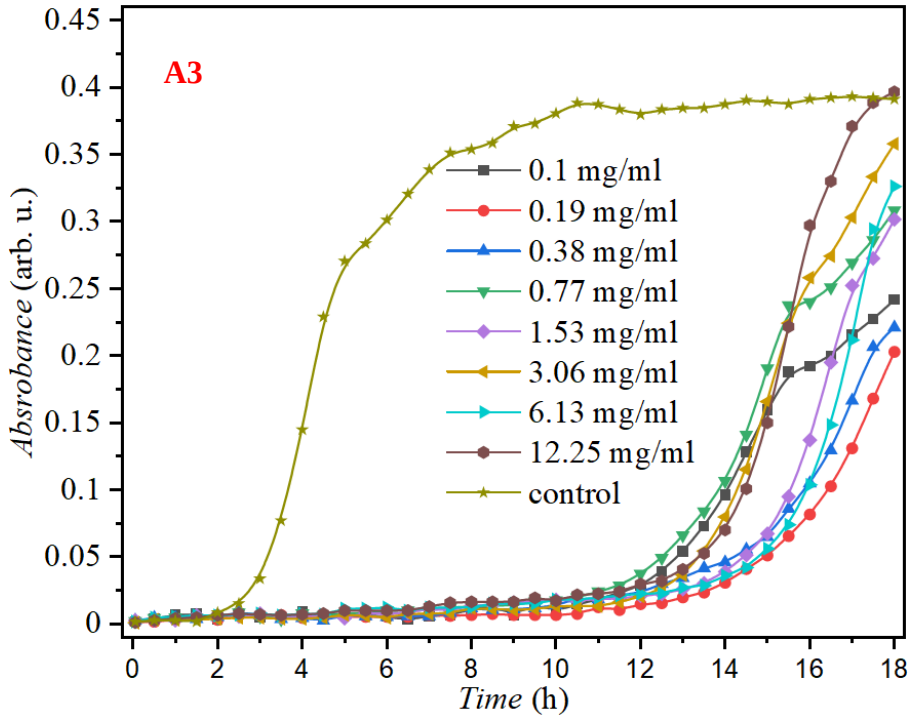

Figure 48: Growth curves of S. aureus with applied L-cysteine-reduced Se NPs: sample A1 (stabilized with PVP-29) - top, A2 (stabilized with PVP)-40 - middle and A3 (stabilized with BSA) - bottom.

The other bacterial culture with applied Se NPs, where growth curves were measured, was *E. coli*. Figure 49 shows results of this measurement (sample A1, sample A2, sample A3). The results show that the growth of bacterial strain *E. coli* was affected only slightly. It can be also seen that the concentration of Se NPs did not affect the growth of the bacterial culture. This result correlates with the result from a previous MIC measurement test, where it was also shown that any selected concentration of Se NPs does not affect the growth of *E. coli*.

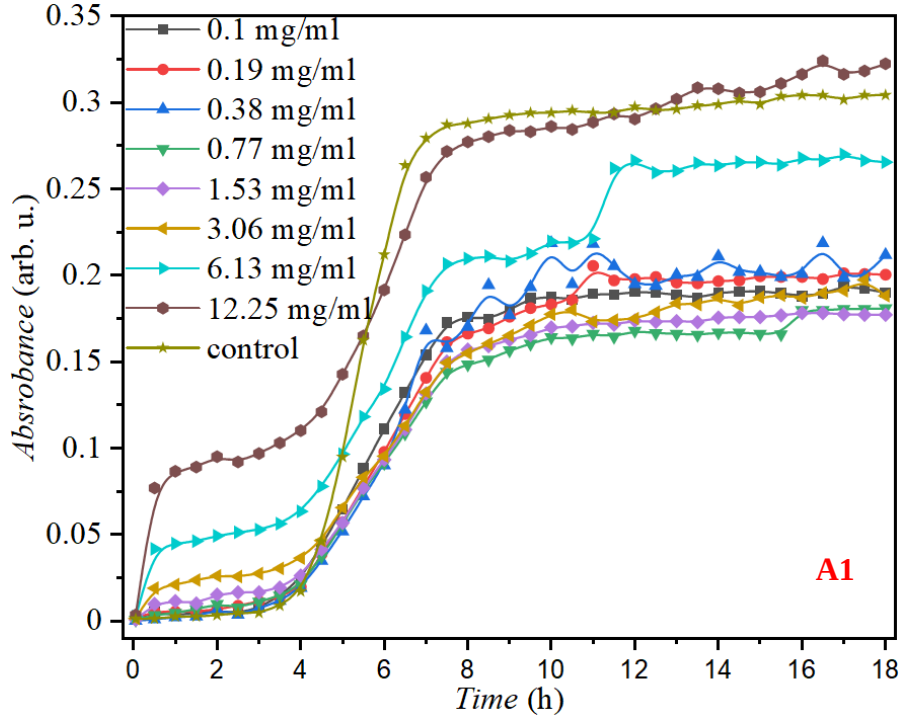

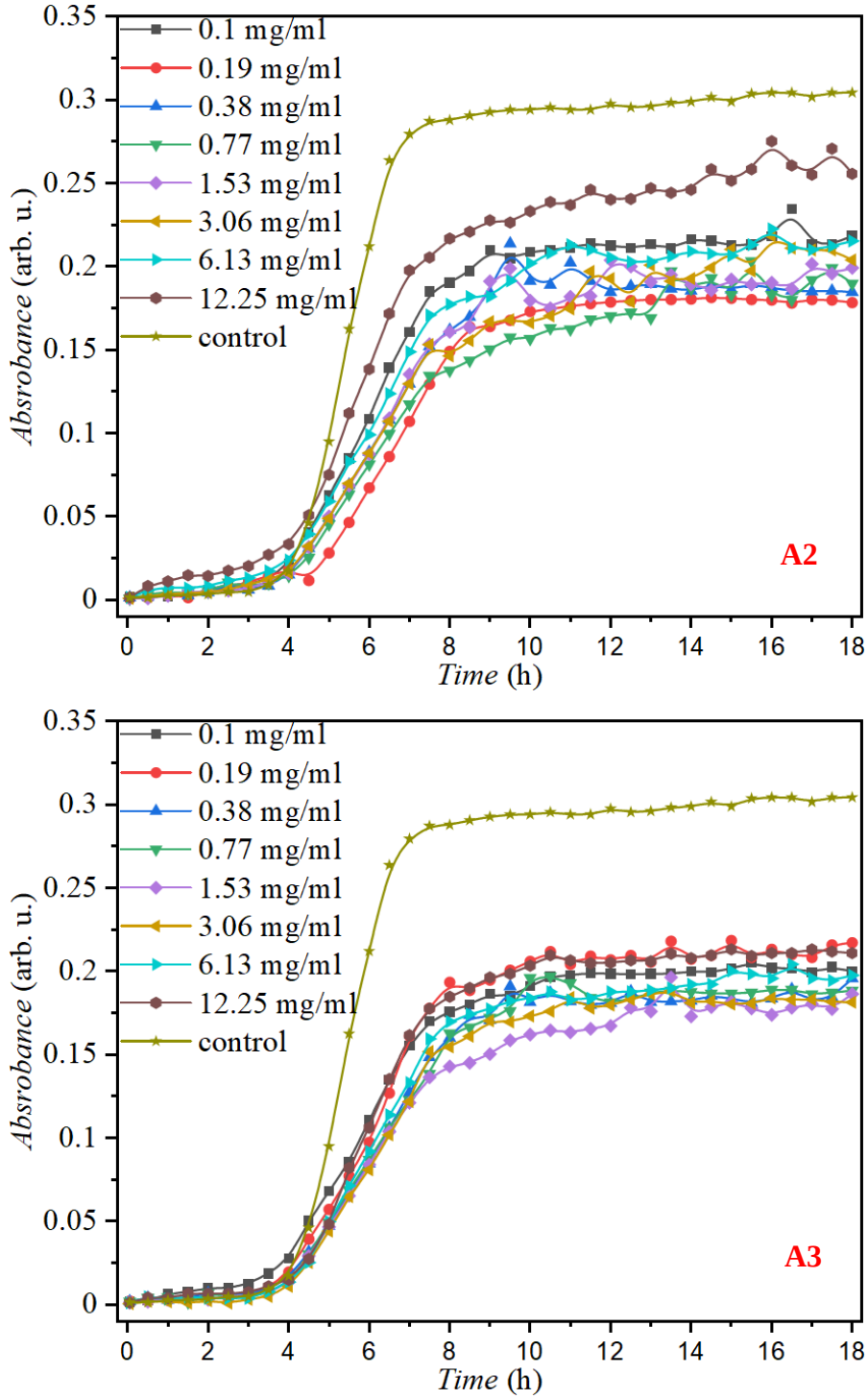

Figure 49: Growth curves of E. coli with applied L-cysteine-reduced Se NPs – samples A1 (stabilized with PVP-29) - top, A2 (stabilized with PVP-40) - middle and A3 (stabilized with BSA) - bottom.

Testing on bacterial culture *S. aureus* showed that Se NPs were able to stop the bacterial growth only partially. In this case, these results point to fact, that Se NPs evince more bacteriostatic rather than a bactericidal effect against *S. aureus* strain. Se NPs have also been tested on bacterial culture. *E. coli*. It was found out, that any concentration of Se NPs (increasing or decreasing) did not affect the growth of the bacteria significantly, which was confirmed as a correlation between MIC testing and measurement of growth curves. The growth of the bacterial culture was suppressed only slightly. In this case, there are several options how results

can be understood. Se NPs did not have any antimicrobial properties against *E. coli* bacterial culture. The concentration of Se NPs was not sufficient to affect the growth, possibly, in the same way as for the above-mentioned Ag NPs, *E. coli* is able to very quickly develop the resistance against antimicrobial agent. From these results, it could be stated that Se NPs against *E. coli* show only a partial bacteriostatic effect.

However, an interesting phenomenon has been found during testing of bacterial culture *S. aureus*, which has not been published in any available literature, yet. The results showed that with increasing concentration of Se NPs, the antimicrobial effect decreased. The results from both MIC and growth curves, where the lag phase was significantly prolonged at higher concentrations, correlated. This refers to the fact that Se NPs at higher concentrations act as bacteriostatic rather than bactericidal compound. This fact is interesting mainly because most available scientific publications state that the antimicrobial effect also increases with increasing concentration of antimicrobial compound [158].

5.3 Plasma treatment of polymer membranes and immobilization of nanoparticles

Due to the composition of polymer membrane, its plasma treatment was complicated. The first issue was related to the process of deposition of amine groups in a vacuum. Since the membrane started to release a big amount of gas, it was necessary to pump the chamber for a very long time. After deposition of the amine groups, it was necessary to immobilize the antimicrobial NPs on the membrane in very short time. The longer the membrane would stand, the more the stability of the deposited groups would decrease due to binding of oxygen, humidity, etc.

In addition, the immobilization process was carried out as a wet chemical reaction, which causes the swelling of the membrane. Although the membrane was able to dry, some amount of humidity was still absorbed in it. It should be noted that membranes with deposited amine groups needed to be stored frozen in a refrigerator, ideally with silica gel beads to prevent binding of moisture. Due to the release of gas from the membrane in vacuum, it was necessary to choose a suitable technique to determine the bindings, which were formed between NPs and polymer membrane. Therefore, the analysis was done by Fourier-transform infrared spectroscopy (FTIR), which does not need to be performed in a vacuum.

Another obstacle was the immobilization of Ag NPs on the membrane. The plasma treated membrane with deposited amino groups was immersed in the reaction solution to synthesize Ag NPs directly on the membrane. It was found that all tested wavelengths of UV-irradiation, used for synthesis of hydrazine-hydrate reduced Ag NPs, affected the stability of the membrane and caused its degradation. The membrane began to dissolve and the solution with Ag NPs evinced a strong turbidity. However, it was obvious from provided antimicrobial tests that the composition of Ag NPs (e.g. silver nitrate used as a precursor, hydrazine hydrate as reductant, and sodium citrate as stabilizer) showed at least partial antimicrobial properties (bacteriostatic properties). Therefore, Ag NPs that were immobilized on the membrane were prepared without UV-irradiation. Under such synthesis condition, it was possible to observe how the individual components of reaction solution affect the final antimicrobial properties of Ag NPs.

5.3.1 Low-pressure plasma deposition of amine groups on polymer membranes

FTIR analysis of low-pressure plasma deposition with polymerization of CPA is shown in Figure 50. According to FTIR spectra of all samples of polymer membranes with immobilized NPs, it can be assumed that combination of various amide groups was present on the membranes with immobilized NPs, namely basic N-H stretching, primary, secondary, and tertiary amides, which have typical peaks at the certain wavenumbers [159].

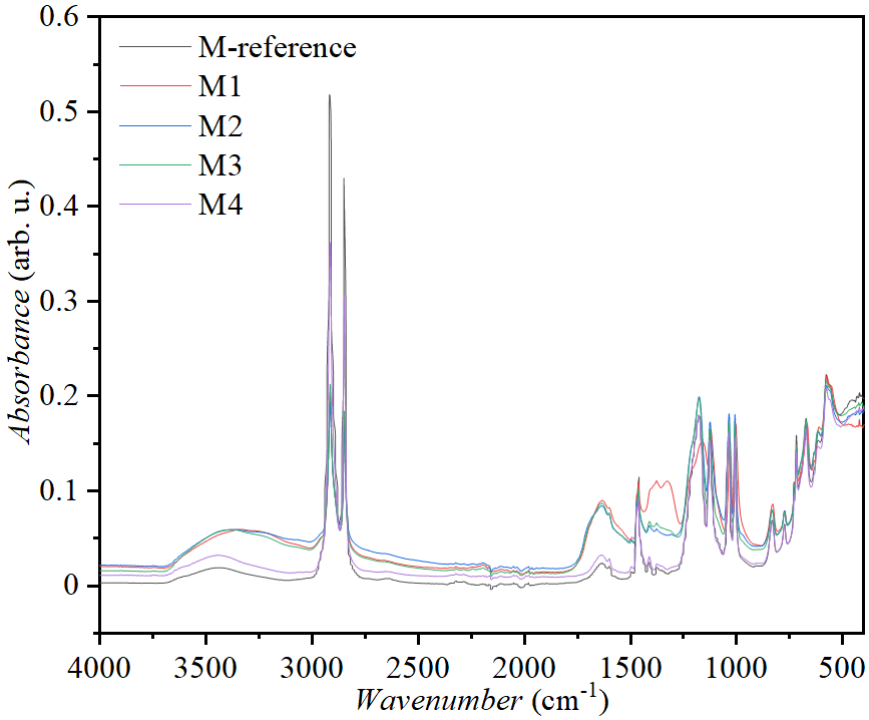

Figure 50: FTIR measurement of polymer membranes with immobilized Ag NPs and Se NPs (low-pressure plasma treatment).

Sample M - reference: pure membrane without applied NPs and without amine groups.

Sample M1: For this sample only 25 mM silver nitrate solution was used. Silver nitrate dissolves in water into Ag^{+} and NO^{3-} ions. These ions further react with the amine groups. According to the FTIR analysis, it can be seen that at the wavenumber of ≈ 3 500 cm^{-1} and in the range from ≈ 2 000 cm^{-1} to ≈ 1 000 cm^{-1} peaks with an increased intensity appeared. Thus, it can be concluded that the silver ions attached to the amine groups on the membrane formed an amide bond. In this case, the region at the ≈ 3 500 cm^{-1} represent N-H stretching and the other region from ≈ 2 000 cm^{-1} to ≈ 1 000 cm^{-1} can be assigned to secondary, primary amides and tertiary. However, in this region, peaks are not visibly sharp, most probably due to humidity of the membrane. Thus, silver ions were able to create these four types of the bindings to the membrane. Akhavan et al. reported that amine groups with silver are able to create stable silver-ammine complexes [135].

Sample M2: In this sample, silver nitrate was used as a precursor and hydrazine hydrate was used as a reductant (without stabilizing agent). From the FTIR analysis, it can be seen that immobilization of Ag NPs there was a change in the region of 3 500 cm^{-1}, similarly to sample M1. The increased intensity also occurred at the region from ≈ 2 000 cm^{-1} to ≈ 1 000 cm^{-1}, but not as significant as in the previous sample M1. Thus, N-H stretching, primary, secondary and tertiary amide groups were formed. However, the humidity of the polymer membranes is present at the shorter wavenumber regions as in the previous sample M1.

Sample M3: Sample M3 is almost identical to sample M2. In this case, the Ag NPs were stabilized with sodium citrate. Thus, in conclusion, it seems that the stabilizing agent did not have any impact on immobilization of Ag NPs on the polymer membrane and all four types of above-mentioned amide bindings were formed (N-H stretching, primary, secondary and tertiary amides).

Sample M4: This sample corresponds to Se NPs sample A1 stabilized with PVP-29 and immobilized on polymer membrane. In this case, the intensity of the FTIR signal increased very

slightly and only in the region of 3 500 cm^{-1}. Therefore, it can be assumed that the Se NPs formed only a basic amide bond (N-H stretching). As only basic amide bond was formed in this case, it can be assumed that smaller amount of Ag NPs created a bind to the polymer membrane in comparison to previous samples M1, M2 and M3, where also other types of amide bindings were formed such as primary, secondary and tertiary amides.

5.3.2 Reactive ion etching immobilization of nanoparticles on polymer membranes

In this group of samples, the amine groups were deposited by RIE with subsequent exposition to flow of ammonia gas. The particles were immobilized as in the previous case, by a wet chemical reaction, where the membranes with deposited groups were immersed directly into the reaction solution with NPs precursors, reducing and/or stabilizing agents. Subsequently, FTIR analysis was performed and the results are shown in Figure 51.

As can be seen from the individual spectra, all of the samples formed mainly basic amide group (N-H stretching). Since the signal intensity is quite low, it can be assumed that the binding of NPs was not that significant as in previous deposition method. However, sample MA1 shows the highest intensity, especially in the region of 3 500 cm^{-1}.

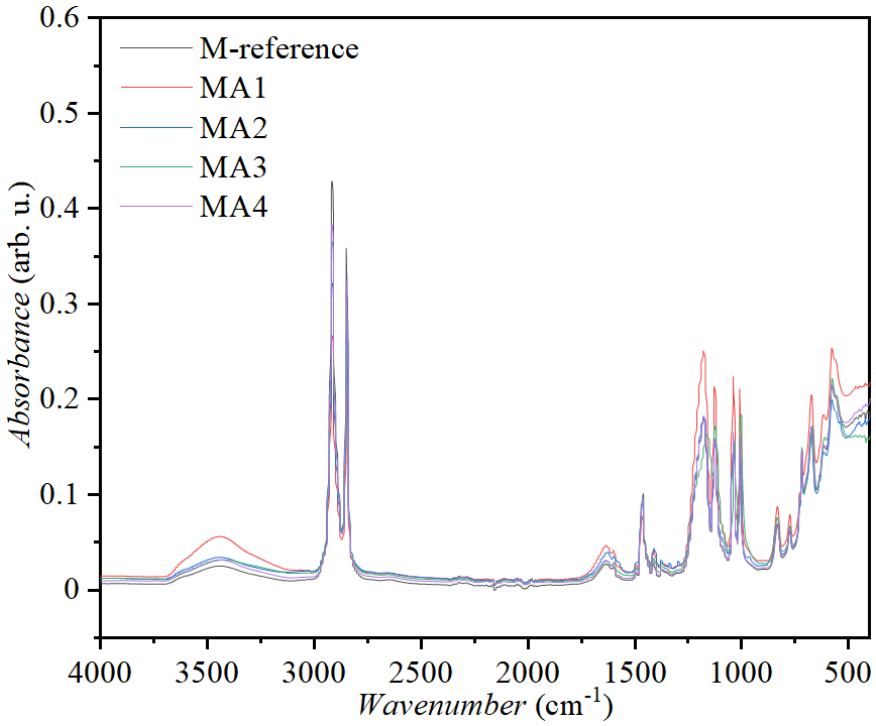

Figure 51: FTIR measurement of polymer membranes with immobilized Ag NPs and Se NPs (RIE treatment with ammonia plasma).

In conclusion, these the two deposition methods, namely low-pressure plasma treatment and RIE showed that immobilized NPs after low-plasma treatment were able to create variety of amide groups (basic, primary, secondary and tertiary). On the other hand, when NPs were immobilized after RIE treatment, only basic amide groups were primarily formed. It should be noted that if humidity is too high (in this case due to the wet chemical immobilization), the peaks corresponding to water molecules can overlap the areas of interest in FTIR spectra, where the amide groups are situated. FTIR spectra of both plasma deposition methods clearly show the attached humidity at the region of N-H stretching at ≈ 3 500 cm^{-1}, where the peaks are not sharp, as well as in the region of ≈ 2 000 cm^{-1} to ≈ 1 000 cm^{-1}. Additionally, membranes are fabricated from a variety of compounds such as LDPE and a filler - strong acidic or alkalic

ionex based on styrene-divinylbenzene copolymer and also PES reinforcing textile. Thus, the signals from the membrane compounds can also overlap the areas in the field of interest (in this case, mostly in the region of ≈ 2 000 cm^{-1} to ≈ 1 000 cm^{-1}). In addition, immobilization of NPs on polymer membrane was performed as a wet chemical process and NPs also consist of various compounds (Ag NPs: silver nitrate, hydrazine hydrate, sodium citrate and Se NPs: sodium selenite, L-cysteine, PVP). When NPs are forming a lot of sub products can be created during the synthesis, which could also react with the deposited amine groups on the membrane and therefore have an impact on final chemical bindings between NPs and polymer membranes. Despite all of these facts, FTIR spectra clearly show the difference between individual samples, where the intensity of peaks significantly changed with immobilization of NPs on polymer membranes in comparison to a reference membrane without functional amine groups and also without NPs (sample M).

5.4 Antimicrobial activity of polymer membranes with immobilized nanoparticles

Final testing of polymer membranes with immobilized NPs was provided via macro dilution method. Photo documentation of this process is depicted in Figure 52, where individual test tubes with applied samples of polymer membranes are shown. It can be seen that sample M1 and MA4 caused high turbidity of the sample, which could be clearly seen by naked eye. Thus, the measurement of absorbance could be negatively affected. It can be also observed that these membranes have changed their color from light beige to orange. It can be assumed, that the NPs immobilized on these membranes (M1 – silver nitrate, MA4 – Se NPs stabilized with PVP-29) were probably oxidized by some of the components in the liquid medium, which negatively affected the stability of the membrane and caused its degradation (dissolution). However, this problem did not occur with remaining samples (M2, M3, M4, MA1, MA2, MA3), so the measurement of absorbance was not negatively affected.

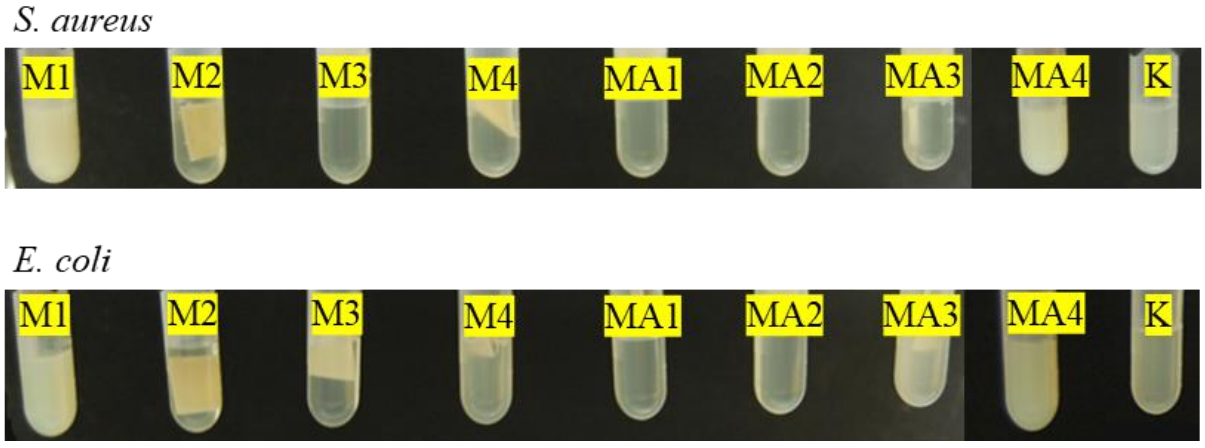

Figure 52: Photos of antimicrobial tests by macro dilution method – samples of polymer membranes with immobilized NPs applied on S. aureus (top) and E. coli (bottom), K = control (only bacterial culture).

Figure 53 shows time dependence of absorbance measurement of membranes with immobilized particles applied against *S. aureus*. This measurement was performed within 3 different time intervals: at the beginning, i.e. right after immersion of membrane to medium with cell culture, after 7 h and after 24 h. As can be seen from results, the turbidity of samples M1 and MA4 negatively affected the measurement, therefore the credibility of the results for these two

samples cannot be evaluated. However, all the remaining samples (M2, M3, M4, MA1, MA2, MA3) successfully stopped the growth of bacteria. To conclude, the membranes with immobilized NPs (except of samples M1 a MA4) evince strong antimicrobial properties with bactericidal effect.

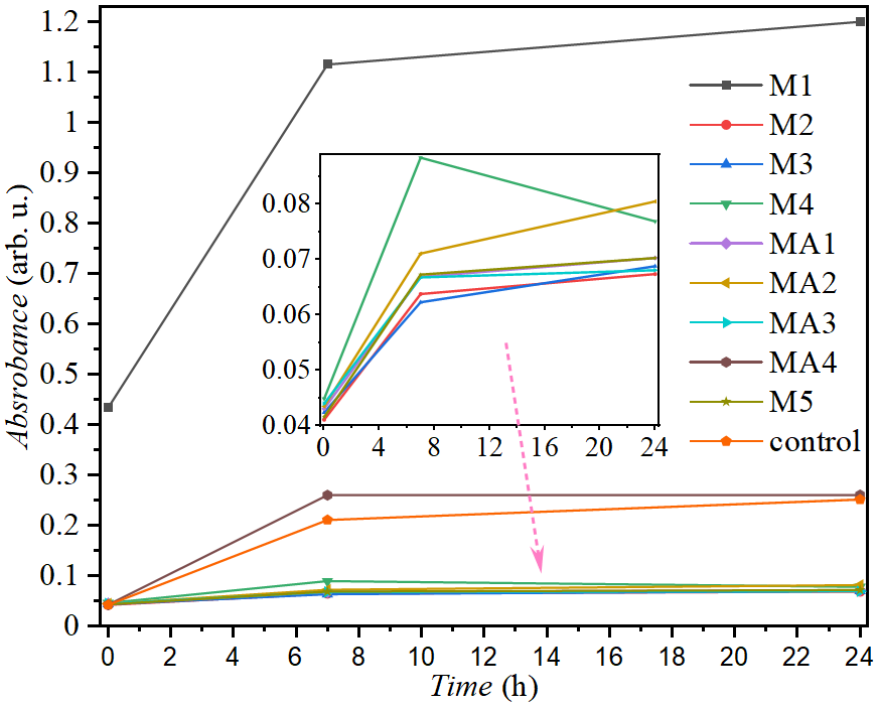

Figure 53: UV-VIS absorption spectroscopy measurement of polymer membranes with immobilized Se NPs applied against S. aureus in 24 h.

Figure *54* shows the results of spectroscopic measurement of how immobilized particles on a polymer membrane act against bacterial culture *E. coli*.

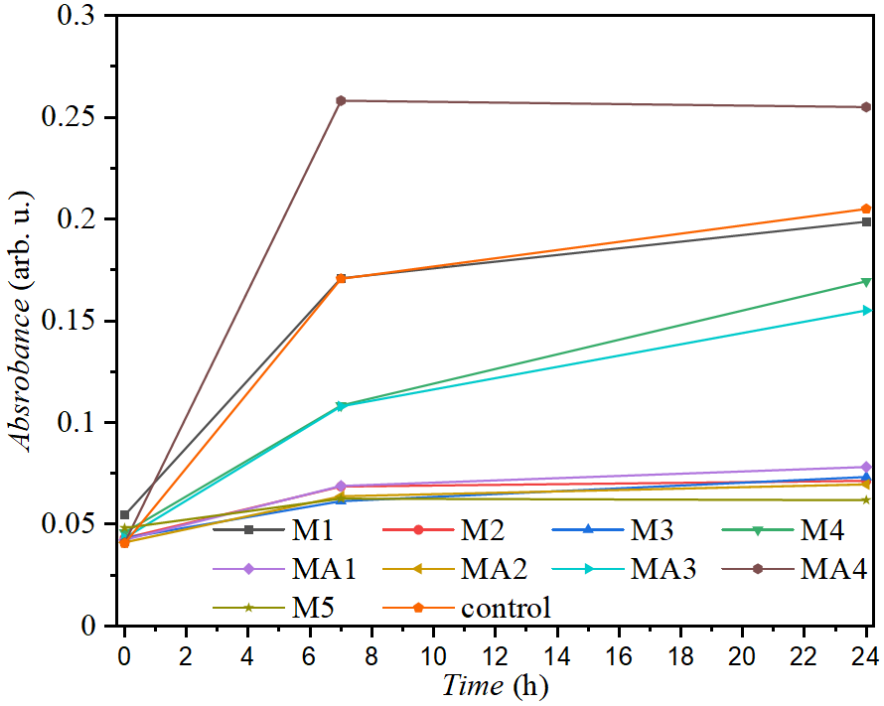

Figure 54: UV-VIS absorption spectroscopy measurement in 24 h – polymer membranes with immobilized Se NPs applied against E. coli.

Sample M1 and MA4, similarly as in the previous case, due to the dissolution of the membrane cannot be evaluated. However, other samples (M2, M3, M4, MA1, MA2, MA3) showed significant antimicrobial effect. Samples M2, M3, MA1 and MA2 successfully inhibited the growth of *E. coli* bacterial culture. Thus, it can be stated that these samples evince strong antimicrobial properties with bactericidal effect. Samples M4 and MA3 show a weaker antimicrobial effect.

Figure 55 also shows above-mentioned spectroscopic measurements but plotted into a bar graph for a better comparison of the two bacterial cultures. Here, it can be clearly seen that samples M1 corresponding to immobilization of only silver nitrate on polymer membrane and MA4 corresponding to immobilization of Se NPs (stabilized with PVP-29) on polymer membrane, do not show any relevant results that could be evaluated due to the dissolution of membranes. From the measured turbidity, it can be assessed that the antimicrobial effect of most samples (except M4 - immobilized Se NPs stabilized with PVP-29 and MA3 - immobilized Ag NPs stabilized with sodium citrate) is very similar.

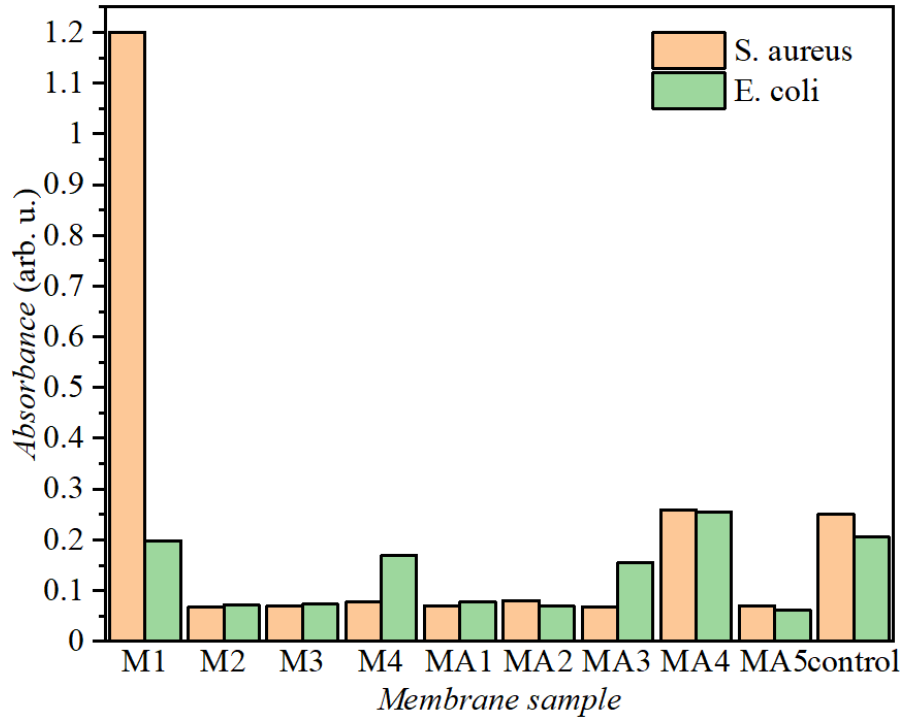

Figure 55: Turbidity measurement after 24 h - immobilized NPs on polymer membranes applied against S. aureus and E. coli.

The inhibition of bacterial growth was calculated from the data of the measured turbidity. The results were plotted into the bar graph in Figure 56 for a better comparison of the two bacterial cultures. All samples (except the mentioned samples with high turbidity M1 and MA4) inhibited the growth of both bacterial cultures by about 80 % except of two samples M4 (immobilized Se NPs stabilized with PVP-29) and MA3 (immobilized Ag NPs stabilized with sodium citrate), which inhibited the growth of only 20-30 %. Thus, it can be said that these samples show a significant antimicrobial effect. Sample M4 represents Se NPs (A1-stabilized with PVP-29) deposited with low-pressure plasma treatment of polymer membrane. In sample MA3 are Ag NPs stabilized with sodium citrate and the polymer membrane was treated with RIE and ammonia plasma. In this case, there are few possible reasons, why the antimicrobial effect was lower than for the other samples. It could by caused by lower amount of immobilized NPs on the polymer membrane or due to the bonding, which changed the antimicrobial properties of these samples.

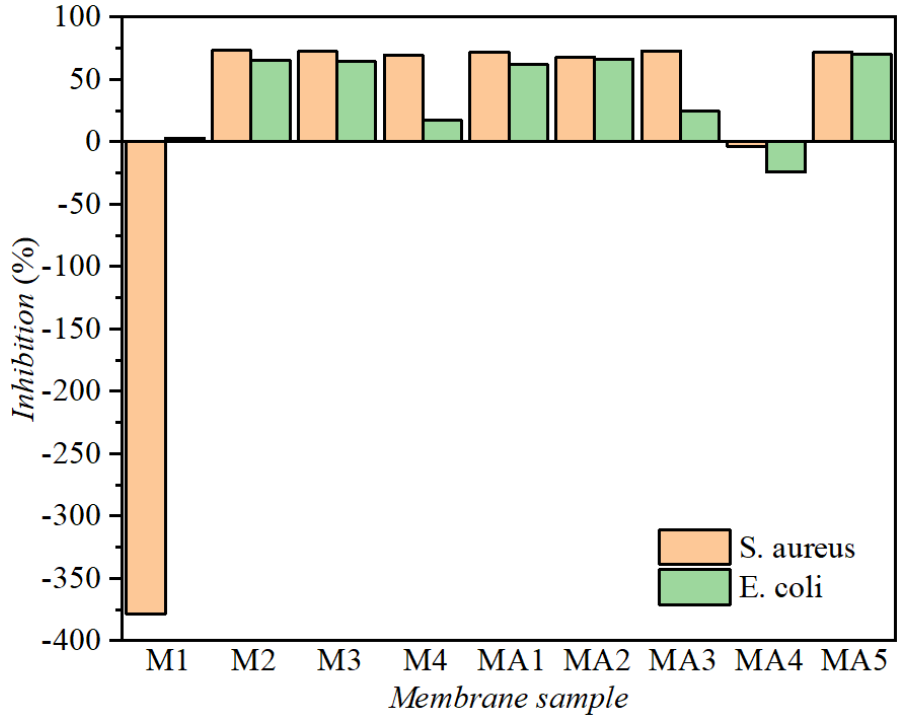

Figure 56: Inhibition after 24 h - immobilized NPs on polymer membranes applied against S. aureus and E. coli

In summary, these experiments showed that the bindings formed between the NPs and the polymer membrane have a significant importance for the final antimicrobial effect. It could be assumed that there could be a synergistic effect of the polymer membrane with bonded NPs and this antimicrobial effect was enhanced in comparison to antimicrobial tests performed on pure NPs (where mostly bacteriostatic effect occurred). It could also be assumed that the type of bond (basic, primary, secondary or tertiary amide) does not affect the antimicrobial efficacy. As well as the deposition method to functionalize the polymers does not have any significant effect on final antimicrobial properties of polymer membranes with immobilized NPs.

In conclusion, it would be appropriate to consider the antimicrobial action of the polymer membrane with immobilized NPs. From the above-mentioned antimicrobial tests, which were performed only on NPs, it was clear that NPs showed more bacteriostatic rather than a bactericidal effect. However, when individual parts of the polymer membranes with immobilized NPs are taken into account, it is not just the NPs that can affect the bacteria. It is necessary to consider also the plasma modification of the membrane, where new functional groups and other highly reactive species have been formed and also the binding between NPs and the membrane, as well as the NPs themselves. Thus, each of these aspects may affect the final antimicrobial properties of as prepared samples.

The synergistic effect of polymer and NPs could also be considered. Here, two interesting scientific papers should be noted. The first, published by Pekárková et al., where Se NPs were used to modify parylene-C micropillars for antimicrobial effect resulting in very low efficacy against *S. aureus* and *E. coli*. They found out that micropillars could have a negative effect against cell cultures [160]. The second scientific paper published by our team (Gablech E. et al.), where a synergistic effect of Se NPs stabilized with PVP-29 mixed with commercial antifungal product was investigated [161]. When Se NPs were mixed with commercial antifungal product, it can be assumed that new chemical bindings between these two compounds were formed. The results showed that this mixture was more effective against fungus *Serpula lacrymans* rather than used individually. Thus, it can be considered that

chemical binding between NPs and polymer membrane can potentially affect the final antimicrobial effect.

6 Conclusion

The main objective of the dissertation thesis was to improve antimicrobial efficiency of commercial polymer membranes used in the food industry for the filtration of milk products, especially whey. These membranes suffer from microbial contamination, which negatively affects not only the filtration process itself but also significantly reduces the life-time of this membrane. Therefore, the aim of this work was to immobilize the suitable antimicrobial NPs on the polymer membrane to achieve antimicrobial properties and thus to protect the membrane from formation of biofilm of microorganisms present in milk and whey. Among various types of NPs exhibiting strong antimicrobial properties, Ag NPs and Se NPs seem to be the most effective antimicrobial agents as reported in the literature. Thus, these NPs were utilized for immobilization on the polymer membrane treated with plasma for deposition of functional amine groups. These groups enabled binding of NPs to membrane by forming amide groups. Such functionalized membranes were tested for antimicrobial properties.

Specific objective 1: Synthesis of NPs

This part of work was devoted to optimization of the preparation processes of individual types of NPs, specifically Ag NPs and Se NPs. Various procedures and factors that could affect the final biological and physico-chemical properties of NPs have been investigated. These factors include various precursors, reducing and stabilizing agents, or physical factors such as temperature or UV radiation. Furthermore, the effect of their concentration and also their various combinations were investigated.

Silver nanoparticles

In the first step, Ag NPs were synthesized using green methods, where reagents such as chitosan or glucose were used as reducing agents. However, these Ag NPs were not suitable for further utilization, mainly due to their low colloidal stability. Therefore, another approach was tested and different factors were investigated. The synthesis was based on silver nitrate used as precursor, hydrazine hydrate as the reducing agent and two different stabilizing agents, SDS and sodium citrate. Firstly, the effect of the concentration of individual agents and two different stabilizing agents was investigated. It was found out that both, the concentration of individual substances and also stabilizing agents, have a significant influence on the final properties of Ag NPs, especially their shape. When the silver nitrate concentration was low (2 mM) and the reducing agent concentration was high (12 mM), the resulting Ag NPs evinced spherical shape with size ranging from 20 nm to 150 nm. With increasing concentration of precursor and decreasing concentration of reductant, the anisotropic form of Ag NPs predominated. Regarding the effect of stabilizers, the presence of sodium citrate promoted the formation of anisotropic form of Ag NPs. However, these samples also showed low colloidal stability and therefore, were not suitable for further experiments.

In another set of experiments, this method was modified and the effect of elevated temperature (30 ºC, 40 ºC, 60 ºC and 80 ºC) on the final properties of Ag NPs was investigated. The results from SEM analysis showed that the temperature also have great effect on final properties of Ag NPs, especially shape and size. With increasing temperature, the shape of Ag NPs changed from anisotropic to spherical, and the particle size decreased (average size decreased from ≈ 100 nm to ≈ 50 nm. However, as in the previous case, these particles showed a short colloidal stability (about 7 days), therefore they were not suitable for further use.

Consequently, the synthesis method was modified again by employing UV radiation with different wavelengths, namely 255 nm, 366 nm and 400 nm. A control sample without any radiation was also prepared in the dark environment. It was found that UV radiation was also

very important factor that can affect final properties of Ag NPs, especially the shape and size. With increasing wavelengths of UV radiation, the shape of Ag NPs changed from spherical to anisotropic (various shapes as rods, triangular plates with truncated tops, spheres). The stability of the particles was also significantly prolonged (including the control sample prepared in darkness) up to 3 weeks after synthesis, which was also confirmed by UV-VIS spectroscopy analysis.

Since the UV-radiation adds additional energy to the reaction system (the temperature of reaction mixtures increased), one more modification of this synthesis was performed by employing a cooling system in combination with UV radiation. The results showed that not only the increasing temperature, but also the decreasing temperature to 15 ºC has an effect on the size and also on the shape of Ag NPs. Final shape of Ag NPs was mainly anisotropic and the stability of these samples lasted for 3 weeks. These Ag NPs were not further used due to the demanding preparation process with the cooling system. Nevertheless, these samples served as a demonstration that both, increasing and decreasing temperatures, affect the resulting properties of Ag NPs.

Selenium nanoparticles

Similarly, to Ag NPs, the synthesis of Se NPs was optimized and several factors were investigated. Se NPs were prepared by a procedure, where selenous acid employed as a precursor was reduced with chitosan, which also served as a stabilizer. However, these Se NPs were not suitable for further utilization due to their low colloidal stability. Subsequently, another type of the synthesis was performed, where sodium selenite was used as a precursor, sodium hydroxide as a reducing agent and glutathione as a reductant and also a stabilizer. Following factors were investigated: mixing of the reaction solution and the presence or absence of sodium hydroxide were tested. However, as the results showed, none of these factors had a significant effect on the resulting properties of Se NPs - only their size changed slightly.

To improve the stability of Se NPs, another type of synthesis approach was performed. This method was invented and optimized in our laboratory. Sodium selenite was used as precursor, L-cysteine was reducing agent and three different stabilizers were used in this synthesis: PVP-29, PVP-40 and BSA. The shape of all types of Se NPs samples was spherical and the stability of these particles was also sufficient (no sediments were seen 2 weeks after synthesis). Subsequent analyzes showed that the various stabilizing agents affected mainly the size of Se NPs. Se NPs stabilized with PVP-29 evinced the smallest size around 40 nm confirmed by STEM and SAXS. Because of the smallest dimensions, Se NPs stabilized with PVP-29 (sample A1) was selected for further experiments, i.e. for immobilization on membrane to achieve its antimicrobial coating.

Specific objective 2: Cytotoxicity of NPs

Silver nanoparticles

Following samples of Ag NPs were tested with MTT assay to determine their cytotoxicity: sample A prepared under UV light of 255 nm, sample B prepared under UV light of 366 nm and sample C prepared under UV light of 400 nm, and sample X prepared in darkness. However, in this part of the work, an obstacle with the stability of Ag NPs occurred. When Ag NPs were dispersed in DMEM medium (originally dispersed in deionized water), Ag NPs rapidly agglomerated (big agglomerates could be seen by naked eye). This problem was partially solved with utilization of ultrasonic bath, which helped to improve their stability for 24 h. After this period big agglomerates appeared again at the bottom of the vessel. Another problem was the preparation of Ag NPs for this assay - Ag NPs were centrifuged and then dried in a small Petri dish to determine the specific concentration and subsequent dilution. However, the yield of Ag

NPs was very small and it was difficult to separate Ag NPs from the Petri dish. However, this analysis showed, although only partially, that with increasing concentration (from 2.5 mg/ml to 220 mg/ml), their toxicity, e.g. cell viability decreased.

Selenium nanoparticles

Two assays were performed to determine the cytotoxicity of Se NPs, namely the XTT cytotoxicity assay and the BrdU proliferation assay. The results of these assays showed interesting results. At higher concentrations, Se NPs (2 mg/ml and 5 mg ml) showed a significant cytotoxic effect. However, with decreasing concentration, they promoted cell growth. This could be explained by the fact that Se is a micronutrient, and at very low concentrations may support some of the cellular processes.

Specific objective 3: Antimicrobial activity of NPs

Silver nanoparticles

The antimicrobial activity of the Ag NPs samples was tested by several methods, namely disk-diffusion method, growth curves measurement and dilution method with subsequent manual counting of grown colonies. The disk-diffusion method showed only a small effect of Ag NPs against *S. aureus,* but no effect against *E. coli*. Therefore, additional tests were performed to determine whether the Ag NPs exhibit antimicrobial properties. Measurement of growth curves showed only partial inhibition of the growth of both bacterial cultures. The third, dilution method confirmed the antimicrobial properties for both bacterial clusters, but more significantly against *S. aureus* culture, where Ag NPs samples A (prepared under UV light of 255 nm) and C (prepared under UV light of 400 nm) inhibited the growth of bacteria by about 50 %, while for *E. coli* only about 30 %. However, from all the performed tests, it was obvious that none of the samples with any concentration was able to completely inhibit the growth of bacterial cultures, which would indicate rather a bacteriostatic than a bactericidal effect.

Selenium nanoparticles

Antimicrobial activity Se NPs were tested on three samples, A1 (stabilized with PVP-29), A2 (stabilized with PVP-40) and A3 (stabilized with BSA). The MIC and growth curves measurements were used to observe the antimicrobial effect. Measurements were performed on two bacterial cultures, *E. coli* and *S. aureus*. The results showed that, similarly to Ag NPs, none of the samples was able to completely inhibit the growth of both bacterial cultures. Again, it can be assumed that Se NPs exhibit antimicrobial properties with a bacteriostatic effect. An interesting phenomenon was also found with testing of *S. aureus* bacterial culture: with increasing concentration of Se NPs, the antimicrobial effect decreased. These results were confirmed by both types of antimicrobial methods.

Specific objective 4: Plasma treatment of polymer membranes and immobilization of NPs

This part of the work was focused on plasma modification of polymer membranes and deposition of amine functional groups and subsequent immobilization of Ag NPs and Se NPs. Two different approaches were used: low-pressure plasma deposition with CPA polymerization and RIE with ammonia plasma utilization. Due to the low stability of the functional groups, the NPs were immobilized immediately after plasma treatment by a wet chemical reaction, i.e. by immersing the membrane directly in the reaction solution of the NPs. It was found that UV-radiation, used for Ag NPs synthesis, had a negative effect on the stability of the membrane, which began to dissolve. Therefore, a new series of experiments was performed. Due to antimicrobial tests of Ag NPs, which showed that the composition of Ag NPs, e.g. silver nitrate, hydrazine hydrate and sodium citrate exhibited antimicrobial properties, the effect of these

individual components, which were immobilized on the membrane, was investigated. The Se NPs of sample A1 (stabilized with PVP-29) were also immobilized on a membrane.

The results of FTIR analysis showed that all types of binded NPs formed different types of amide binds - basic, primary, secondary and tertiary. Low-pressure plasma treatment proved to be a more suitable way of membrane modification than RIE with ammonia plasma because in case of utilization of low-pressure plasma, NPs were able to form different types of amide bonds from basic to tertiary, while in case of utilization of RIE with ammonia plasma only basic amide binds.

Specific objective 5: Antimicrobial activity of polymer membranes with immobilized NPs

The antimicrobial activity of the polymer membrane with immobilized NPs was tested by a microdilution method against bacterial strains *S. aureus* and *E. coli*. The results showed that NPs immobilized by both types of plasma modification of polymer membrane evinced a strong inhibitory effect on both bacterial cultures. It was also found that all membranes with immobilized NPs (except for samples M1 and MA4 since the immersion of the membranes into medium caused their dissolution and abnormal turbidity of samples) evinced strong antimicrobial effect against both bacterial cultures and inhibited their growth by about 80 %. However, it was found out that the immobilized NPs on the polymer membrane showed significantly higher antimicrobial effect than the NPs applied themselves (confirmed by antimicrobial tests).

In conclusion, this dissertation thesis required interdisciplinary approach as several different areas were investigated such as NPs synthesis and optimization, polymer treatment by plasma, testing of cytotoxicity and antimicrobial properties. Several challenging issues occurred during the experiments - especially linked with the stability of the membrane and the stability of the NPs themselves. The anex polymer membrane dissolved in some reagents, and therefore only a catex membrane was used for all types of experiments because it showed slightly better stability. The membrane also caused problems when analyzed with vacuum methods - it extensively released a gas and therefore, it was necessary to pump the chamber for a very long time to achieve a suitable level of vacuum. Finally, when NPs were immobilized on the surface of the membrane by the wet chemical process, the membrane swelled and a significant moisture remained absorbed in the membrane, which made it difficult to interpret the FTIR results, Therefore, the membrane samples with immobilized NPs had to be kept in a dry box for a month. A large number of experiments and subsequent analyzes have been performed, which have shown that both Se NPs and Ag NPs can evince strong antimicrobial effect. It was also found that antimicrobial activity can be significantly affected by the binding of NPs to membrane and also synergistic effect could be considered. According to antimicrobial tests of polymer membranes with immobilized NPs, the antimicrobial effect is affected not only by NPs per se but also by plasma treated membrane, its functional groups and other highly reactive species that were formed during this treatment.

7 References

1. Daufin, G., et al., *Recent and emerging applications of membrane processes in the food and dairy industry.* Food and Bioproducts Processing, 2001. **79**(2): p. 89-102.
2. Pouliot, Y., *Membrane processes in dairy technology—From a simple idea to worldwide panacea.* International Dairy Journal, 2008. **18**(7): p. 735-740.
3. Aguero, R., et al., *Membrane processes for whey proteins separation and purification. A review.* Current Organic Chemistry, 2017. **21**(17): p. 1740-1752.
4. Wen-Qiong, W., et al., *Whey protein membrane processing methods and membrane fouling mechanism analysis.* Food chemistry, 2019. **289**: p. 468-481.
5. Kowalik-Klimczak, A., *The possibilities of using membrane filtration in the dairy industry.* Journal of Machine Construction and Maintenance-Problemy Eksploatacji, 2017.
6. Kumar, P., et al., *Perspective of membrane technology in dairy industry: A review.* Asian-Australasian Journal of Animal Sciences, 2013. **26**(9): p. 1347.
7. Charcosset, C., *Classical and recent applications of membrane processes in the food industry.* Food Engineering Reviews, 2021. **13**(2): p. 322-343.
8. Chamberland, J., et al., *Biofouling of ultrafiltration membrane by dairy fluids: Characterization of pioneer colonizer bacteria using a DNA metabarcoding approach.* Journal of dairy science, 2017. **100**(2): p. 981-990.
9. Kaur, N., et al., *Recent developments in purification techniques and industrial applications for whey valorization: A review.* Chemical Engineering Communications, 2020. **207**(1): p. 123-138.
10. Anand, S. and D. Singh, *Resistance of the constitutive microflora of biofilms formed on whey reverse-osmosis membranes to individual cleaning steps of a typical clean-in-place protocol.* Journal of dairy science, 2013. **96**(10): p. 6213-6222.
11. Kochkodan, V.M. and V.K. Sharma, *Graft polymerization and plasma treatment of polymer membranes for fouling reduction: A review.* Journal of Environmental Science and Health, Part A, 2012. **47**(12): p. 1713-1727.
12. Wood, T.L., et al., *Living biofouling-resistant membranes as a model for the beneficial use of engineered biofilms.* Proceedings of the National Academy of Sciences, 2016. **113**(20): p. E2802-E2811.
13. Mehrabi, Z., et al., *Bienzymatic modification of polymeric membranes to mitigate biofouling.* Separation and Purification Technology, 2020. **237**: p. 116464.
14. Sun, X.-F., et al., *Graphene oxide–silver nanoparticle membrane for biofouling control and water purification.* Chemical Engineering Journal, 2015. **281**: p. 53-59.
15. Saion, E., E. Gharibshahi, and K. Naghavi, *Size-controlled and optical properties of monodispersed silver nanoparticles synthesized by the radiolytic reduction method.* International journal of molecular sciences, 2013. **14**(4): p. 7880-7896.
16. Zain, N.M., A.G.F. Stapley, and G. Shama, *Green synthesis of silver and copper nanoparticles using ascorbic acid and chitosan for antimicrobial applications.* Carbohydrate Polymers, 2014. **112**(0): p. 195-202.
17. Abou El-Nour, K.M.M., et al., *Synthesis and applications of silver nanoparticles.* Arabian Journal of Chemistry, 2010. **3**(3): p. 135-140.

18. Prabhu, S. and E. Poulose, *Silver nanoparticles: mechanism of antimicrobial action, synthesis, medical applications, and toxicity effects.* International Nano Letters, 2012. **2**(1): p. 1-10.

19. Tran, Q.H. and A.-T. Le, *Silver nanoparticles: synthesis, properties, toxicology, applications and perspectives.* Advances in Natural Sciences: Nanoscience and Nanotechnology, 2013. **4**(3): p. 033001.

20. Mohan, S., et al., *Completely green synthesis of dextrose reduced silver nanoparticles, its antimicrobial and sensing properties.* Carbohydrate Polymers, 2014. **106**(0): p. 469-474.

21. Moritz, M. and M. Geszke-Moritz, *The newest achievements in synthesis, immobilization and practical applications of antibacterial nanoparticles.* Chemical Engineering Journal, 2013. **228**: p. 596-613.

22. Camargo, P.H., et al., *Controlled synthesis: nucleation and growth in solution*, in *Metallic Nanostructures*. 2015, Springer. p. 49-74.

23. Wiley, B., et al., *Shape-controlled synthesis of metal nanostructures: the case of silver.* Chemistry–A European Journal, 2005. **11**(2): p. 454-463.

24. Shameli, K., et al., *Investigation of antibacterial properties silver nanoparticles prepared via green method.* Chemistry Central Journal, 2012. **6**(1): p. 73.

25. Nayak, V., et al., *Potentialities of selenium nanoparticles in biomedical science.* New Journal of Chemistry, 2021. **45**(6): p. 2849-2878.

26. Salem, S.S., et al., *Bactericidal and in-vitro cytotoxic efficacy of silver nanoparticles (Ag-NPs) fabricated by endophytic actinomycetes and their use as coating for the textile fabrics.* Nanomaterials, 2020. **10**(10): p. 2082.

27. Rujido-Santos, I., et al., *Silver nanoparticles assessment in moisturizing creams by ultrasound assisted extraction followed by sp-ICP-MS.* Talanta, 2019. **197**: p. 530-538.

28. Mathur, P., et al., *Pharmaceutical aspects of silver nanoparticles.* Artificial cells, nanomedicine, and biotechnology, 2018. **46**(sup1): p. 115-126.

29. Klębowski, B., et al., *Applications of noble metal-based nanoparticles in medicine.* International journal of molecular sciences, 2018. **19**(12): p. 4031.

30. EFSA Panel on Food Contact Materials, E., et al., *Safety assessment of the substance silver nanoparticles for use in food contact materials.* EFSA Journal, 2021. **19**(8): p. e06790.

31. Kalaivani, R., et al., *Synthesis of chitosan mediated silver nanoparticles (Ag NPs) for potential antimicrobial applications.* Frontiers in Laboratory Medicine, 2018. **2**(1): p. 30-35.

32. Nasrollahzadeh, M., et al., *Recent developments in the plant-mediated green synthesis of Ag-based nanoparticles for environmental and catalytic applications.* The Chemical Record, 2019. **19**(12): p. 2436-2479.

33. Bin, Q., M. Wang, and L. Wang, *Ag nanoparticles decorated into metal-organic framework (Ag NPs/ZIF-8) for electrochemical sensing of chloride ion.* Nanotechnology, 2020. **31**(12): p. 125601.

34. Zhang, K., et al., *Label-free and stable serum analysis based on Ag-NPs/PSi surface-enhanced Raman scattering for noninvasive lung cancer detection.* Biomedical optics express, 2018. **9**(9): p. 4345-4358.

35. Guzmán, M.G., J. Dille, and S. Godet, *Synthesis of silver nanoparticles by chemical reduction method and their antibacterial activity.* Int J Chem Biomol Eng, 2009. **2**(3): p. 104-111.

36. Luo, S., et al., *In situ and controllable synthesis of Ag NPs in tannic acid-based hyperbranched waterborne polyurethanes to prepare antibacterial polyurethanes/Ag NPs composites.* RSC advances, 2018. **8**(64): p. 36571-36578.

37. Mohamed, D.S., et al., *Antimicrobial activity of silver-treated bacteria against other multi-drug resistant pathogens in their environment.* Antibiotics, 2020. **9**(4): p. 181.

38. Ottoni, C., et al., *Environmental impact of biogenic silver nanoparticles in soil and aquatic organisms.* Chemosphere, 2020. **239**: p. 124698.

39. Chhabria, S. and K. Desai, *Selenium nanoparticles and their applications.* Encyclopedia of Nanoscience and Nanotechnology, 2016. **20**: p. 1-32.

40. Wang, Q., et al., *Red selenium nanoparticles and gray selenium nanorods as antibacterial coatings for PEEK medical devices.* Journal of Biomedical Materials Research Part B: Applied Biomaterials, 2016. **104**(7): p. 1352-1358.

41. Zhang, S.-Y., et al., *Synthesis of selenium nanoparticles in the presence of polysaccharides.* Materials Letters, 2004. **58**(21): p. 2590-2594.

42. Ingole, A.R., et al., *Green synthesis of selenium nanoparticles under ambient condition.* Chalcogenide Lett, 2010. **7**(7): p. 485-489.

43. Glantreo. *Selenium Nanoparticle Application*. 2021 [cited 2021; Available from: https://glantreo.com/multidimensional-application-of-selenium-nanoparticles/.

44. Tran, P.A. and T.J. Webster, *Selenium nanoparticles inhibit Staphylococcus aureus growth.* International journal of nanomedicine, 2011. **6**: p. 1553.

45. Medina Cruz, D., G. Mi, and T.J. Webster, *Synthesis and characterization of biogenic selenium nanoparticles with antimicrobial properties made by Staphylococcus aureus, methicillin-resistant Staphylococcus aureus (MRSA), Escherichia coli, and Pseudomonas aeruginosa.* Journal of Biomedical Materials Research Part A, 2018. **106**(5): p. 1400-1412.

46. MemBrain, s.r.o. 2021 [cited 2021; Available from: https://www.membrain.cz/.

47. Jiránková, H., *Membránové procesy v potravinářství a mlékárenství.* Pardubice: Ústav environmentálního a chemického inženýrství, UPa,[cit. 2017-06-06]. Dostupný z http://www. czemp. cz/sites/default/files/clanek/1071/prilohy/1. mempro-mlk. pdf.

48. Selatile, M.K., et al., *Recent developments in polymeric electrospun nanofibrous membranes for seawater desalination.* RSC advances, 2018. **8**(66): p. 37915-37938.

49. Honarparvar, S., et al., *Frontiers of Membrane Desalination Processes for Brackish Water Treatment: A Review.* Membranes, 2021. **11**(4): p. 246.

50. Bernauer, B., et al., *Membránové procesy*. 1 ed. 2012, Praha: VŠCHT. 296.

51. Ečer, J.a.K., J. *Membránové procesy v mlékárenském průmyslu*. Mlékárenské listy, 2014. **č. 145**.

52. Křivčík, J., *Iontově selektivní membrány*. 2013, MemBrain, s.r.o. p. 44.

53. Akar, N., et al., *Investigation of characterization and biofouling properties of PES membrane containing selenium and copper nanoparticles.* Journal of Membrane Science, 2013. **437**: p. 216-226.

54. Kochkodan, V. and N. Hilal, *A comprehensive review on surface modified polymer membranes for biofouling mitigation.* Desalination, 2015. **356**: p. 187-207.

55. Sedlarik, V., *Antimicrobial modifications of polymers.* Biodegradation-Life of Science, 2013: p. 187-204.

56. Zhu, J., et al., *Polymeric antimicrobial membranes enabled by nanomaterials for water treatment.* Journal of Membrane Science, 2018. **550**: p. 173-197.

57. Bansal, B. and X.D. Chen, *A critical review of milk fouling in heat exchangers.* Comprehensive reviews in food science and food safety, 2006. **5**(2): p. 27-33.

58. Chambers, J.V., *The microbiology of raw milk.* Dairy microbiology handbook, 2002: p. 39-89.

59. Tang, X., et al., *Biofilm Contamination of Ultrafiltration and Reverse Osmosis Plants.* Biofilms in the Dairy Industry, 2015: p. 138-153.

60. Anand, S., et al., *Development and control of bacterial biofilms on dairy processing membranes.* Comprehensive Reviews in Food Science and Food Safety, 2014. **13**(1): p. 18-33.

61. Schlosser, Š., *Mikulášek P.(red.): Tlakové membránové procesy.* Chemické listy, 2014. **108**(10): p. 990-990.

62. Jiránková, H., *INTEGROVANÉ MEMBRÁNOVÉ PROCESY.*

63. Palatý, Z., *Membránové procesy.* Chem. Listy, 2012. **106**: p. 1086-1088.

64. Sari Erkan, H., N. Bakaraki Turan, and G. Önkal Engin, *Chapter Five - Membrane Bioreactors for Wastewater Treatment*, in *Comprehensive Analytical Chemistry*, D.S. Chormey, et al., Editors. 2018, Elsevier. p. 151-200.

65. Thombre, N.V., et al., *Ultrasound induced cleaning of polymeric nanofiltration membranes.* Ultrasonics sonochemistry, 2020. **62**: p. 104891.

66. Saleh, T.A. and V.K. Gupta, *Nanomaterial and polymer membranes: synthesis, characterization, and applications*. 2016: Elsevier.

67. Gul, A., J. Hruza, and F. Yalcinkaya, *Fouling and Chemical Cleaning of Microfiltration Membranes: A Mini-Review.* Polymers, 2021. **13**(6): p. 846.

68. Zondervan, E. and B. Roffel, *Evaluation of different cleaning agents used for cleaning ultra filtration membranes fouled by surface water.* Journal of Membrane Science, 2007. **304**(1-2): p. 40-49.

69. Vohlídal, J., *Polymer degradation: a short review.* Chemistry Teacher International, 2021. **3**(2): p. 213-220.

70. Zakria, H.S., et al., *Immobilization techniques of a photocatalyst into and onto a polymer membrane for photocatalytic activity.* RSC Advances, 2021. **11**(12): p. 6985-7014.

71. Mijnendonckx, K., et al., *Antimicrobial silver: uses, toxicity and potential for resistance.* Biometals, 2013. **26**(4): p. 609-621.

72. Zhang, X.-F., et al., *Silver nanoparticles: synthesis, characterization, properties, applications, and therapeutic approaches.* International journal of molecular sciences, 2016. **17**(9): p. 1534.

73. Beyene, H.D., et al., *Synthesis paradigm and applications of silver nanoparticles (AgNPs), a review.* Sustainable materials and technologies, 2017. **13**: p. 18-23.

74. Natsuki, J., T. Natsuki, and Y. Hashimoto, *A review of silver nanoparticles: synthesis methods, properties and applications.* Int. J. Mater. Sci. Appl, 2015. **4**(5): p. 325-332.

75. Durán, N., et al., *Silver nanoparticles: A new view on mechanistic aspects on antimicrobial activity.* Nanomedicine: nanotechnology, biology and medicine, 2016. **12**(3): p. 789-799.

76. Cha, S.-H., et al., *Shape-dependent biomimetic inhibition of enzyme by nanoparticles and their antibacterial activity.* ACS nano, 2015. **9**(9): p. 9097-9105.

77. Yin, J., et al., *Attachment of silver nanoparticles (AgNPs) onto thin-film composite (TFC) membranes through covalent bonding to reduce membrane biofouling.* Journal of membrane science, 2013. **441**: p. 73-82.

78. Haider, M.S., et al., *Aminated polyethersulfone-silver nanoparticles (AgNPs-APES) composite membranes with controlled silver ion release for antibacterial and water treatment applications.* Materials Science and Engineering: C, 2016. **62**: p. 732-745.

79. Das, R., S. Gang, and S.S. Nath, *Preparation and antibacterial activity of silver nanoparticles.* Journal of Biomaterials and nanobiotechnology, 2011. **2**: p. 472.

80. Lin, W., et al., *The advancing of selenium nanoparticles against infectious diseases.* Frontiers in Pharmacology, 2021: p. 1971.

81. Khurana, A., et al., *Therapeutic applications of selenium nanoparticles.* Biomedicine & Pharmacotherapy, 2019. **111**: p. 802-812.

82. Geoffrion, L.D., et al., *Naked selenium nanoparticles for antibacterial and anticancer treatments.* ACS omega, 2020. **5**(6): p. 2660-2669.

83. Guisbiers, G., et al., *Inhibition of E. coli and S. aureus with selenium nanoparticles synthesized by pulsed laser ablation in deionized water.* International journal of nanomedicine, 2016. **11**: p. 3731.

84. Xu, C., et al., *Biogenic synthesis of novel functionalized selenium nanoparticles by Lactobacillus casei ATCC 393 and its protective effects on intestinal barrier dysfunction caused by enterotoxigenic Escherichia coli K88.* Frontiers in microbiology, 2018. **9**: p. 1129.

85. Ahmed, M., et al., *Wound dressing properties of functionalized environmentally biopolymer loaded with selenium nanoparticles.* Journal of Molecular Structure, 2021. **1225**: p. 129138.

86. Khiralla, G.M. and B.A. El-Deeb, *Antimicrobial and antibiofilm effects of selenium nanoparticles on some foodborne pathogens.* LWT-Food Science and Technology, 2015. **63**(2): p. 1001-1007.

87. Filipović, N., et al., *Comparative study of the antimicrobial activity of selenium nanoparticles with different surface chemistry and structure.* Frontiers in bioengineering and biotechnology, 2021. **8**: p. 1591.

88. Huang, T., et al., *Engineering highly effective antimicrobial selenium nanoparticles through control of particle size.* Nanoscale, 2019. **11**(31): p. 14937-14951.

89. Singh, Y., et al., *Approaches to increasing yield in evaporation/condensation nanoparticle generation.* Journal of Aerosol Science, 2002. **33**(9): p. 1309-1325.

90. Lin, Z., et al., *Rapid synthesis of metallic and alloy micro/nanoparticles by laser ablation towards water.* Applied Surface Science, 2020. **504**: p. 144461.

91. Sharma, V.K., R.A. Yngard, and Y. Lin, *Silver nanoparticles: Green synthesis and their antimicrobial activities.* Advances in Colloid and Interface Science, 2009. **145**(1-2): p. 83-96.

92. Escobar-Ramírez, M.C., et al., *Antimicrobial activity of Se-nanoparticles from bacterial biotransformation.* Fermentation, 2021. **7**(3): p. 130.

93. Kailasa, S.K., et al., *Antimicrobial activity of silver nanoparticles*, in *Nanoparticles in pharmacotherapy*. 2019, Elsevier. p. 461-484.

94. Palza, H., *Antimicrobial polymers with metal nanoparticles.* International journal of molecular sciences, 2015. **16**(1): p. 2099-2116.

95. Mikhailova, E.O., *Silver Nanoparticles: Mechanism of action and probable bio-application.* Journal of Functional Biomaterials, 2020. **11**(4): p. 84.

96. Yin, I.X., et al., *The antibacterial mechanism of silver nanoparticles and its application in dentistry.* International journal of nanomedicine, 2020. **15**: p. 2555.

97. Ahmad, S.A., et al., *Bactericidal activity of silver nanoparticles: a mechanistic review.* Materials Science for Energy Technologies, 2020.

98. Steve, W. and W. Thomas, *Efficacy and mechanism of selenium nanoparticles as antibacterial agents.* Frontiers in Bioengineering and Biotechnology, 2016. **4**.

99. Truong, L.B., et al., *Selenium Nanomaterials to Combat Antimicrobial Resistance.* Molecules, 2021. **26**(12): p. 3611.

100. Reller, L.B., et al., *Antimicrobial susceptibility testing: a review of general principles and contemporary practices.* Clinical infectious diseases, 2009. **49**(11): p. 1749-1755.

101. Balouiri, M., M. Sadiki, and S.K. Ibnsouda, *Methods for in vitro evaluating antimicrobial activity: A review.* Journal of pharmaceutical analysis, 2016. **6**(2): p. 71-79.

102. Piddock, L.J., *Techniques used for the determination of antimicrobial resistance and sensitivity in bacteria.* Journal of applied bacteriology, 1990. **68**(4): p. 307-318.

103. *Mueller Hinton Agar and Mueller Hinton Broth: Composition, Preparation and Differences*. [cited 2022; Available from: https://labmal.com/2019/11/20/mueller-hinton-agar-and-mueller-hinton-broth/.

104. Manual, O.T., *Laboratory methodologies for bacterial antimicrobial susceptibility testing.* OIE Ref Lab Antimicrob Resist, 2012.

105. Tendencia, E.A., *Disk diffusion method*, in *Laboratory manual of standardized methods for antimicrobial sensitivity tests for bacteria isolated from aquatic animals and environment*. 2004, Aquaculture Department, Southeast Asian Fisheries Development Center. p. 13-29.

106. Garibo, D., et al., *Green synthesis of silver nanoparticles using Lysiloma acapulcensis exhibit high-antimicrobial activity.* Scientific reports, 2020. **10**(1): p. 1-11.

107. Ram, D., *Isolation of antimicrobial actinomycetes from the soil surrounding different medicinal plants of saurashtra and characterization of antimicrobial compounds therefrom.*

108. Sagar, A. *Mueller and Hinton developed Mueller Hinton Agar (MHA) in 1941 for the isolation of pathogenic Neisseria species. Nowadays, it is more commonly used for the routine susceptibility testing of non-fastidious microorganism by the Kirby-Bauer disk diffusion technique.* 2018 [cited 2022; Available from: https://microbiologyinfo.com/mueller-hinton-agar-mha-composition-principle-uses-and-preparation/.

109. Valgas, C., et al., *Screening methods to determine antibacterial activity of natural products.* Brazilian journal of microbiology, 2007. **38**: p. 369-380.

110. Benabbou, R., et al., *Inhibition of Listeria monocytogenes by a combination of chitosan and divergicin M35.* Canadian journal of microbiology, 2009. **55**(4): p. 347-355.

111. Simner, P.J., et al., *Two-site evaluation of the colistin broth disk elution test to determine colistin in vitro activity against Gram-negative bacilli.* Journal of clinical microbiology, 2019. **57**(2): p. e01163-18.

112. Monod, J., *The growth of bacterial cultures.* Annual review of microbiology, 1949. **3**(1): p. 371-394.

113. Peleg, M. and M.G. Corradini, *Microbial growth curves: what the models tell us and what they cannot.* Critical reviews in food science and nutrition, 2011. **51**(10): p. 917-945.

114. T Garrison, A. and R. W Huigens III, *Eradicating bacterial biofilms with natural products and their inspired analogues that operate through unique mechanisms.* Current topics in medicinal chemistry, 2017. **17**(17): p. 1954-1964.

115. Bernauer, U., et al., *" SCIENTIFIC ADVICE on the safety of nanomaterials in cosmetics (SCCS)"-SCCS/1618/2020-Preliminary Advice*. 2020.

116. Baccaro, M., et al., *Ageing, dissolution and biogenic formation of nanoparticles: how do these factors affect the uptake kinetics of silver nanoparticles in earthworms?* Environmental Science: Nano, 2018. **5**(5): p. 1107-1116.

117. Schultz, C.L., et al., *Aging reduces the toxicity of pristine but not sulphidised silver nanoparticles to soil bacteria.* Environmental Science: Nano, 2018. **5**(11): p. 2618-2630.

118. Ribeiro, F., et al., *Bioaccumulation of silver in Daphnia magna: Waterborne and dietary exposure to nanoparticles and dissolved silver.* Science of The Total Environment, 2017. **574**: p. 1633-1639.

119. Fard, J.K., S. Jafari, and M.A. Eghbal, *A review of molecular mechanisms involved in toxicity of nanoparticles.* Advanced pharmaceutical bulletin, 2015. **5**(4): p. 447.

120. Grijalva, M., et al., *Cytotoxic and antiproliferative effects of nanomaterials on cancer cell lines: a review.* Unraveling the Safety Profile of Nanoscale Particles and Materials—From Biomedical to Environmental Applications, 2018: p. 63-85.

121. Aslantürk, Ö.S., *In vitro cytotoxicity and cell viability assays: principles, advantages, and disadvantages.* Genotoxicity-A predictable risk to our actual world, 2018. **2**: p. 64-80.

122. Riss, T., et al., *Cytotoxicity assays: in vitro methods to measure dead cells.* Assay Guidance Manual [Internet], 2019.

123. AC Wahab, N.F., et al., *Methods in Cytotoxicity Testing: A Review.* Recent Patents on Materials Science, 2017. **10**(1): p. 50-59.

124. Adan, A., Y. Kiraz, and Y. Baran, *Cell proliferation and cytotoxicity assays.* Current pharmaceutical biotechnology, 2016. **17**(14): p. 1213-1221.

125. Firouzjaei, M.D., et al., *Recent advances in functionalized polymer membranes for biofouling control and mitigation in forward osmosis.* Journal of Membrane Science, 2020. **596**: p. 117604.

126. Biswas, P. and R. Bandyopadhyaya, *Biofouling prevention using silver nanoparticle impregnated polyethersulfone (PES) membrane: E. coli cell-killing in a continuous cross-flow membrane module.* Journal of colloid and interface science, 2017. **491**: p. 13-26.

127. Chan, C.-M., T.-M. Ko, and H. Hiraoka, *Polymer surface modification by plasmas and photons.* Surface science reports, 1996. **24**(1-2): p. 1-54.

128. Qi, L., et al., *Polymeric membrane ion-selective electrodes with anti-biofouling properties by surface modification of silver nanoparticles.* Sensors and Actuators B: Chemical, 2021. **328**: p. 129014.

129. Liston, E., L. Martinu, and M. Wertheimer, *Plasma surface modification of polymers for improved adhesion: a critical review.* Journal of adhesion science and technology, 1993. **7**(10): p. 1091-1127.

130. Manakhov, A., et al., *Carboxyl-anhydride and amine plasma coating of PCL nanofibers to improve their bioactivity.* Materials & Design, 2017. **132**: p. 257-265.

131. Manakhov, A., et al., *Deposition of stable amine coating onto polycaprolactone nanofibers by low pressure cyclopropylamine plasma polymerization.* Thin Solid Films, 2015. **581**: p. 7-13.

132. Oehr, C., *Plasma surface modification of polymers for biomedical use.* Nuclear Instruments and Methods in Physics Research Section B: Beam Interactions with Materials and Atoms, 2003. **208**: p. 40-47.

133. Tylkowski, B., et al., *Applications of silver nanoparticles stabilized and/or immobilized by polymer matrixes.* Physical Sciences Reviews, 2017. **2**(7).

134. Park, S.-H., et al., *Direct incorporation of silver nanoparticles onto thin-film composite membranes via arc plasma deposition for enhanced antibacterial and permeation performance.* Journal of membrane science, 2016. **513**: p. 226-235.

135. Akhavan, B., et al., *Direct covalent attachment of silver nanoparticles on radical-rich plasma polymer films for antibacterial applications.* Journal of Materials Chemistry B, 2018. **6**(37): p. 5845-5853.

136. Brewis, D., *Adhesion to polymers: how important are weak boundary layers?* International journal of adhesion and adhesives, 1993. **13**(4): p. 251-256.

137. Yasuda, H., *Plasma for modification of polymers.* Journal of Macromolecular Science—Chemistry, 1976. **10**(3): p. 383-420.

138. Jiang, H., et al., *Plasma-enhanced deposition of silver nanoparticles onto polymer and metal surfaces for the generation of antimicrobial characteristics.* Journal of Applied Polymer Science, 2004. **93**(3): p. 1411-1422.

139. Airoudj, A., L. Ploux, and V. Roucoules, *Effect of plasma duty cycle on silver nanoparticles loading of cotton fabrics for durable antibacterial properties.* Journal of Applied Polymer Science, 2015. **132**(1).

140. Hosseini, S., et al., *Preparation and surface modification of PVC/SBR heterogeneous cation exchange membrane with silver nanoparticles by plasma treatment.* Journal of Membrane Science, 2010. **365**(1-2): p. 438-446.

141. Taheri, S., et al., *Binding of nanoparticles to aminated plasma polymer surfaces is controlled by primary amine density and solution PH.* The Journal of Physical Chemistry C, 2018. **122**(26): p. 14986-14995.

142. Agnihotri, S., S. Mukherji, and S. Mukherji, *Immobilized silver nanoparticles enhance contact killing and show highest efficacy: elucidation of the mechanism of bactericidal action of silver.* Nanoscale, 2013. **5**(16): p. 7328-7340.

143. McMichael, K. *Amines- Reactions* 2021 [cited 2022; Available from: https://chem.libretexts.org/Bookshelves/Organic_Chemistry/Book%3A_Organic_Chemistry_-_A_Carbonyl_Early_Approach_(McMichael)/01%3A_Chapters/1.20%3A_Amines-_Reactions.

144. Tran, H.V., et al., *Synthesis, characterization, antibacterial and antiproliferative activities of monodisperse chitosan-based silver nanoparticles.* Colloids and Surfaces A: Physicochemical and Engineering Aspects, 2010. **360**(1-3): p. 32-40.

145. Luo, C., et al., *The role of poly (ethylene glycol) in the formation of silver nanoparticles.* Journal of colloid and interface science, 2005. **288**(2): p. 444-448.

146. Darroudi, M., et al., *Fabrication and characterization of gelatin stabilized silver nanoparticles under UV-light.* International journal of molecular sciences, 2011. **12**(9): p. 6346-6356.

147. Yu, B., et al., *Positive surface charge enhances selective cellular uptake and anticancer efficacy of selenium nanoparticles.* Inorganic chemistry, 2012. **51**(16): p. 8956-8963.

148. Oldenburg, S.J. Silver Nanoparticles: Properties and Applications [cited 2015 1.4.2015]; Available from: http://www.sigmaaldrich.com/materials-science/nanomaterials/silver-nanoparticles.html.

149. Velgosova, O., et al., *Effect of storage conditions on long-term stability of Ag nanoparticles formed via green synthesis.* International Journal of Minerals, Metallurgy, and Materials, 2017. **24**(10): p. 1177-1182.

150. Al-Thabaiti, S.A., et al., *Formation and characterization of surfactant stabilized silver nanoparticles: a kinetic study.* Colloids and Surfaces B: Biointerfaces, 2008. **67**(2): p. 230-237.

151. Nguyen, T.H.N., T.D. Nguyen, and M.T. Cao, *Fast and simple synthesis of triangular silver nanoparticles under the assistance of light.* Colloids and Surfaces A: Physicochemical and Engineering Aspects, 2020. **594**: p. 124659.

152. Stamplecoskie, K.G. and J.C. Scaiano, *Light emitting diode irradiation can control the morphology and optical properties of silver nanoparticles.* Journal of the American Chemical Society, 2010. **132**(6): p. 1825-1827.

153. Graves Jr, J.L., et al., *Rapid evolution of silver nanoparticle resistance in Escherichia coli.* Frontiers in genetics, 2015. **6**: p. 42.

154. Lin, Z.-H. and C.C. Wang, *Evidence on the size-dependent absorption spectral evolution of selenium nanoparticles.* Materials Chemistry and Physics, 2005. **92**(2-3): p. 591-594.

155. Srivastava, G.K., et al., *Comparison between direct contact and extract exposure methods for PFO cytotoxicity evaluation.* Scientific Reports, 2018. **8**(1): p. 1-9.

156. Crane, A.M. and S.K. Bhattacharya, *The use of bromodeoxyuridine incorporation assays to assess corneal stem cell proliferation*, in *Corneal Regenerative Medicine*. 2013, Springer. p. 65-70.

157. Shahid, M., et al., *A critical review of selenium biogeochemical behavior in soil-plant system with an inference to human health.* Environmental Pollution, 2018. **234**: p. 915-934.

158. Ramos, J.F. and T.J. Webster, *Cytotoxicity of selenium nanoparticles in rat dermal fibroblasts.* International journal of nanomedicine, 2012. **7**: p. 3907.

159. León-Mancilla, B., et al., *Physico-chemical characterization of collagen scaffolds for tissue engineering.* Journal of applied research and technology, 2016. **14**(1): p. 77-85.

160. Pekarkova, J., et al., *Modifications of Parylene by Microstructures and Selenium Nanoparticles: Evaluation of Bacterial and Mesenchymal Stem Cell Viability.* Frontiers in Bioengineering and Biotechnology, 2021. **9**.

161. Gablech, E., et al., *Selenium nanoparticles with boron salt-based compound act synergistically against the brown-rot Serpula lacrymans.* International Biodeterioration & Biodegradation, 2022. **169**: p. 105377.